
Probabilistic analysis of
Coxeter statistics
and
STIT tessellations

RUHR UNIVERSITY BOCHUM



DOCTORAL THESIS

presented to the Faculty of Mathematics
at the Ruhr University Bochum
in consideration for the award of the academic grade of

Doctor rerum naturalium

by

Kathrin Meier

April 2023

“Can you forgive me for not trusting you? For not telling you? ... I only feared that you would fail as I had failed. I only dreaded that you would make my mistakes.”

Albus Dumbledore
Harry Potter and the Deathly Hallows

Abstract

Probabilistic analysis can deal with a wide variety of mathematical objects. In this thesis, we focus on statistics of Coxeter groups and STIT tessellations.

The first part of the thesis deals on two statistics of Coxeter groups, namely the generalized d -inversions and generalized d -descents. Interim results combine probabilistic properties like the covariance of random variable with combinatorial properties of Coxeter groups. The dependency graph method is used to conclude a central limit for these statistics.

The second part of the thesis investigates second-order properties of a specific type of STIT tessellation called Mondrians. We examine the (co-)variance for the number of maximal edges and the weighted total edge length. Additionally, Mondrian analogues of the pair-correlation functions for the random edge length measure and the random vertex process, as well as the cross-correlation function for these functions, are deduced.

The last chapter of the thesis deals with probabilistic analysis of different types of line segments in planar isotropic STIT tessellations. Probabilities are deduced for some geometrical and metrical properties of these.

Acknowledgement

First of all, I would like to express my deepest thanks to Professor Christoph Thäle to convince me continuing my math study as a PhD student, and Professor Christian Stump for introducing me to so many aspects in Coxeter theory and Coxeter statistics. I thank them wholeheartedly for their support during all the times I struggled with different kind of challenges and their confidence especially in the last months of my studies.

I thank Dennis Jahn, Tilman Möller, Galen Dorpalen-Barry for their help when dealing with mathematical, programming and private problems. Furthermore I thank Nils Heerten, Benedikt Rednoß, Carolin Kleemann, Tristan Schiller and Marius Butzek for all the times we met for Wizard-Wednesday and never ending discussions about Harry Potter. I thank Dennis Jahn and Carina Betken for sharing the office with me and for all the help during this time. Further, I thank Tanja Schiffmann for her help with all my questions and concerns, and her support during my time at university.

Moreover, I thank Carina Betken, Galen Dorpalen-Barry and Tilman Möller for proofreading of this thesis and their fruitfull comments.

I owe my deepest gratitude to my mother, stepfather and brother for their endless love and support during the whole time. Finally, I thank Jan-Kristian for his love, his support and his patience.

Contents

1	Introduction	1
2	Background on Coxeter statistics	5
2.1	Finite Coxeter systems and root systems	5
2.2	Probabilistic background and Coxeter group statistics	7
2.3	Inversion and descent statistics	8
3	Probabilistic analysis of Coxeter statistics	15
3.1	Main results	15
3.1.1	Set-Up	15
3.1.2	Central limit theorems	18
3.2	Random inversions for finite root systems	20
3.3	Concrete variances	25
3.3.1	Type A_{n-1}	26
3.3.2	Type B_n	30
3.3.3	Type C_n	38
3.3.4	Type D_n	39
3.4	Central limit theorems	41
3.4.1	The dependency graph method	41
3.4.2	Central limit theorems for antichains in root posets and d -descents . .	42
3.4.3	Central limit theorems for d -inversions	44
4	Background on STIT tessellations	49
4.1	Probability measures and tessellations	49
4.2	Construction of a STIT tessellation	51
4.3	Properties of STIT tessellations	53
5	Probabilistic analysis of Mondrian tessellations	55
5.1	Main results	55
5.1.1	Set-up	55
5.1.2	Variances	56

5.1.3	Correlation Function	58
5.2	Expected value and variance for Mondrian tessellations	61
5.2.1	The point intersection measure and expected values	61
5.2.2	The segment intersection measure and variances	62
5.3	Pair- and cross-correlations	68
5.3.1	Preparatory calculations	68
5.3.2	Edge pair-correlations for Mondrian tessellations	77
5.3.3	Edge-vertex cross-correlations for Mondrian tessellations	80
5.3.4	Vertex pair-correlations for Mondrian tessellations	83
6	Probabilistic analysis of line segments	87
6.1	Set-up	87
6.2	Refined analysis of I-segments	89
6.3	Geometrical and metrical properties of line segments	91
6.3.1	Geometrical properties of sides	91
6.3.2	Metric properties	95
	Bibliography	101

List of Figures

1.1	Planar isotropic STIT tessellation and weighted planar Mondrian tessellation.	3
2.1	Root poset for the Coxeter group of type A_4 .	9
2.2	Root poset for the Coxeter group of type B_4 .	10
2.3	Inversions & descents of a signed Permutations $\sigma \in B_3$.	11
2.4	Inversions & descents of a signed Permutations $\sigma \in C_3$.	13
2.5	Inversions & descents of a forked signed Permutations $\sigma \in D_3$.	14
3.1	Root poset and one-line notation for 2-inversions & 2-descents in A_4 .	17
3.2	3-descents for B_4, C_4 and D_4 in their respective one-line notation.	18
4.1	Schematic construction of a planar Mondrian tessellation.	51
4.2	Parametrization of a line in \mathbb{R}^2 .	52
4.3	Schematic visualization of an iteration of Y_0 with Y_1 .	54
5.1	Pair- and cross-correlation functions $g_{\mathcal{E}}(r), g_{\mathcal{E}, \mathcal{V}}(r)$, and $g_{\mathcal{V}}(r)$.	60
5.2	Projection of a horizontal line segment to E_1 .	64
5.3	Visualization of the Lebesgue measure after a diagonal-shift of a line segment in \mathbb{R}^2 .	72
6.1	Line segments of a planar STIT tessellation.	88
6.2	Visualization of edges adjacent to one terminus.	92
6.3	Probabilities for typical edges adjacent to 0, 1 terminus or 2 termini.	93
6.4	Probabilities for the number of vertices of a typical side.	94
6.5	Probabilities for the number of sides adjacent to a typical side.	95
6.6	Densities for the length of a random edge on a typical I-segment.	96
6.7	Densities for the length of an I-segment covering a typical edge.	97
6.8	Densities for the length of an I-segment covering a typical side.	98

Chapter 1

Introduction

This thesis consists of three parts. All of these deal with the analysis of probabilistic aspects, with the first part focusing on Coxeter groups and the latter two on planar STIT tessellations.

Coxeter and Weyl groups are a large family of groups with connections to symmetry and geometry. One of the best known examples of a Coxeter group is the symmetric group. Permutations have been studied in various fields of mathematics like algebraic combinatorics, group theory or probability (see for example [7, 10, 26]). Within this area of research, statistics and especially those being normal distributed, are of interest. Widely known are the statistics of descents and inversions, which can be expressed by comparing permutation entries. An *inversion* of $\pi \in \mathfrak{S}_n$ is given by a pair (i, j) with $1 \leq i < j \leq n$ and $\pi(i) > \pi(j)$. A *descent* can then be described as an inversion with distance 1, *i.e.*, it is given by i with $1 \leq i \leq n - 1$ and $\pi(i) > \pi(i + 1)$. The *inversion statistic* and *descent statistic* now count the number of inversions and descents of a permutation, respectively. Random variables may be associated to these statistics. These describe the number of inversions or descents a permutations is likely to have, when picking it uniformly at random from \mathfrak{S}_n . The random variables \mathcal{X}_{des} and \mathcal{X}_{inv} are known to fulfill a central limit theorem, *i.e.*, their normalized version converges in distribution to the normal Gaussian distribution (see [2]).

From this starting point, the aim of the first part of the thesis is to generalize these statistics in two different ways. These results are joint work with Christian Stump published in [21]. Bona [7] and Pike [26] studied *d-inversions* of permutations by restricting the distance between the compared permutation entries to be at most d . Similarly, one may define *d-descents* for permutations as comparisons with a distance of exactly d . For a permutation $\pi \in \mathfrak{S}_n$, the number of *d-descents* and *d-inversions* is then given by

$$\begin{aligned} \text{des}_d(\pi) &= |\{1 \leq i \leq n - d \mid \pi(i) > \pi(i + d)\}| \\ \text{inv}_d(\pi) &= |\{1 \leq i < j \leq \min\{i + d, n\} \mid \pi(i) > \pi(j)\}| \end{aligned}$$

respectively. For the associated random variable of d -inversions, $\mathcal{X}_{\text{inv}_d}$, Bona [7] and Pike [26] conclude a central limit theorem for fixed d and for $d = d_n$ as a function of n . One sees for example [26, Theorem 4]. Pike additionally concludes rates of convergence if d_n grows faster than $n^{2/3}$ and slower than $n^{1/3}$. The second generalization of these statistics pertains their current limitation towards permutations. Following a similar approach as Kahle and Stump in [14], we expand these statistics to other finite Weyl groups. The aforementioned authors gave a description of the descent and inversion statistic in terms of roots and proved normality of these in finite Coxeter groups.

As a main result, we prove the central limit theorem for d -inversions and antichains along with the rate of convergence in classical types under some additional condition on the growth behavior of $d = d_n$. The result for antichains implies the central limit for d -descents.

A STIT tessellation is a special model describing a cell division process which is **stable under iteration**. They were introduced by Nagel and Weiss in [24]. A planar STIT tessellation can be described colloquially as follows. Start with a bounded and convex window of observation $W \subset \mathbb{R}^2$. After some random time, which depends on some properties of W , this window is cut by a random line. The driving measure of such a line is dependent on W again. This line segment divides W into two smaller windows (called cells), which are subject to the same procedure of being split. For some threshold t , the union of these line segments dividing W into smaller cells is a *STIT tessellation* of W at time t . It is denoted by $Y(t, W)$. A visualization of two STIT tessellations is given in Figure 1.1.

A lot of research has been done about those STIT tessellations (see for example [20, 23, 28, 29, 30, 34]). In particular, Schreiber and Thäle deduced in [28] formulas for the variance of the total number of maximal edges and for the total number of vertices for general driving measures. Likewise, abstract formulas are derived for the vertex pair-correlation and the edge-vertex cross-correlation for a general case. As in other studies about STIT tessellations, Schreiber and Thäle explicitly investigated *isotropic STIT tessellations*, *i.e.*, those in which the driving measure is rotation invariant. For these tessellations, more concrete formulas could be deduced.

Another special class of STIT tessellations are planar Mondrian tessellations. In this special case, the splitting lines are restricted to only axis-parallel cutting directions. The concrete measure on the splitting line can include some weight parameter $p \in (0, 1)$ for disparate probabilities of appearance for the two directions. We call tessellations with this driving measure *weighted Mondrian tessellations*. A visualization of a weighted planar Mondrian tessellation with $p = 0.5$ is given in Figure 1.1.

Their name is reminiscent of works by the Dutch artist Piet Mondrian, which are characterized by a grid of vertical and horizontal lines. Knowledge Mondrian tessellations are widely used in machine learning literature. More precisely, they are used in random forest learning

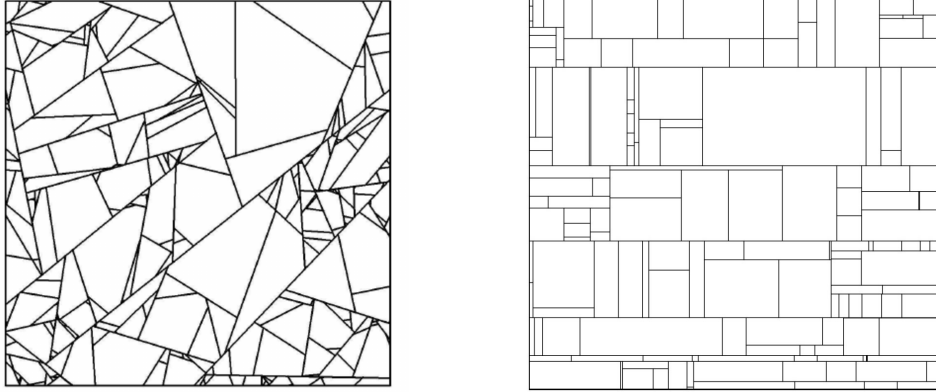


FIGURE 1.1: Planar isotropic STIT tessellation (left) [22, Figure 1] and weighted planar Mondrian tessellation with $p = 0.5$ (right) [3, Figure 2].

[15, 16] or kernel methods [1]. Their property of being stable under iteration makes them extremely suitable for incorporating new data into an existing model. Their wide field of application makes it desirable investigating second-order properties of these special class of STIT tessellations. Thus, we present results specifying the formulas for the variance and covariance of the number of maximal edges and weighted total edge length for weighted Mondrian tessellations. Additionally, Mondrian analogues of the pair- and cross-correlation functions are derived. These results are joint work with Carina Betken, Tom Kaufmann and Christoph Thäle [3].

Due to their easy accessibility, isotropic STIT tessellations are subject to other aspects of studies. Those may be considered for different kinds of line segments. Following notation of [17], we distinguish between three kinds of line segments, called I-segments, J-segments and K-segments. A *K-segment* is an edge without any internal vertex. A *J-segment* is a side of a cell of the tessellation. An *I-segment*, also called a maximal edge, is a union of collinear edges, which can not be extended by another one. Exemplary properties studied in the context of line segments are the distribution of their length, birth time or the number of internal vertices (see [8, 17, 20, 34]). Cowan added some aspects about geometrical properties of different line segments in [8].

The main results of Chapter 6 are the refinement of I-segments regarding some weight functions and a more specified analysis of geometrical and metrical properties of line segments in which the birth time of covering I-segments is considered.

This thesis is organized as follows.

- We will commence by presenting the necessary background on definitions and notations of finite crystallographic root systems in Section 2.1, as well as the needed aspects from probability theory and Coxeter statistics in Section 2.2.

-
- In Chapter 3 we begin by presenting the main results in Section 3.1 followed by an interim result connecting the covariance as a probabilistic statement with a combinatorial aspect of positive roots in Section 3.2. Elaborate calculations in Section 3.3 will lead to concrete formulas for the variances of d -descents and d -inversions in irreducible types. Lastly, introduction and application of the dependency graph method will give rise to the main results in Section 3.4.
 - Moving on to the second aspect of the thesis, Chapter 4 begins with necessary definitions and notation about probability measures and tessellations in Section 4.1. This is followed by more specific information about the construction of STIT tessellations in Section 4.2 and relevant properties of these in Section 4.3.
 - In Chapter 5, we first present the main results in Section 5.1. We then proceed to calculate the variance and covariance of the number of maximal edges and the weighted total edge length of a Mondrian tessellation in Section 5.2. In order to compute the pair- and cross-correlation function some extensive integral computations are outsourced to Section 5.3.1. Results for the pair-correlation functions can then be found in Section 5.3.2 and Section 5.3.4, and for the cross-correlation in Section 5.3.3.
 - In Chapter 6, we investigate the properties of line segments in isotropic planar STIT tessellations. We begin by extending the basic definitions and notations of STIT tessellations and line segments in Section 6.1. We then present our first results concerning the refinement of I-segments by adding weight functions and how this affects their distributions in Section 6.2. Next, we derive geometrical properties of line segment in Section 6.3.1, before turning to their metrical properties, specifically their length distributions, in Section 6.3.2.

Chapter 2

Background on Coxeter statistics

In this chapter, we set up notation and terminology concerning Coxeter systems and Coxeter statistics, which we will use in Chapter 3. In Section 2.1, we start by recalling basic definitions and important properties about Coxeter systems, for which we roughly follow [5] and [12]. Additionally, Section 2.2 gives the most relevant probabilistic theory needed to analyze Coxeter group statistics. In Section 2.3, we investigate the known statistics of inversions and descents in detail and prepare for their generalization.

2.1 Finite Coxeter systems and root systems

Let \mathcal{S} be a finite set with cardinality n . A *Coxeter matrix* is defined to be a function $m : \mathcal{S} \times \mathcal{S} \mapsto \{1, 2, \dots, \infty\}$ which satisfies $m(s, s') = m(s', s) \geq 1$ for all $s, s' \in \mathcal{S}$, and $m(s, s') = 1$ if and only if $s = s'$. The generating set \mathcal{S} along with relations $(ss')^{m(s, s')} = e$, where e is the identity element, form a group W which we call *Coxeter group*. Together with its set of *simple reflections* \mathcal{S} we call the pair (W, \mathcal{S}) a *Coxeter system*. The cardinality of \mathcal{S} is called the *rank* of W and whenever $|W| < \infty$, the Coxeter group is said to be *finite*. The set of all *reflections* in W is given by $\mathcal{R} = \{wsw^{-1} | w \in W, s \in \mathcal{S}\}$.

The Coxeter matrix can also be represented by an undirected graph, called the *Coxeter diagram*, which vertex set is given by \mathcal{S} , and an unordered pair $\{s, s'\}$ forming an edge if $m(s, s') \geq 3$. Whenever $m(s, s') \geq 4$, the edge is labeled by that number. A system (W, \mathcal{S}) is *irreducible* if the Coxeter diagram is connected.

In what follows, let V be an n -dimensional Euclidean vector space with inner product $\langle \cdot, \cdot \rangle$. For each $0 \neq \alpha \in V$, we define the reflection r_α orthogonal to α by

$$r_\alpha(\lambda) = \lambda - 2 \frac{\langle \lambda, \alpha \rangle}{\langle \alpha, \alpha \rangle} \alpha \in V$$

for $\lambda \in V$. A finite set $\Phi \subset V$ is called a finite *root system* if for all $\alpha \in \Phi$ the following two conditions are satisfied:

- i) $\Phi \cap \mathbb{R}\alpha = \{-\alpha, \alpha\}$,
- ii) $r_\alpha(\Phi) = \Phi$.

Elements of Φ are called *roots*. A subset $\Delta = \{\alpha_1, \dots, \alpha_n\} \subseteq \Phi$ is called the set of *simple roots* if it is linear independent and every other root $\beta \in \Phi$ can be expressed as a linear combination with either non-negative or non-positive coefficients. A choice of simple roots splits Φ into *positive roots* Φ^+ and *negative roots* Φ^- ,

$$\Phi^+ = \left\{ \sum_{i=1}^n \lambda_i \alpha_i \mid \lambda_i \in \mathbb{R}_+ \right\} \cap \Phi \quad \text{and} \quad \Phi^- = \left\{ \sum_{i=1}^n \lambda_i \alpha_i \mid \lambda_i \in \mathbb{R}_- \right\} \cap \Phi = -\Phi^+.$$

Given these sets of roots it is clear that $\Delta \subseteq \Phi^+ \subset \Phi = \Phi^+ \cup \Phi^- \subseteq V$.

Given a finite root system Φ we define its Weyl group $W(\Phi)$ by

$$W(\Phi) = \langle r_\beta \mid \beta \in \Phi \rangle \subseteq GL(V).$$

It turns out that $W(\Phi)$ is generated by $\mathcal{S} = \{r_\alpha \mid \alpha \in \Delta\}$, that $(W(\Phi), \mathcal{S})$ is a finite Coxeter system, and that every finite Coxeter system can be obtained from a finite root system.

A root system Φ is called *crystallographic* if all $\alpha, \beta \in \Phi$ satisfy the integrality criterion

$$2 \frac{\langle \alpha, \beta \rangle}{\langle \alpha, \alpha \rangle} \in \mathbb{Z}.$$

Equivalently, for all $s, s' \in \mathcal{S}$ the corresponding entry $m(s, s')$ of the Coxeter matrix satisfies $m(s, s') = \{1, 2, 3, 4, 6\}$.

The set of positive roots comes with a natural partial order induced by the cover relation $\beta \prec \gamma$ if $\gamma - \beta \in \Delta$. We refer to Φ^+ with this partial order as the *root poset*. A set of pairwise incomparable roots in Φ^+ is called an *antichain*. Moreover, the root poset is ranked by the *height* of a root $\beta = \sum_{i=1}^n \lambda_i \alpha_i \in \Phi^+$, which is defined as the sum of its coefficients, *i.e.*, $ht(\beta) = \sum_{i=1}^n \lambda_i$. The height of the root poset is $h - 1$ for the *Coxeter number* h of the related Coxeter group. The *order* of two roots $\beta, \gamma \in \Phi^+$ is set to be the order of the product of the associated reflections s_β, s_γ , *i.e.*,

$$\text{ord}(\beta, \gamma) = \text{ord}(s_\beta s_\gamma) = \min\{k \in \mathbb{N}_{>0} \mid (s_\beta s_\gamma)^k = e\}.$$

For any subset $\Gamma \subseteq \Delta$, the group W_Γ generated by r_α for $\alpha \in \Gamma$ is called a *parabolic subgroup* of W . For this, we also define the corresponding set of positive roots Φ_Γ^+ which are non-negative linear combinations of Γ , *i.e.*, $\Phi_\Gamma^+ = \Phi^+ \cap \text{span}(\Gamma)$. Moreover, we let $W^\Gamma = \{w \in W \mid w(\alpha) \in \Phi^+ \text{ for all } \alpha \in \Gamma\}$ be the *parabolic quotient*. Given $\Gamma \subseteq \Delta$, each

group element $w \in W$ can be written as a unique decomposition $w = w^\Gamma \cdot w_\Gamma$ with $w^\Gamma \in W^\Gamma$ and $w_\Gamma \in W_\Gamma$, see [5].

2.2 Probabilistic background and Coxeter group statistics

Let W be a finite Coxeter group. A *statistic* is simply a map $\text{st} : W \rightarrow \mathbb{N}$. One may now study the probabilistic properties of st by asking for its value on an element in W chosen uniformly at random. More formally, this finite random variable X_{st} is defined by its probabilities

$$\mathbb{P}(X_{\text{st}} = k) = \frac{|\{w \in W \mid \text{st}(w) = k\}|}{|W|}.$$

We study probabilistic properties of such random variables based on different statistics later in Chapter 3. For this, we recall necessary probabilistic notations and properties. Let X be a finite random variable on \mathbb{N} . Here, finite means that only finitely many values are obtained. Its *expected value* and its *variance* are

$$\mathbb{E}[X] = \sum_{k \in \mathbb{N}} \mathbb{P}(X = k) \cdot k \quad \text{and} \quad \mathbb{V}[X] = \mathbb{E}[(X - \mathbb{E}[X])^2] = \mathbb{E}[X^2] - \mathbb{E}[X]^2,$$

respectively. Moreover, given a second such random variable Y , the *covariance* of X and Y is

$$\text{Cov}(X, Y) = \text{Cov}(Y, X) = \mathbb{E}[XY] - \mathbb{E}[X]\mathbb{E}[Y].$$

Note that $\text{Cov}(X, X) = \mathbb{V}[X]$ and that X and Y are *independent* if $\text{Cov}(X, Y) = 0$.

The variance of a sum of such random variables $\mathcal{X} = \sum_{i=1}^k X_i$ can be calculated using the linearity of the covariance:

$$\mathbb{V}[\mathcal{X}] = \sum_{i,j=1}^k \text{Cov}(X_i, X_j) = \sum_{i=1}^k \mathbb{V}[X_i] + \sum_{\substack{i,j=1 \\ i \neq j}}^k \text{Cov}(X_i, X_j).$$

Finally, let $\mathcal{X}^{(n)}$ be a sequence of such random variables. We call $\mathcal{X}^{(n)}$ *asymptotically normal* if its normalized version converges in distribution towards the standard Gaussian distribution, denoted by $\mathcal{N}(0, 1)$. More formally, this is

$$\frac{\mathcal{X}^{(n)} - \mathbb{E}[\mathcal{X}^{(n)}]}{\mathbb{V}[\mathcal{X}^{(n)}]^{1/2}} \xrightarrow{\mathcal{D}} \mathcal{N}(0, 1),$$

where $X^{(n)} \xrightarrow{\mathcal{D}} X$ means

$$\lim_{n \rightarrow \infty} \mathbb{E}[f(X^{(n)})] = \mathbb{E}[f(X)]$$

for all bounded, continuous functions f .

2.3 Inversion and descent statistics

Statistics on Coxeter groups are often introduced for the special case of the symmetric group \mathfrak{S}_n , which coincides with the Coxeter group of type A_{n-1} , before they are generalized to other types. Two very well studied statistics are inversions and descents, for which we recall their definitions and visualizations.

Given a permutation $\pi \in \mathfrak{S}_n$, an *inversion* is a pair (i, j) with $1 \leq i < j \leq n$ for which $\pi(i) > \pi(j)$. A *descent* is an inversion of distance 1, *i.e.*, i is a descent of $\pi \in \mathfrak{S}_n$ if $1 \leq i \leq n - 1$ and $\pi(i) > \pi(i + 1)$. For $\pi \in \mathfrak{S}_n$, the sets

$$\text{Inv}(\pi) = \{(i, j) \mid 1 \leq i < j \leq n \text{ and } \pi(i) > \pi(j)\}, \quad (2.1)$$

$$\text{Des}(\pi) = \{i \mid 1 \leq i \leq n \text{ and } \pi(i) > \pi(i + 1)\}, \quad (2.2)$$

are called the *inversion set* and *descent set* of π , respectively. Then, $\text{inv}(\pi) = |\text{Inv}(\pi)|$ and $\text{des}(\pi) = |\text{Des}(\pi)|$ count the number of inversions and descents in π , respectively.

Example 2.3.1 Let $\pi = [2, 5, 1, 4, 3] \in \mathfrak{S}_5$ be a permutation written in one-line notation. The sets of inversions and descents are

$$\text{Inv}(\pi) = \{(1, 3), (2, 3), (2, 4), (2, 5), (4, 5)\} \quad \text{and} \quad \text{Des}(\pi) = \{2, 4\}.$$

respectively.

For generalizations to other finite Coxeter groups, we follow the notation of Kahle and Stump [14] and define *W-inversions* and *W-descents* by

$$\text{Inv}(\pi) = \{\beta \in \Phi^+ \mid \pi(\beta) \in \Phi^-\} \text{ and } \text{Des}(\pi) = \{\beta \in \Delta \mid \pi(\beta) \in \Phi^-\}, \quad (2.3)$$

respectively. These definitions allow us to expand the idea of the inversion and descent statistic to other objects of finite Weyl groups denoted again by $\text{inv}(\pi) = |\text{Inv}(\pi)|$ and $\text{des}(\pi) = |\text{Des}(\pi)|$. The next paragraphs will provide explanations of the coherence between the two definitions as well as visualizations in classical Weyl groups. For this, we use $\{e_1, \dots, e_n\}$ to denote the standard basis vectors of \mathbb{R}^n .

Type A_{n-1} : We consider \mathfrak{S}_n as a Coxeter group of type A_{n-1} . Its root system $\Delta \subseteq \Phi^+ \subseteq \Phi$ can be realized by

$$\{e_{i+1} - e_i \mid 1 \leq i \leq n - 1\} \subseteq \{e_j - e_i \mid 1 \leq i < j \leq n\} \subseteq \{e_i - e_j \mid 1 \leq i \neq j \leq n\}.$$

A visualization of the corresponding root poset is given in Figure 2.1. Simplifying notation, we write $[ij]$ for $e_j - e_i$.

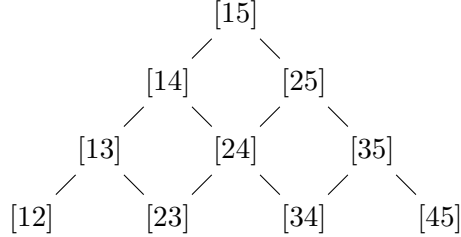


FIGURE 2.1: Root poset for the Coxeter group of type A_4 .

By Equation (2.3), a positive root $\beta = e_j - e_i$ is an inversion if

$$\pi(\beta) = e_{\pi(j)} - e_{\pi(i)} \in \Phi^-,$$

where the last assertion implies that $\pi(i) > \pi(j)$ by the definition of Φ^- . Since $\beta \in \Phi^+$, it is $i < j$, and thus the pair (i, j) is an inversion in the sense of Equation (2.2).

The same thoughts with restriction to simple roots lead to the coherence between A_{n-1} -descents in (2.3) and the given description in terms of one-line-notation in (2.2).

Example 2.3.2 Let $\pi = [2, 5, 1, 4, 3] \in \mathfrak{S}_5$ be the permutation from Example 2.3.1. Its inversion and descent sets denoted according both definitions are,

$$\begin{aligned} \text{Inv}(\pi) &= \{ (1, 3), (2, 3), (2, 4), (2, 5), (4, 5) \}, \\ \text{Inv}(\pi) &= \{ e_3 - e_1, e_3 - e_2, e_4 - e_2, e_5 - e_2, e_5 - e_4 \} \end{aligned}$$

and

$$\begin{aligned} \text{Des}(\pi) &= \{ 2, 4 \}, \\ \text{Des}(\pi) &= \{ e_3 - e_2, e_4 - e_3 \} \end{aligned}$$

respectively.

Since

$$e_j - e_i = \sum_{k=i}^{j-1} (e_{k+1} - e_k) = (e_{i+1} - e_i) + \cdots + (e_j - e_{j-1}) \in \Phi^+$$

we have $\text{ht}(e_j - e_i) = j - i$. Thus, the distance of the entries being compared in a permutation written in one-line notation equals the height of the corresponding root.

Type B_n : One may realize the irreducible root system of type B_n using standard basis vectors of \mathbb{R}^n and set $\Delta \subseteq \Phi^+ \subseteq \Phi$ to be

$$\begin{aligned} \{e_1\} \cup \{e_{i+1} - e_i | 1 \leq i \leq n-1\} &\subseteq \{e_i | 1 \leq i \leq n\} \cup \{e_j \pm e_i | 1 \leq i < j \leq n\} \\ &\subseteq \{\pm e_i | 1 \leq i \leq n\} \cup \{e_j \pm e_i | 1 \leq i \neq j \leq n\}. \end{aligned}$$

A visualization of the root poset is given in Figure 2.2. Similar to roots $[ij]$ already seen in type A_{n-1} , we write $[\tilde{k}\ell]$ for roots of the form $e_\ell + e_k$ and $[i]$ for e_i .

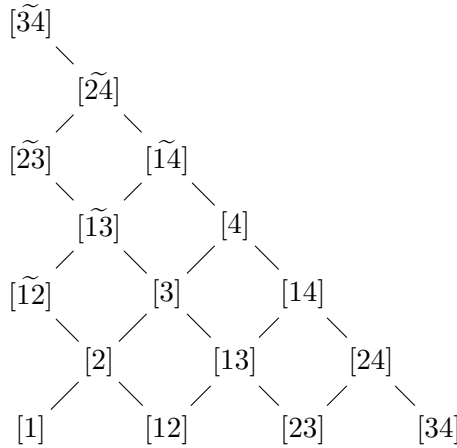


FIGURE 2.2: Root poset for the Coxeter group of type B_4 .

The height for $\beta = e_j - e_i$ is the same as in A_{n-1} . For the other roots, we have

$$e_j + e_i = 2e_1 + \sum_{\ell=1}^{i-1} (e_{\ell+1} - e_\ell) + \sum_{k=1}^{j-1} (e_{k+1} - e_k) \quad \text{and} \quad e_i = e_1 + \sum_{k=1}^{i-1} (e_{k+1} - e_k).$$

This yields the following description of the height:

$$\text{ht}(\beta) = \begin{cases} j - i & \text{if } \beta = e_j - e_i, \\ i & \text{if } \beta = e_i, \\ i + j & \text{if } \beta = e_j + e_i. \end{cases}$$

Elements of the Coxeter group of type B_n may be represented by *signed permutations*. That is,

$$B_n = \{\pi : \{\pm 1, \pm 2, \dots, \pm n\} \rightarrow \{\pm 1, \pm 2, \dots, \pm n\} \mid \pi \text{ is bijective and } \pi(-i) = -\pi(i)\}.$$

To find an interpretation analogous to (2.1) and (2.2) of descents and inversions for signed

permutations, we set

$$\text{Inv}^+(\pi) = \{(i, j) \mid 1 \leq i < j \leq n \text{ and } \pi(i) > \pi(j)\}, \quad (2.4)$$

$$\text{Inv}^-(\pi) = \{\widetilde{(i, j)} \mid 1 \leq i < j \leq n \text{ and } -\pi(i) > \pi(j)\}, \quad (2.5)$$

$$\text{Inv}^\circ(\pi) = \{i \mid 1 \leq i \leq n \text{ and } \pi(i) < 0\} = \{i \mid 1 \leq i \leq n \text{ and } -\pi(i) > \pi(i)\}, \quad (2.6)$$

which we relate to as positive, negative and neutral inversions, respectively. We then define the descents and inversions by

$$\text{Des}(\pi) = \{i \mid 0 \leq i \leq n-1 \text{ and } \pi(i) > \pi(i+1)\} \text{ with } \pi(0) = 0, \quad (2.7)$$

$$\text{Inv}(\pi) = \text{Inv}^+(\pi) \cup \text{Inv}^-(\pi) \cup \text{Inv}^\circ(\pi), \quad (2.8)$$

respectively. The comparisons of permutation entries taken into account for these kind of inversions are shown in Figure 2.3.

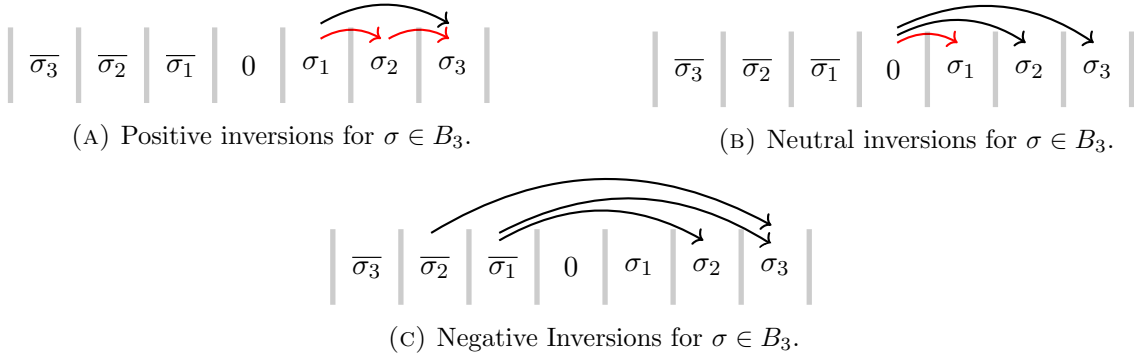


FIGURE 2.3: Visualization of inversions for a signed permutation $\sigma \in B_3$. Descents are marked in red.

We will show that these kinds of comparisons in one-line notation correspond to roots of the form $e_j - e_i$, $e_j + e_i$ and e_i , respectively. For this, we recall the sign function to be

$$\text{sgn}(x) = \begin{cases} +1 & \text{if } x > 0, \\ 0 & \text{if } x = 0, \\ -1 & \text{if } x < 0, \end{cases}$$

for any $x \in \mathbb{R}$.

Proposition 2.3.3 *Let Φ^+ be the set of positive roots for type B_n and $\pi \in B_n$. Then*

$$\text{Inv}^+(\pi) = \{\beta = e_j - e_i \in \Phi^+ \mid \pi(\beta) \in \Phi^-\},$$

$$\text{Inv}^-(\pi) = \{\beta = e_j + e_i \in \Phi^+ \mid \pi(\beta) \in \Phi^-\},$$

$$\text{Inv}^\circ(\pi) = \{\beta = e_i \in \Phi^+ \mid \pi(\beta) \in \Phi^-\}.$$

Proof. The proof follows similar ideas already shown in the paragraph for type A_n . We will show that the stated sets coincide with the sets given for positive, negative and neutral inversions in (2.4), (2.5) and (2.6).

First, let $e_j - e_i \in \text{Inv}^+(\pi)$. It is $\pi(e_j - e_i) = \text{sgn}(\pi(j)) e_{|\pi(j)|} - \text{sgn}(\pi(i)) e_{|\pi(i)|} \in \Phi^-$. Then, by definition of Φ^- one distinguishes

$$\begin{aligned} e_j - e_i \in \text{Inv}^+(\pi) \Leftrightarrow & \quad (\text{sgn}(\pi(j)) > 0 \quad \wedge \quad \text{sgn}(\pi(i)) > 0 \quad \wedge \quad |\pi(j)| < |\pi(i)|) \\ & \vee \quad (\text{sgn}(\pi(j)) < 0 \quad \wedge \quad \text{sgn}(\pi(i)) > 0) \\ & \vee \quad (\text{sgn}(\pi(j)) < 0 \quad \wedge \quad \text{sgn}(\pi(i)) < 0 \quad \wedge \quad |\pi(j)| < |\pi(i)|), \end{aligned}$$

where \wedge, \vee are the logical connectives “and” and “or”, respectively. These three cases simplify to $\pi(i) > \pi(j)$, and since $j > i$, it follows that (i, j) is a positive inversions in the sense of (2.4).

The proofs for the other two identities follow analogous arguments. □

Remark 2.3.4 Talking about inversions often includes a colloquial description as *comparing an entry to every other on its right*. Based on Figure 2.3, one might argue that some comparisons, e.g. between $\overline{\sigma_2}$ and σ_1 , are missing. However, these comparisons are completely determined by comparison of their negative versions σ_2 and $\overline{\sigma_1}$, which is taken into account by our definitions. Thus, it is reasonable to constrain to comparisons of two entries $\overline{\sigma_i}$ and σ_j if and only if $i \leq j$.

Type C_n : The root system for a Coxeter group of type C_n slightly differs from the one given for groups of type B_n . We may choose an applicable root system $\Delta \subseteq \Phi^+ \subseteq \Phi$ as

$$\begin{aligned} \{2e_1\} \cup \{e_{i+1} - e_i | 1 \leq i \leq n-1\} & \subseteq \{2e_i | 1 \leq i \leq n\} \cup \{e_j \pm e_i | 1 \leq i < j \leq n\} \\ & \subseteq \{\pm 2e_i | 1 \leq i \leq n\} \cup \{e_j \pm e_i | 1 \leq i \neq j \leq n\}. \end{aligned}$$

The height of some roots however differs from the case for type B_n . For $e_j - e_i$, the decomposition into simple roots and their height is given as before. Moreover, it is

$$e_j + e_i = 2e_1 + \sum_{\ell=1}^{i-1} (e_{\ell+1} - e_\ell) + \sum_{k=1}^{j-1} (e_{k+1} - e_k) \quad \text{and} \quad e_i = 2e_1 + 2 \sum_{k=1}^{i-1} (e_{k+1} - e_k).$$

This yields the following description of the height of $\beta \in \Phi^+$:

$$\text{ht}(\beta) = \begin{cases} j - i & \text{if } \beta = e_j - e_i, \\ 2i - 1 & \text{if } \beta = 2e_i, \\ i + j - 1 & \text{if } \beta = e_j + e_i. \end{cases}$$

Elements of Coxeter groups of type C_n can be represented by signed permutation as in type B_n . The one-line-notation for type C_n however omits the entry $\sigma(0) = 0$. This guarantees that the height of a root still equals the distance of entries which are compared in one-line notation. The inversion and descent sets are as defined for type B_n in Equations (2.7) and (2.8). Visualizations are given in Figure 2.4.

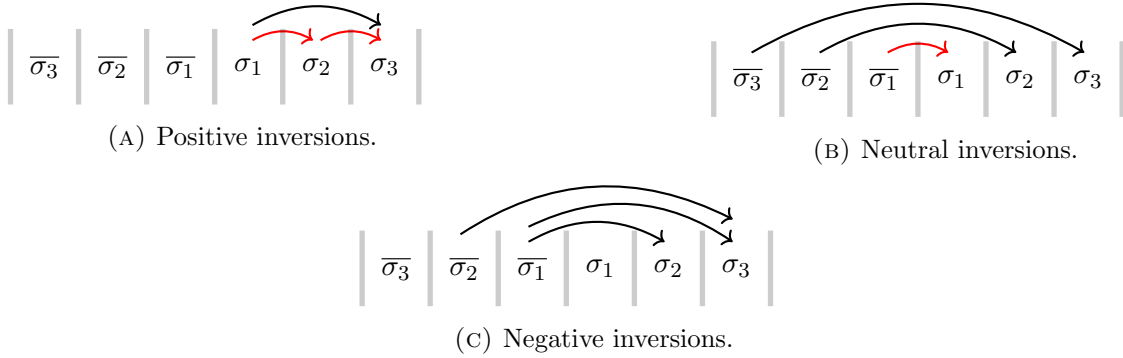


FIGURE 2.4: Visualization of inversions for a signed permutation $\sigma \in C_3$. Descents are marked in red.

Type D_n : The root system of type D_n may be realized by setting $\Delta \subseteq \Phi^+ \subseteq \Phi$ as

$$\{e_2 + e_1\} \cup \{e_{i+1} - e_i | 1 \leq i \leq n - 1\} \subseteq \{e_j \pm e_i | 1 \leq i < j \leq n\} \subseteq \{e_j \pm e_i | 1 \leq i \neq j \leq n\}.$$

The decomposition of roots of the form $e_j - e_i$ is the same as before. For the other roots, we have

$$e_j + e_i = (e_2 + e_1) + \sum_{k=2}^{j-1} (e_{k+1} - e_k) + \sum_{\ell=1}^{i-1} (e_{\ell+1} - e_\ell).$$

Thus, the height of $\beta \in \Phi^+$ in type D_n is given as

$$\text{ht}(\beta) = \begin{cases} j - i & \text{if } \beta = e_j - e_i, \\ i + j - 2 & \text{if } \beta = e_j + e_i. \end{cases}$$

The elements of Coxeter groups of type D_n can be viewed as a subset of those of type B_n with the restriction to an even number of negative entries, *i.e.*,

$$D_n = \left\{ \pi \in B_n \mid \prod_{i=1}^n \pi(i) > 0 \right\}.$$

Our choice of visualizing elements of type D_n follows the idea in [25] and is shown in Figure 2.5. The inversion set for an element $\pi \in D_n$ is given by the union of $\text{Inv}^+(\pi)$ and $\text{Inv}^-(\pi)$.

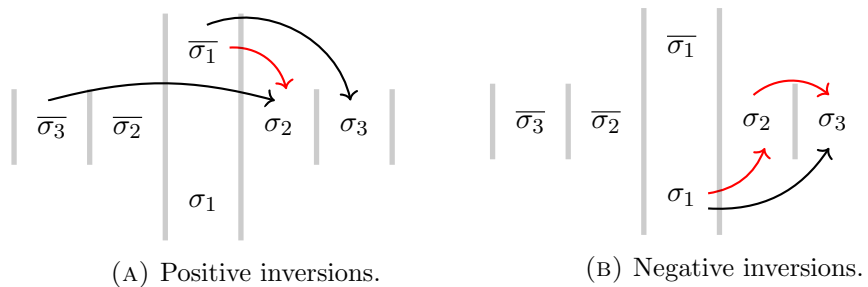


FIGURE 2.5: Visualization of inversions for a forked signed permutation $\sigma \in D_3$. Descents are marked in red.

For the descent and inversion statistics, Kahle and Stump showed a central limit for all finite Coxeter groups in [14]. Another generalization can be done by restricting the distance between permutation entries which are considered for comparisons. Such kinds of generalization were already started by Bona [7] and Pike [26] for the symmetric group by introducing d -inversions. In Chapter 3, we will define two statistics as generalizations of descents and inversion in a similar sense as in [7, 26] but in general finite Weyl groups, and prove their asymptotic normality.

Chapter 3

Probabilistic analysis of Coxeter statistics

This chapter covers the results from joint work with Christian Stump in [21]. We introduce generalized d -inversions and generalized d -descents in finite Weyl groups as natural analogues of inversions and descents in Definition 3.1.1, and give the main results in Theorem 3.1.3, 3.1.5 and Corollary 3.1.4. For this we will combine algebraic and stochastic properties and use the dependency graph method to conclude the central limit. Moreover, whenever our method is applicable we will provide a bound on the rate of convergence, see Theorem 3.1.3 and Corollary 3.4.2.

3.1 Main results

Before presenting the main results of this chapter, we will introduce generalized d -inversions and generalized d -descents in finite Weyl groups. As in Chapter 2 we will give visualization for all classical types.

3.1.1 Set-Up

As seen in Section 2.3, the distance of the permutation entries considered for comparison equals the height of the corresponding roots in the root poset. Thus, the following generalization of descents and inversions according to their height seems reasonable and will find an interpretation in one-line notation for all classical types.

Definition 3.1.1 ([21, Definition 2.4]) Let Φ be a finite crystallographic root system with

positive roots Φ^+ and let $d \in \mathbb{N}$. We set

$$\Phi_{\text{des}}^{(d)} = \{\beta \in \Phi^+ | ht(\beta) = d\} \quad \text{and} \quad \Phi_{\text{inv}}^{(d)} = \{\beta \in \Phi^+ | ht(\beta) \leq d\}. \quad (3.1)$$

A generalized d -descent of an element $w \in W$ is an inversion inside of $\Phi_{\text{des}}^{(d)}$ and a generalized d -inversion of an element $w \in W$ is an inversion inside $\Phi_{\text{inv}}^{(d)}$.

For better readability, we will drop the term generalized in the rest of this thesis. In type A, d -inversions coincide with the generalized descents defined by Bona [7] and Pike [26]. However, we refer to this statistic as d -inversions to emphasize that it involves multiple comparisons. We decided to use the expression d -descents to describe a statistic which does not seem to be investigated yet.

These statistics generalize the known inversions and descents in such a way that if $d = 1$, the d -descents and d -inversions match the definition of descents. Moreover, if $d = h - 1$, with h being the Coxeter number and thus $h - 1$ the height of the root poset, d -inversions are the same as usual inversions.

The comparisons of permutation entries taken into account for the statistics of d -descents and d -inversions can be visualized for classical Weyl groups as follows.

Type A_n : Given the root system for A_n as before. For $n = 4$ and $d = 2$, we have

$$\Phi_{\text{des}}^{(2)} = \{[13], [24], [35]\} \quad \text{and} \quad \Phi_{\text{inv}}^{(2)} = \{[12], [23], [34], [45], [13], [24], [35]\}.$$

The set of d -descents now only considers comparisons of entries with distance exactly two (see Figure 3.1 left). The set of d -inversions considers all comparisons with a distance at most 2 (see Figure 3.1 right).

We continue by giving visualizations for d -descents in other classical types. Due to complexity, we will refrain from pictorial descriptions of d -inversions in other types than A_n .

Types B_n , C_n , and D_n : Using the root system for the classical types as given before. With $n = 4$ and $d = 3$, we have

$$\Phi_{\text{des}}^{(3)} = \{[\tilde{1}2], [3], [14]\} \quad , \quad \Phi_{\text{des}}^{(3)} = \{[2], [\tilde{1}3], [14]\} \quad , \quad \Phi_{\text{des}}^{(3)} = \{[\tilde{1}4], [\tilde{2}3], [14]\}.$$

for B_4 , C_4 and D_4 , respectively. These sets indicate that permutation entries of distance 3 are compared. However, these comparisons are subject to the additional restriction that $\bar{\sigma}_i$ and σ_j are compared if and only if $i < j$ (see Remark 2.3.4). Relevant comparisons are illustrated using the respective visualizations for permutations of these groups in Figure 3.2.

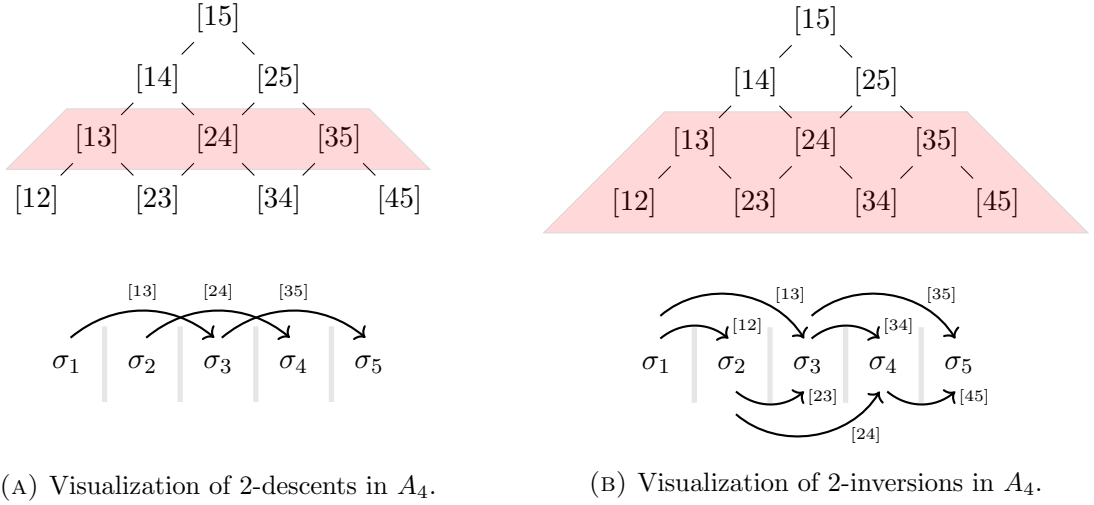


FIGURE 3.1: Top: Root poset of type A_4 with highlighted roots of $\Phi_{\text{des}}^{(2)}$ (left) and $\Phi_{\text{inv}}^{(2)}$ (right). Bottom: One line notation of $\sigma \in \mathfrak{S}_5$ with marked comparisons according to the subset of roots described above.

After having defined generalized d -descents and d -inversions in terms of roots, we now define their related random variables. Let $\beta \in \Phi^+$ and define the corresponding Bernoulli random variable, *i.e.*, a random variable only taking values 0 and 1, as an indicator, whether β is an inversion of an element w chosen uniformly at random in W . More formally, this is

$$\mathcal{X}_\beta(w) = \begin{cases} 1 & \text{if } w(\beta) \in \Phi^- , \\ 0 & \text{if } w(\beta) \in \Phi^+ . \end{cases} \quad (3.2)$$

Another way describing this Bernoulli random variable is

$$\mathbb{P}[\mathcal{X}_\beta = 1] = \frac{|\{w \in W \mid w(\beta) \in \Phi^-\}|}{|W|}, \quad \mathbb{P}[\mathcal{X}_\beta = 0] = \frac{|\{w \in W \mid w(\beta) \in \Phi^+\}|}{|W|}. \quad (3.3)$$

Given a subset $\Psi \subseteq \Phi^+$, we set $\mathcal{X}_\Psi(w) = \sum_{\beta \in \Psi} \mathcal{X}_\beta(w)$. Then \mathcal{X}_Ψ counts the number of inversions of w within a given subset Ψ .

For example, one may think of Ψ as the set of simple roots which would result in the statistic of descents. When $\Psi = \Phi^+$ is the entire set of positive roots, then \mathcal{X}_Ψ is the number of inversions. We are interested in what other choices of Ψ might lead to a central limit of \mathcal{X}_Ψ . One necessary restriction is given by $|\Psi| \rightarrow \infty$. However, this is not the only limitation as the following example shows.

Example 3.1.2 ([21, Example 2.3]) Let Φ be the root system of type A_{n-1} as before and

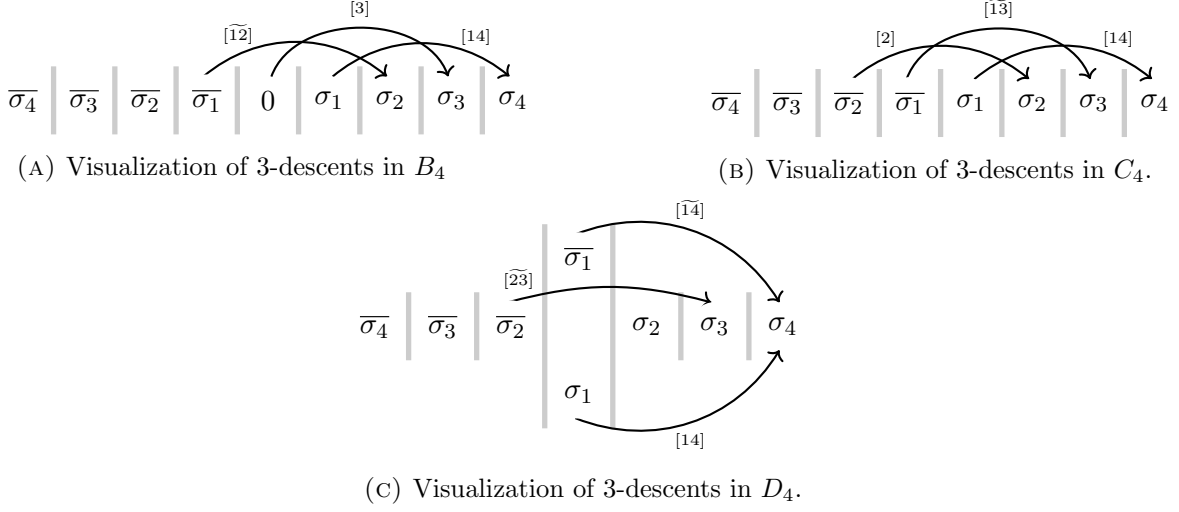


FIGURE 3.2: Visualization of 3-descents in different Weyl groups using their respective one-line notation.

consider

$$\Psi^{(n)} = \{e_i - e_1 \mid 2 \leq i \leq n\} \subseteq \Phi^+.$$

This clearly implies $|\Psi^{(n)}| \rightarrow \infty$ as n tends to infinity. Since we've seen that $e_i - e_1$ corresponds to the comparisons of the i -th and 1st entry of a permutation $\pi \in \mathfrak{S}_n$, it is

$$\mathcal{X}_{\Psi^{(n)}}(\pi) = |\{i \mid 2 \leq i \leq n \text{ and } \pi(i) > \pi(1)\}| = \pi(1) - 1.$$

This implies that $\mathcal{X}_{\Psi^{(n)}}$ does not have a central limit since it is uniformly distributed with

$$\mathbb{P}(\mathcal{X}_{\Psi^{(n)}}(\pi) = k) = \frac{1}{n-1}$$

for all $0 \leq k \leq n-1$ and $n \in \mathbb{N}_{\geq 2}$.

3.1.2 Central limit theorems

Having the probabilistic description for the statistic of d -descents and d -inversions at hand, we are able to state our main results. We start with a result concerning asymptotic normality of antichains, which easily implies the corresponding result for d -descents.

Theorem 3.1.3 ([21, Theorem 2.6]) *Let $\{\Phi^{(n)}\}_{n \geq 1}$ be a sequence of finite crystallographic root systems and let $\{\Psi^{(n)}\}_{n \geq 1}$ be a sequence of antichains with $\Psi^{(n)} \subset \Phi^{(n)}$ and $|\Psi^{(n)}| \rightarrow \infty$. The corresponding random variable $\mathcal{X}_{\Psi^{(n)}}$ is then asymptotically normal. The rate of convergence in distribution towards the standard Gaussian distribution is bounded by $|\Psi^{(n)}|^{-1/2}$.*

Since roots of the same height are pairwise incomparable, the sets $\Phi_{\text{des}}^{(d)}$ are antichains for any d . The desired central limit for d -descents follows directly.

Corollary 3.1.4 ([21, Corollary 2.7]) *Let $\{\Phi^{(n)}\}_{n \geq 1}$ be a sequence of finite crystallographic root systems and let $\{d_n\}_{n \geq 1}$ be a sequence of integers such that $|\Phi_{\text{des}}^{(d_n)}| \rightarrow \infty$. The corresponding random variable $\mathcal{X}_{\Phi_{\text{des}}^{(d_n)}}$ is then asymptotically normal with its rate of convergence bounded by $|\Phi_{\text{des}}^{(d_n)}|^{-1/2}$.*

The proof of Theorem 3.1.3 provided in this thesis makes use of the dependency graph method. However, the same result can be obtained by a result of Sommers [31], together with a result of Kahle and Stump [14]. Providing a detailed alternative proof using the dependency graph method will add information on bounds on the rate of convergence.

Next, we will state the analogous result for d -inversions. However, we will give bounds on the rate of convergence in a separate corollary.

Theorem 3.1.5 ([21, Theorem 2.8]) *Let $\{\Phi^{(n)}\}_{n \geq 1}$ be a sequence of finite crystallographic root systems and let $\{d_n\}_{n \geq 1}$ be a sequence of integers such that $|\Phi_{\text{inv}}^{(d_n)}| \rightarrow \infty$. The corresponding random variable $\mathcal{X}_{\Phi_{\text{inv}}^{(d_n)}}$ is then asymptotically normal.*

The bound on the rate of convergence is strongly dependent on the ranks of the root systems and their relation to $\{d_n\}_{n \geq 1}$. The following corollary provides bounds on the rates of convergence whenever our used method is applicable. Without loss of generality, we assume that for all n every root poset $\Phi^{(n)}$ contains at least one root of height d_n .

Corollary 3.1.6 ([21, Corollary 2.9]) *Let r_n be the rank of $\Phi^{(n)}$ and let $\Phi^{(n)} = \bigcup_i \Phi_i$ be the decomposition into its irreducible components. Set*

- r_A to be the rank of the union of those components Φ_i for which $\text{rk}(\Phi_i) < d_n$,
- r_B to be the rank of the union of those components Φ_i for which $d_n \leq \text{rk}(\Phi_i) \leq d_n^2$, and
- r_C to be the rank of the union of those components Φ_i for which $d_n^2 < \text{rk}(\Phi_i)$.

We then have the following bounds on the rates of convergence:

- if r_A grows linearly in r_n , we have the bound $r_n^{-1/2}$,
- if r_B grows linearly in r_n and d_n grows faster than $r_n^{2/3}$, we have the bound $r_n \cdot d_n^{-3/2}$,
- if r_C grows linearly in r_n and d_n grows slower than $r_n^{1/3}$, we have the bound $r_n^{-1/2} \cdot d_n^{3/2}$.

Given these bounds on the rate of convergence and assuming that $\Phi^{(n)}$ is irreducible, we can confirm the rate of convergence which were already observed in the case of the symmetric

group in [26].

To conclude this section, we will give an overview on the following sections. The asymptotic normality for d -descents as stated in Corollary 3.1.4 will follow from a more general result in Theorem 3.1.3 about antichains. Known Coxeter-theoretic results are used to provide an alternative proof of this theorem, which also provides rate of convergence. Although concrete variances of d -descents are not needed, they are stated in Section 3.3 for classical types.

Unfortunately, we do not have a general consideration for d -inversions. The concrete formulas for their variances in classical types are given in Theorem 3.3.1, 3.3.5, 3.3.13 and 3.3.14. Based on these, a lower bound will be deduced in Lemma 3.4.6. The dependency graph method then provides the asymptotic normality and, whenever possible, bounds on the rate of convergence.

The attempt to interpret d -inversions as a special case of *order ideals* in the root poset, *i.e.*, subsets $\Psi \subseteq \Phi^+$ such that $\beta \leq \gamma \in \Psi$ implies $\beta \in \Psi$, failed in providing a counter example in terms of a sequence which does not have a central limit, as well as in providing a more general reason to always having a central limit. We state this as an open problem.

Question. *Do sequences of order ideals of increasing cardinality always have a central limit?*

3.2 Random inversions for finite root systems

The aim of this section is to understand the interaction between random variables \mathcal{X}_β with $\beta \in \Phi^+$. The two main results are Theorem 3.2.1, exhibiting a connection between the covariance as a probabilistic statement and Coxeter-theoretic assertions, and Theorem 3.2.7, describing the independence of two distinct sets of random variables and thereby preparing for the later use of the dependency graph method.

Theorem 3.2.1 ([21, Theorem 3.1]) *Let $\beta, \gamma \in \Phi^+$ and \mathcal{X}_β and \mathcal{X}_γ as in (3.2). We then have*

$$\text{Cov}(\mathcal{X}_\beta, \mathcal{X}_\gamma) = \pm \left(\frac{1}{4} - \frac{1}{2 \cdot \text{ord}(\beta, \gamma)} \right),$$

with the sign being positive if $\langle \beta, \gamma \rangle \geq 0$ and negative if $\langle \beta, \gamma \rangle \leq 0$. In particular, \mathcal{X}_β and \mathcal{X}_γ are independent if and only if β and γ are orthogonal.

Remark 3.2.2 ([21, Remark 3.2]) *Instead of the order, one may use the angle between the two positive roots to describe the covariance. For $\beta, \gamma \in \Phi^+$, the angle is*

$$\varphi = \angle(\beta, \gamma) = \arccos \left(\frac{\langle \beta, \gamma \rangle}{|\beta| \cdot |\gamma|} \right),$$

and thus

$$\text{Cov}(\mathcal{X}_\beta, \mathcal{X}_\gamma) = \frac{1}{4} - \frac{\varphi}{2\pi}.$$

This avoids the case distinction based on the inner product.

We start preparing for the proof of Theorem 3.2.1 by partitioning the Weyl group W depending on the property of changing the sign of positive roots $\beta, \gamma \in \Phi^+$. For given signs $\varepsilon, \delta \in \{+, -\}$, we define

$$W^{(\varepsilon\delta)}(\beta, \gamma) = \{w \in W \mid \varepsilon \cdot w(\beta) \in \Phi^+, \delta \cdot w(\gamma) \in \Phi^+\} \subseteq W$$

as those elements in the Weyl group that send a pair of positive roots β and γ to positive or negative roots depending on the given signs ε, δ , respectively. We are only interested in the relation of the cardinalities of these four sets and state them in the following proposition.

Proposition 3.2.3 ([21, Proposition 3.4]) *Let $\beta, \gamma \in \Phi^+$. Then*

$$\begin{aligned} |W^{(++)}(\beta, \gamma)| &= |W^{(--) }(\beta, \gamma)|, \\ |W^{(+-)}(\beta, \gamma)| &= |W^{(-+)}(\beta, \gamma)|. \end{aligned}$$

If in addition $\beta \neq \gamma$, then

$$\begin{aligned} |W^{(++)}(\beta, \gamma)| &= (\text{ord}(\beta, \gamma) - 1) \cdot |W^{(+-)}(\beta, \gamma)| \text{ if } \langle \beta, \gamma \rangle \geq 0, \\ |W^{(+-)}(\beta, \gamma)| &= (\text{ord}(\beta, \gamma) - 1) \cdot |W^{(++)}(\beta, \gamma)| \text{ if } \langle \beta, \gamma \rangle \leq 0. \end{aligned}$$

This implies equal cardinality of all four sets if and only if β and γ are orthogonal

The idea of this proof is to break it down to the two dimensional subspace $\text{span}\{\beta, \gamma\}$ and the parabolic subgroup generated by simple roots related to β and γ . For this, it is of importance that the random variable \mathcal{X}_β , *i.e.*, the property of an element changing the sign of β , only depends on elements of the parabolic subgroup.

Lemma 3.2.4 ([21, Lemma 3.5]) *Let $\Gamma \subseteq \Delta$ and let $w = w^\Gamma \cdot w_\Gamma \in W$ be the unique parabolic decomposition of w . For any $\beta \in \Phi_\Gamma^+$, it then holds that*

$$w(\beta) \in \Phi^+ \iff w_\Gamma(\beta) \in \Phi^+.$$

Proof. By the definition of positive roots, every root in Φ_Γ^+ is a nonnegative linear combination of elements in Γ . Hence, elements of the parabolic quotient W^Γ keep such roots positive, *i.e.*, $w^\Gamma(\Phi_\Gamma^+) \in \Phi^+$.

First, let $w_\Gamma(\beta) \in \Phi^+$. Since $\beta \in \Phi_\Gamma^+$, it easily follows that $w_\Gamma(\beta) \in \Phi_\Gamma^+$. Applying an

element of the parabolic quotient generated by Γ , it is $w(\beta) = w^\Gamma(w_\Gamma(\beta)) \in \Phi^+$. Second, let $w_\Gamma(\beta) \notin \Phi^+$. Then $w_\Gamma(\beta) \in \Phi_\Gamma^-$, and reuse of the above argument leads to $w(\beta) = w^\Gamma(w_\Gamma(\beta)) \in \Phi^-$. \square

Using Lemma 3.2.4, we check that the random variable \mathcal{X}_β indeed only depends on the parabolic root subsystem which contains β .

Corollary 3.2.5 ([21, Corollary 3.6]) *Let $\Gamma \subseteq \Delta$ and W_Γ its parabolic subgroup. For $\beta \in \Phi_\Gamma^+$, the random variable \mathcal{X}_β is independent of whether it is considered on W or on W_Γ .*

Proof. Since \mathcal{X}_β is a Bernoulli random variable, it is enough to check that

$$\begin{aligned} \mathbb{P}[\mathcal{X}_\beta = 1] &= \frac{|\{w \in W \mid w(\beta) \in \Phi^-\}|}{|W|} = \frac{|W^\Gamma| \cdot |\{w \in W_\Gamma \mid w(\beta) \in \Phi^-\}|}{|W^\Gamma| \cdot |W_\Gamma|} \\ &= \frac{|\{w \in W_\Gamma \mid w(\beta) \in \Phi^-\}|}{|W_\Gamma|}. \end{aligned} \quad \square$$

After Corollary 3.2.5, we can use Lemma 3.2.4 to prove Proposition 3.2.3.

Proof of Proposition 3.2.3. Starting with the first two identities. We write w_\circ for the longest element of W . The map $w \mapsto w_\circ \cdot w$ is known to be a bijection on W interchanging inversions and non-inversions,

$$\text{Inv}(w_\circ \cdot w) = \Phi^+ \setminus \text{Inv}(w).$$

For elements of the given sets, it is

$$w \in W^{(\varepsilon, \delta)} \Leftrightarrow w_\circ \cdot w \in W^{(-\varepsilon, -\delta)}.$$

For proving the other two identities, let $\text{span}\{\beta, \gamma\}$ be the linear subspace of V spanned by the two positive roots $\beta, \gamma \in \Phi^+$. Then, one can find simple roots $\Gamma = \{\alpha, \alpha'\} \subseteq \Delta$ such that

$$w(\text{span}\{\beta, \gamma\}) = \text{span}(\Gamma),$$

for some element $w \in W$. In particular, $w(\beta), w(\gamma) \in \Phi_\Gamma^+$. Note that $W = w \cdot W$ is a bijection on W , and since we are only interested in the cardinalities, we may assume $w = e$ and $\beta, \gamma \in \Phi_\Gamma^+$. By Lemma 3.2.4, it holds that

$$W^{(\varepsilon, \delta)}(\beta, \gamma) = W^\Gamma \times W_\Gamma^{(\varepsilon, \delta)}(\beta, \gamma).$$

This simplifies the anticipated equalities to statements regarding groups of dihedral type only.

Thus,

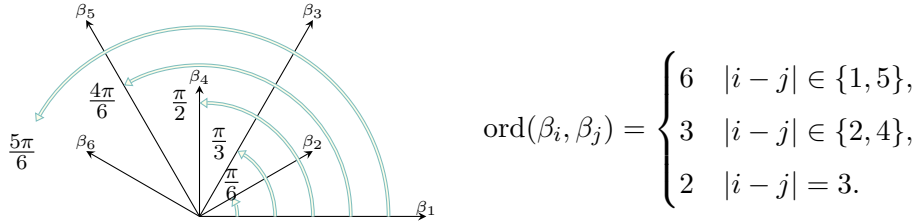
$$\begin{aligned} |W^{(++)}(\beta, \gamma)| &= (\text{ord}(s_\beta s_\gamma) - 1) \cdot |W^{(+-)}(\beta, \gamma)| \text{ if } \langle \beta, \gamma \rangle \geq 0, \\ |W^{(+-)}(\beta, \gamma)| &= (\text{ord}(s_\beta s_\gamma) - 1) \cdot |W^{(++)}(\beta, \gamma)| \text{ if } \langle \beta, \gamma \rangle \leq 0 \end{aligned}$$

need to be checked for types $A_1 \times A_1, A_2, B_2, C_2, G_2$ to conclude the proposition. \square

Example 3.2.6 ([21, Example 3.7]) Consider the Weyl group W of type G_2 , with simple reflections $\mathcal{S} = \{s, t\}$ and the set of all reflections

$$\mathcal{R} = \{s, sts, ststs, tstst, tst, t\}.$$

For a set of positive roots $\Phi^+ = \{\beta_1, \dots, \beta_6\}$ we write $s_{\beta_1}, \dots, s_{\beta_6}$ in the same order. Given the root system of G_2 one can deduce $\text{ord}(\beta_i, \beta_j)$.



Investigating the explicit inversion set of elements in G_2 we get

$$\begin{aligned} \text{Inv}(e) &= \{\} & \text{Inv}(ststst) &= \{\beta_1, \beta_2, \beta_3, \beta_4, \beta_5, \beta_6\} \\ \text{Inv}(s) &= \{\beta_1\} & \text{Inv}(tstst) &= \{\beta_2, \beta_3, \beta_4, \beta_5, \beta_6\} \\ \text{Inv}(st) &= \{\beta_1, \beta_2\} & \text{Inv}(tsts) &= \{\beta_3, \beta_4, \beta_5, \beta_6\} \\ \text{Inv}(sts) &= \{\beta_1, \beta_2, \beta_3\} & \text{Inv}(tst) &= \{\beta_4, \beta_5, \beta_6\} \\ \text{Inv}(stst) &= \{\beta_1, \beta_2, \beta_3, \beta_4\} & \text{Inv}(ts) &= \{\beta_5, \beta_6\} \\ \text{Inv}(ststs) &= \{\beta_1, \beta_2, \beta_3, \beta_4, \beta_5\} & \text{Inv}(t) &= \{\beta_6\} \end{aligned}$$

and obtain for example for β_2 and β_4 the following decomposition

$$\begin{aligned} W^{(++)}(\beta_2, \beta_4) &= \{e, s, ts, t\}, & W^{(+-)}(\beta_2, \beta_4) &= \{tsts, tst\}, \\ W^{(--) }(\beta_2, \beta_4) &= \{stst, ststs, ststst, tstst\}, & W^{(-+)}(\beta_2, \beta_4) &= \{st, sts\}. \end{aligned}$$

One easily checks with $\langle \beta_2, \beta_4 \rangle > 0$ that

$$\begin{aligned} |W^{(++)}(\beta_2, \beta_4)| &= |W^{(--) }(\beta_2, \beta_4)|, & |W^{(+-)}(\beta_2, \beta_4)| &= |W^{(-+)}(\beta_2, \beta_4)|, \\ |W^{(++)}(\beta_2, \beta_4)| &= \underbrace{(\text{ord}(\beta_2, \beta_4) - 1)}_{=3} \cdot |W^{(+-)}(\beta_2, \beta_4)|. \end{aligned}$$

We are finally able to prove Theorem 3.2.1. For this, we express the covariance in terms of

expected values and use the decomposition of W in Proposition 3.2.3 to write it as a function of $\text{ord}(\beta, \gamma)$.

Proof of Theorem 3.2.1. We write

$$\begin{aligned} \text{Cov}(\mathcal{X}_\beta, \mathcal{X}_\gamma) &= \mathbb{E}[\mathcal{X}_\beta \cdot \mathcal{X}_\gamma] - \mathbb{E}[\mathcal{X}_\beta] \cdot \mathbb{E}[\mathcal{X}_\gamma] = \mathbb{P}[\mathcal{X}_\beta = \mathcal{X}_\gamma = 1] - \frac{1}{4} \\ &= \frac{|W^{(-)}(\beta, \gamma)|}{|W|} - \frac{1}{4}. \end{aligned}$$

By the first two equalities in Proposition 3.2.3, the denominator of the first term can be rewritten, such that

$$\text{Cov}(\mathcal{X}_\beta, \mathcal{X}_\gamma) = \frac{|W^{(-)}(\beta, \gamma)|}{2 \cdot (|W^{(-)}(\beta, \gamma)| + |W^{(+-)}(\beta, \gamma)|)} - \frac{1}{4}.$$

First let $\beta = \gamma$. Then $W^{(+-)}(\beta, \gamma) = \emptyset$ and we can conclude $\text{Cov}(\mathcal{X}_\beta, \mathcal{X}_\gamma) = \mathbb{V}[X_\beta] = \frac{1}{4}$.

Now let $\beta \neq \gamma$ and assume $\langle \beta, \gamma \rangle \leq 0$. The fourth equality in Proposition 3.2.3 then gives

$$\begin{aligned} \text{Cov}(\mathcal{X}_\beta, \mathcal{X}_\gamma) &= \frac{|W^{(-)}(\beta, \gamma)|}{2 \cdot (|W^{(-)}(\beta, \gamma)| + (\text{ord}(\beta, \gamma) - 1) \cdot |W^{(-)}(\beta, \gamma)|)} - \frac{1}{4} \\ &= \frac{1}{2 \cdot \text{ord}(\beta, \gamma)} - \frac{1}{4}, \end{aligned}$$

as stated. For $\langle \beta, \gamma \rangle \geq 0$, one uses the third equality in Proposition 3.2.3 for analogous calculations. \square

The last statement in this chapter deals with the independence of two orthogonal sets of roots. We call $\Psi, \Psi' \subseteq \Phi^+$ *orthogonal* if and only if $\text{ord}(\beta, \gamma) = 2$ for all $\beta \in \Psi$ and $\gamma \in \Psi'$. Moreover, let $A = \{A_i\}_{i=1}^m$ and $B = \{B_i\}_{i=1}^k$ be two finite sets of random variables with vectors of possible outcomes $a = (a_1, \dots, a_m)$ and $b = (b_1, \dots, b_k)$, respectively. We call A and B *independent* if and only if $\mathbb{P}[A = a, B = b] = \mathbb{P}[A = a] \mathbb{P}[B = b]$. If $\mathbb{P}[B = b] \neq 0$, this is equivalent to $\mathbb{P}[A = a \mid B = b] = \mathbb{P}[A = a]$. The independence of orthogonal sets of random variables is a necessary property for the later use of the dependency graph method. Its proof uses the unique decomposition of W into a parabolic subgroup and parabolic quotient similar to the proof of Proposition 3.2.3.

Theorem 3.2.7 *Let $\Psi, \Psi' \subseteq \Phi^+$. If Ψ and Ψ' are orthogonal, then the sets $\{\mathcal{X}_\beta\}_{\beta \in \Psi}$ and $\{\mathcal{X}_\gamma\}_{\gamma \in \Psi'}$ of random variables are independent.*

Proof of Theorem 3.2.7. Let $\Psi, \Psi' \subseteq \Phi^+$ be two orthogonal sets of roots. As in the proof of

Proposition 3.2.3, there exists an element $w \in W$ such that

$$w(\text{span}(\Psi)) = \text{span}(\Gamma),$$

for some simple roots $\Gamma \subseteq \Delta$. Since W preserves the inner product on V , it keeps $w(\Psi')$ in the orthogonal complement of $\text{span}(\Gamma)$.

We aim to prove independence for the sets $\{\mathcal{X}_\beta\}_{\beta \in \Psi}$ and $\{\mathcal{X}_\gamma\}_{\gamma \in \Psi'}$. To shorten notation, let $\mathcal{X} = \{\mathcal{X}_\beta\}_{\beta \in \Psi}$ and $\mathcal{X}' = \{\mathcal{X}_\gamma\}_{\gamma \in \Psi'}$. We only need to show

$$\mathbb{P}[\mathcal{X}' = \delta \mid \mathcal{X} = \varepsilon] = \mathbb{P}[\mathcal{X}' = \delta]$$

for any fixed outcomes $\varepsilon \in \{0, 1\}^{|\Psi|}$ and $\delta \in \{0, 1\}^{|\Psi'|}$. As already seen in Lemma 3.2.4, the outcome of \mathcal{X} depends only on the parabolic subgroup W_Γ . On the other hand, since the random variables of \mathcal{X}' live in the orthogonal complement of $\text{span}(\Gamma)$, the outcome $\mathcal{X}' = \delta$ only depends on the parabolic quotient W^Γ and is fixed pointwise by W_Γ .

We will provide precise calculations to support our argumentation. For better readability, we write

$$\varepsilon \cdot w(\Psi) \in \Phi^- \quad \text{if for all } \beta \in \Psi \text{ we have } \begin{cases} w(\beta) \in \Phi^- & \text{if } \varepsilon(\beta) = 1, \\ w(\beta) \in \Phi^+ & \text{if } \varepsilon(\beta) = 0, \end{cases}$$

and analogously $\delta \cdot w(\Psi') \in \Phi^-$.

We then can conclude, by the properties of W_Γ and W^Γ described above,

$$\begin{aligned} \mathbb{P}[\mathcal{X}' = \delta \mid \mathcal{X} = \varepsilon] &= \frac{\mathbb{P}[\mathcal{X}' = \delta, \mathcal{X} = \varepsilon]}{\mathbb{P}[\mathcal{X} = \varepsilon]} = \frac{|\{w \in W \mid \varepsilon \cdot w(\Psi) \in \Phi^-, \delta \cdot w(\Psi') \in \Phi^-\}|}{|\{w \in W \mid \varepsilon \cdot w(\Psi) \in \Phi^-\}|} \\ &= \frac{|\{w^\Gamma \in W^\Gamma, w_\Gamma \in W_\Gamma \mid \varepsilon \cdot w_\Gamma(\Psi) \in \Phi^-, \delta \cdot w^\Gamma(\Psi') \in \Phi^-\}|}{|W^\Gamma| \cdot |\{w_\Gamma \in W_\Gamma \mid \varepsilon \cdot w_\Gamma(\Psi) \in \Phi^-\}|} \\ &= \frac{|\{w \in W^\Gamma \mid \delta \cdot w(\Psi') \in \Phi^-\}|}{|W^\Gamma|} \\ &= \frac{|\{w \in W \mid \delta \cdot w(\Psi') \in \Phi^-\}|}{|W|} \\ &= \mathbb{P}[\mathcal{X}' = \delta]. \end{aligned} \quad \square$$

3.3 Concrete variances

In this chapter, we provide concrete formulas for the variances of d -descents and d -inversions in all irreducible types A, B, C and D . Calculations for type A will be done in great detail, whereas analogous considerations for all other types will be suppressed. The concrete

variances for d -descents are not further used but are provided for its own sake. Explicit calculations of the variance for d -inversions are necessary to conclude a lower bound for the variance in Lemma 3.4.6. This is needed to finally derive the asymptotic normality as claimed in Theorem 3.1.5.

3.3.1 Type A_{n-1}

In this section, we provide the variances for d -descents and d -inversions of type A_{n-1} , which depend on the relation between d and n . The results for d -inversions are already known from [26, Theorem 1].

Theorem 3.3.1 ([21, Theorem 4.1]) *Let \mathcal{X}_Ψ as in (3.2) and $\Phi_{\text{des}}^{(d)}, \Phi_{\text{inv}}^{(d)}$ as in (3.1). For $d < n$ we have*

$$\mathbb{V}[\mathcal{X}_{\Phi_{\text{des}}^{(d)}}] = \begin{cases} \frac{1}{12}(n+d) & \text{if } 2d \leq n, \\ \frac{1}{4}(n-d) & \text{if } 2d \geq n. \end{cases}$$

$$\mathbb{V}[\mathcal{X}_{\Phi_{\text{inv}}^{(d)}}] = \begin{cases} \frac{1}{18}d^3 + \frac{1}{24}d^2 + (\frac{1}{12}n - \frac{1}{72})d & \text{if } 2d \leq n, \\ -\frac{1}{6}d^3 + (\frac{1}{3}n - \frac{7}{24})d^2 + (-\frac{1}{6}n^2 + \frac{5}{12}n - \frac{1}{8})d + (\frac{1}{36}n^3 - \frac{1}{12}n^2 + \frac{1}{18}n) & \text{if } 2d \geq n. \end{cases}$$

We have divided the proof into a sequence of lemmas. We first set

$$N_a = \{\beta \in \Phi^+ \mid \text{ht}(\beta) = a\} = \{[ij] \mid 1 \leq i < j = i + a \leq n\}$$

for $1 \leq a \leq n-1$. The set N_a then contains all positive roots of height a and we partition the set of positive roots according to their height, *i.e.* $\Phi^+ = N_1 \cup N_2 \cup \dots \cup N_{n-1}$.

The following lemma describes the cardinality of these sets, *i.e.* the number of roots of a given height.

Lemma 3.3.2 ([21, Lemma 4.2]) *We have*

$$N_a \neq \emptyset \iff 1 \leq a < n \quad \text{and} \quad |N_a| = n - a \text{ for } 1 \leq a < n.$$

Proof. One may rewrite $N_a = \{[i, i+a] \mid 1 \leq i \leq n-a\}$, from which we can easily conclude the stated cardinalities. \square

For positive roots $[ij]$ and their corresponding reflections $s_{[ij]}$, one can check

$$\begin{aligned} \langle [ij], [ik] \rangle, \langle [ji], [ki] \rangle &> 0, \\ \langle [ji], [ik] \rangle, \langle [ij], [ki] \rangle &< 0, \end{aligned} \quad \text{and} \quad \text{ord}(s_{[ij]}s_{[k\ell]}) = \begin{cases} 1 & \text{if } |\{i, j\} \cap \{k, \ell\}| = 2, \\ 2 & \text{if } |\{i, j\} \cap \{k, \ell\}| = 0, \\ 3 & \text{if } |\{i, j\} \cap \{k, \ell\}| = 1, \end{cases}$$

by identifying reflections $s_{[ij]} = (i, j)$ as transpositions on the symmetric group.

With Theorem 3.2.1, we can conclude that the covariance of $\mathcal{X}_{[ij]}, \mathcal{X}_{[k\ell]}$ is zero if and only if $\{i, j\} \cap \{k, \ell\} = \emptyset$. If $k \neq j$ we have

$$\text{Cov}(\mathcal{X}_{[ij]}, \mathcal{X}_{[ik]}) = \text{Cov}(\mathcal{X}_{[ji]}, \mathcal{X}_{[ki]}) = \frac{1}{12}, \quad \text{Cov}(\mathcal{X}_{[ji]}, \mathcal{X}_{[ik]}) = \text{Cov}(\mathcal{X}_{[ij]}, \mathcal{X}_{[ki]}) = -\frac{1}{12}. \quad (3.4)$$

In order to compute the variance we are interested in the number of pairs with non-zero covariances. These are provided in the following lemma.

Lemma 3.3.3 ([21, Lemma 4.3]) *For $1 \leq a, b < n$, we have*

$$\begin{aligned} \left| \{[ij], [k\ell] \in N_a \times N_b \mid i = k, j \neq \ell\} \right| &= \left| \{[ij], [k\ell] \in N_a \times N_b \mid i \neq k, j = \ell\} \right| \\ &= \begin{cases} n - \max\{a, b\} & a \neq b, \\ 0 & a = b, \end{cases} \end{aligned}$$

for the number of pairs with positive covariance and

$$\begin{aligned} \left| \{[ij], [k\ell] \in N_a \times N_b \mid i = \ell, j \neq k\} \right| &= \left| \{[ij], [k\ell] \in N_a \times N_b \mid j = k, i \neq \ell\} \right| \\ &= n - \min\{n, a + b\} \end{aligned}$$

for the number of pairs with negative covariance.

Proof. First, we observe that if $a = b$, the two sets in the first equality are empty. For all other cases, we use

$$N_c = \{[i, i + c] \mid 0 < i \leq n - c\} = \{[j - c, j] \mid c < j \leq n\}$$

as an alternative description for N_a and N_b to obtain the given counting formulas. As an example, we may write

$$\begin{aligned}
 \left| \{[ij], [k\ell] \in N_a \times N_b \mid i = k, j \neq \ell\} \right| &= \left| \{[ij], [i\ell] \in N_a \times N_b \mid j \neq \ell\} \right| \\
 &= \left| \{[i, i+a], [i, i+b] \in N_a \times N_b \mid \right. \\
 &\qquad \qquad \qquad \left. 0 < i \leq \min\{n-a, n-b\}\} \right| \\
 &= n - \max\{a, b\}. \quad \square
 \end{aligned}$$

Given the number of pairs with non-zero covariances depending on the height of these roots, we can conclude the concrete variances for type A .

Proof of Theorem 3.3.1. Combining Lemma 3.3.2, 3.3.3 and Equation (3.4), we obtain for $a = b = d$ that

$$\mathbb{V}[\mathcal{X}_{\Phi_{\text{des}}^{(d)}}] = \frac{1}{4}|N_d| - \frac{2}{12}(n - \min\{n, 2d\}).$$

This is equivalent to the two cases given for $\mathbb{V}[\mathcal{X}_{\Phi_{\text{des}}^{(d)}}]$. For the variance of d -inversions, we have

$$\mathbb{V}[\mathcal{X}_{\Phi_{\text{inv}}^{(d)}}] = \frac{1}{4} \sum_{1 \leq a \leq d} |N_a| + \frac{2}{12} \sum_{1 \leq a \neq b \leq d} (n - \max\{a, b\}) - \frac{2}{12} \sum_{1 \leq a, b \leq d} (n - \min\{n, a+b\}),$$

where the first term comes from the single variances of $\mathcal{X}_{[ij]}$ for all $[ij] \in \Phi_{\text{inv}}^{(d)}$. The second sum contains the covariances for pairs of random variables $(\mathcal{X}_{[ij]}, \mathcal{X}_{[ik]})$. It can be rewritten as

$$\sum_{1 \leq a \neq b \leq d} (n - \max\{a, b\}) = 2 \cdot \sum_{1 \leq a < b \leq d} (n - b) = 2 \cdot \left(-\frac{1}{6}(d-1)d(2d-3n+2) \right).$$

The third sum combines the covariances for pairs of random variables $(\mathcal{X}_{[ij]}, \mathcal{X}_{[ki]})$. We first note that the summands are zero for $a+b \geq n$. Thus, we may rewrite the sum as

$$\sum_{1 \leq a, b \leq d} (n - \min\{n, a+b\}) = \sum_{\substack{1 \leq a, b \leq d \\ a+b \leq n}} (n - (a+b)) = \sum_{1 \leq a \leq d} \sum_{1 \leq b \leq \min\{n-a, d\}} (n - (a+b)).$$

We start with the first case of $2d \leq n$. Since $a, b \leq d$, it is $d \leq n-a$, and we can simplify the second sum of the last expression to obtain

$$\sum_{1 \leq a, b \leq d} (n - \min\{n, a+b\}) = \sum_{1 \leq a \leq d} \sum_{1 \leq b \leq d} (n - (a+b)) = d^2(-d+n-1).$$

Assume next $2d \geq n$. We further consider two cases $d \leq n - a$ and $d > n - a$ to conclude

$$\begin{aligned} \sum_{1 \leq a, b \leq d} (n - \min\{n, a + b\}) &= \sum_{1 \leq a \leq n-d} \sum_{1 \leq b \leq d} (n - (a + b)) + \sum_{n-d < a \leq d} \sum_{1 \leq b \leq n-a} (n - (a + b)) \\ &= -\frac{1}{2}d(n-2)(d-n) + \frac{1}{6}(2d-n)(d^2 - dn + n^2 - 3n + 2). \end{aligned}$$

Combining these sums depending on the case distinction provides the variance. \square

For visualization which pairs of roots are considered for the different summations, we give an example.

Example 3.3.4 ([21, Example 4.4]) Let $n = 6$ and $d = 4$. Given the definition of N_a for $1 \leq a \leq 4$, the set $\Phi_{\text{inv}}^{(4)}$ can be partitioned into

$$\begin{aligned} N_1 &= \{[12], [23], [34], [45], [56]\}, & |N_1| &= 5, \\ N_2 &= \{[13], [24], [35], [46]\}, & |N_2| &= 4, \\ N_3 &= \{[14], [25], [36]\}, & |N_3| &= 3, \\ N_4 &= \{[15], [26]\}, & |N_4| &= 2. \end{aligned}$$

By Theorem 3.3.1, the variance is

$$\mathbb{V}[\mathcal{X}_{\Phi_{\text{inv}}^{(d)}}] = \frac{1}{4} \sum_{1 \leq a \leq d} |N_a| + \frac{2}{12} \sum_{1 \leq a \neq b \leq d} (n - \max\{a, b\}) - \frac{2}{12} \sum_{1 \leq a, b \leq d} (n - \min\{n, a + b\}).$$

The first sum makes use of the cardinality of N_a for $1 \leq a \leq 4$, which leads to

$$\frac{1}{4}(5 + 4 + 3 + 2) = \frac{7}{2}.$$

Moreover, we consider the relevant pairs (a, b) for the other two summations. For the first summations with $1 \leq a \neq b \leq d = 4$, we have

$$\{(1, 2), (1, 3), (1, 4), (2, 1), (2, 3), (2, 4), (3, 1), (3, 2), (3, 4), (4, 1), (4, 2), (4, 3)\}$$

which gives

$$\frac{2}{12} \sum_{1 \leq a \neq b \leq d} (n - \max\{a, b\}) = \frac{2}{12} (2 \cdot (6 - 2) + 4 \cdot (6 - 3) + 6 \cdot (6 - 4)) = \frac{16}{3}.$$

For example, consider $a = 1, b = 3$. Since the above sum counts all pairs $([ij], [k\ell]) \in (N_a, N_b)$ with $i = k, j \neq \ell$, we can write down these pairs explicitly:

$$\left| \{[ij], [k\ell] \in N_1 \times N_3 \mid i = k, j \neq \ell\} \right| = \left| \{[12][14], [23][25], [34][36]\} \right| = 3 = n - \max\{a, b\}.$$

Similarly, possible pairs (a, b) for the third sum with $1 \leq a, b \leq d$ are

$$\{(1, 1), (1, 2), (1, 3), (1, 4), (2, 1), (2, 2), (2, 3), (3, 1), (3, 2), (4, 1)\}$$

which lead to a third summand of

$$-\frac{2}{12} \sum_{1 \leq a, b \leq d} (n - \min\{n, a + b\}) = -\frac{2}{12} (1 \cdot (6 - 2) + 2 \cdot (6 - 3) + 3 \cdot (6 - 4) + 4 \cdot (6 - 5)) = -\frac{10}{3}.$$

With all three sums, we obtain

$$\mathbb{V}[\mathcal{X}_{\Phi_{\text{inv}}^{(4)}}] = \frac{7}{2} + \frac{16}{3} - \frac{10}{3} = \frac{11}{2}.$$

3.3.2 Type B_n

In this section, we provide the variances for d -descents and d -inversions of type B_n .

Theorem 3.3.5 ([21, Theorem 4.5]) *Let \mathcal{X}_{Ψ} as in (3.2) and $\Phi_{\text{des}}^{(d)}, \Phi_{\text{inv}}^{(d)}$ as in (3.1). For $1 \leq d \leq 2n - 1$, we then have*

$$\mathbb{V}[\mathcal{X}_{\Phi_{\text{des}}^{(d)}}] = \begin{cases} \frac{1}{24}d + \frac{1}{12}n + \frac{1}{12} & \text{if } d \leq \frac{n}{2}, \\ & d \text{ even,} \\ \frac{1}{24}d + \frac{1}{12}n + \frac{1}{24} & \text{if } d \leq \frac{n}{2}, \\ & d \text{ odd,} \\ \frac{1}{24}d + \frac{1}{12}n + \frac{1}{6} & \text{if } \frac{n}{2} < d \leq \frac{2n}{3}, \\ & d \text{ even,} \\ \frac{1}{24}d + \frac{1}{12}n + \frac{1}{8} & \text{if } \frac{n}{2} < d \leq \frac{2n}{3}, \\ & d \text{ odd,} \\ \frac{1}{24}d + \frac{1}{12}n & \text{if } \frac{2n}{3} < d \leq n, \\ & d \text{ even,} \\ \frac{1}{24}d + \frac{1}{12}n + \frac{1}{8} & \text{if } \frac{2n}{3} \leq d \leq n, \\ & d \text{ odd,} \\ -\frac{1}{8}d + \frac{1}{4}n & \text{if } n \leq d, \\ & d \text{ even,} \\ -\frac{1}{8}d + \frac{1}{4}n + \frac{1}{8} & \text{if } n \leq d, \\ & d \text{ odd.} \end{cases}$$

$$\mathbb{V}[\mathcal{X}_{\Phi_{\text{inv}}^{(d)}}] = \left\{ \begin{array}{ll} \frac{1}{36}d^3 + \frac{1}{48}d^2 + (\frac{1}{12}n + \frac{1}{72})d & \begin{array}{l} \text{if } d \leq \frac{n}{2}, \\ d \text{ even,} \end{array} \\ \frac{1}{36}d^3 + \frac{1}{48}d^2 + (\frac{1}{12}n + \frac{1}{72})d + \frac{1}{48} & \begin{array}{l} \text{if } d \leq \frac{n}{2}, \\ d \text{ odd,} \end{array} \\ \frac{1}{36}d^3 + \frac{3}{16}d^2 + (-\frac{1}{12}n + \frac{7}{72})d + (\frac{1}{24}n^2 - \frac{1}{24}n) & \begin{array}{l} \text{if } \frac{n}{2} \leq d \leq \frac{2n}{3}, \\ d \text{ even,} \end{array} \\ \frac{1}{36}d^3 + \frac{3}{16}d^2 + (-\frac{1}{12}n + \frac{7}{72})d + (\frac{1}{24}n^2 - \frac{1}{24}n + \frac{1}{48}) & \begin{array}{l} \text{if } \frac{n}{2} \leq d < \frac{2n}{3}, \\ d \text{ odd,} \end{array} \\ \frac{1}{36}d^3 + (\frac{1}{6}n - \frac{1}{36})d + (-\frac{1}{24}n^2 + \frac{1}{24}n) & \begin{array}{l} \text{if } \frac{2n}{3} \leq d \leq n, \\ d \text{ even,} \end{array} \\ \frac{1}{36}d^3 + (\frac{1}{6}n + \frac{7}{72})d + (-\frac{1}{24}n^2 - \frac{1}{24}n + \frac{1}{24}) & \begin{array}{l} \text{if } \frac{2n}{3} \leq d \leq n, \\ d \text{ odd,} \end{array} \\ -\frac{1}{12}d^3 + (\frac{1}{3}n - \frac{1}{24})d^2 + (-\frac{1}{3}n^2 + \frac{1}{6}n - \frac{1}{24})d + (\frac{1}{9}n^3 + \frac{1}{18}n) & \begin{array}{l} \text{if } n \leq d, \\ d \text{ even,} \end{array} \\ -\frac{1}{12}d^3 + (\frac{1}{3}n - \frac{1}{24})d^2 + (-\frac{1}{3}n^2 + \frac{1}{6}n + \frac{1}{12})d + (\frac{1}{9}n^3 - \frac{1}{36}n + \frac{1}{24}) & \begin{array}{l} \text{if } n \leq d, \\ d \text{ odd.} \end{array} \end{array} \right.$$

We divide the proof into a sequence of lemmas similar to the proof given for type A . We start again with partitioning the set of positive roots according to their height and their form into

$$\begin{aligned} N_a &= \{[ij] \mid 1 \leq i < j \leq n \mid j - i = a\}, \\ O_a &= \{[i] \mid 1 \leq i \leq n \mid i = a\}, \\ P_a &= \{[\tilde{ij}] \mid 1 \leq i < j \leq n \mid j + i = a\}. \end{aligned}$$

Then, the roots of height a are $N_a \cup O_a \cup P_a$. In addition to Lemma 3.3.2, we have the following cardinalities.

Lemma 3.3.6 ([21, Lemma 4.6]) *We have*

- $O_a \neq \emptyset \Leftrightarrow 1 \leq a \leq n$ and $|O_a| = 1$ for $1 \leq a \leq n$
- $P_a \neq \emptyset \Leftrightarrow 3 \leq a \leq 2n - 1$ and $|P_a| = \begin{cases} \lfloor \frac{a-1}{2} \rfloor & \text{if } 3 \leq a \leq n \\ \lfloor \frac{2n-a+1}{2} \rfloor & \text{if } n+1 \leq a \leq 2n-1 \end{cases}$

Proof. This follows directly from the definition. □

Due to the higher number of interactions between positive roots, the situation is slightly more delicate than in type A_{n-1} . We therefore describe the covariances between different kind of

roots separately. To this end, we introduce the sets

$$N_{\leq d} = \bigcup_{a=1}^d N_a, \quad O_{\leq d} = \bigcup_{a=1}^d O_a, \quad P_{\leq d} = \bigcup_{a=1}^d P_a.$$

Proposition 3.3.7 ([21, Proposition 4.7]) *For $1 \leq d \leq 2n - 1$, we have*

$$2 \cdot \text{Cov}(\mathcal{X}_{P_{\leq d}}, \mathcal{X}_{N_{\leq d}}) = \begin{cases} -\frac{1}{18}d^3 + \frac{1}{16}d^2 + \frac{7}{72}d & \text{if } d \leq \frac{n}{2}, \\ & d \text{ even}, \\ -\frac{1}{18}d^3 + \frac{1}{16}d^2 + \frac{1}{18}d - \frac{1}{16} & \text{if } d \leq \frac{n}{2}, \\ & d \text{ odd}, \\ \frac{1}{6}d^3 + (-\frac{1}{3}n + \frac{1}{16})d^2 + (\frac{1}{6}n^2 + \frac{1}{24})d + (-\frac{1}{36}n^3 + \frac{1}{36}n) & \text{if } \frac{n}{2} \leq d \leq \frac{2n}{3}, \\ & d \text{ even}, \\ \frac{1}{6}d^3 + (-\frac{1}{3}n + \frac{1}{16})d^2 + (\frac{1}{6}n^2)d + (-\frac{1}{36}n^3 + \frac{1}{36}n - \frac{1}{16}) & \text{if } \frac{n}{2} \leq d \leq \frac{2n}{3}, \\ & d \text{ odd}, \\ \frac{1}{6}d^3 + (-\frac{1}{3}n - \frac{1}{8})d^2 + (\frac{1}{6}n^2 + \frac{1}{4}n - \frac{1}{12})d + (-\frac{1}{36}n^3 - \frac{1}{12}n^2 + \frac{1}{9}n) & \text{if } \frac{2n}{3} \leq d \leq n, \\ & d \text{ even}, \\ \frac{1}{6}d^3 + (-\frac{1}{3}n - \frac{1}{8})d^2 + (\frac{1}{6}n^2 + \frac{1}{4}n)d + (-\frac{1}{36}n^3 - \frac{1}{12}n^2 + \frac{1}{36}n - \frac{1}{24}) & \text{if } \frac{2n}{3} \leq d \leq n, \\ & d \text{ odd}, \\ -\frac{1}{18}d^3 + (\frac{1}{4}n + \frac{1}{24})d^2 + (-\frac{1}{3}n^2 - \frac{1}{6}n - \frac{1}{36})d + (\frac{1}{9}n^3 + \frac{1}{6}n^2 + \frac{1}{18}n) & \text{if } n \leq d, \\ & d \text{ even}, \\ -\frac{1}{18}d^3 + (\frac{1}{4}n + \frac{1}{24})d^2 + (-\frac{1}{3}n^2 - \frac{1}{6}n + \frac{1}{18})d + (\frac{1}{9}n^3 - \frac{1}{6}n^2 - \frac{1}{36}n - \frac{1}{24}) & \text{if } n \leq d, \\ & d \text{ odd}. \end{cases}$$

$$2 \cdot \text{Cov}(\mathcal{X}_{N_{\leq d}}, \mathcal{X}_{O_{\leq d}}) = \begin{cases} -\frac{1}{8}d^2 - \frac{1}{8}d & \text{if } d \leq \frac{n}{2}, \\ \frac{3}{8}d^2 + (-\frac{1}{2}n + \frac{1}{8})d + (\frac{1}{8}n^2 - \frac{1}{8}n) & \text{if } \frac{n}{2} \leq d \leq n. \end{cases}$$

$$2 \cdot \text{Cov}(\mathcal{X}_{P_{\leq d}}, \mathcal{X}_{O_{\leq d}}) = \begin{cases} \frac{1}{8}d^2 - \frac{1}{4}d & \text{if } d \leq n, \\ & d \text{ even,} \\ \frac{1}{8}d^2 - \frac{1}{4}d + \frac{1}{8} & \text{if } d \leq n, \\ & d \text{ odd,} \\ -\frac{1}{8}d^2 + \frac{1}{2}nd + (-\frac{1}{4}n^2 - \frac{1}{4}n) & \text{if } n \leq d, \\ & d \text{ even,} \\ -\frac{1}{8}d^2 + \frac{1}{2}nd + (-\frac{1}{4}n^2 - \frac{1}{4}n + \frac{1}{8}) & \text{if } n \leq d, \\ & d \text{ odd.} \end{cases}$$

$$\text{Cov}(\mathcal{X}_{P_{\leq d}}, \mathcal{X}_{P_{\leq d}}) = \begin{cases} \frac{1}{36}d^3 - \frac{1}{12}d^2 + \frac{1}{18}d & \text{if } d \leq n, \\ & d \text{ even,} \\ \frac{1}{36}d^3 - \frac{1}{12}d^2 + \frac{7}{72}d - \frac{1}{24} & \text{if } d \leq n, \\ & d \text{ odd,} \\ -\frac{1}{36}d^3 + (\frac{1}{12}n + \frac{1}{24})d^2 + (-\frac{1}{6}n - \frac{1}{72})d + (-\frac{1}{36}n^3 + \frac{1}{24}n^2 + \frac{5}{72}n) & \text{if } n \leq d, \\ & d \text{ even,} \\ -\frac{1}{36}d^3 + (\frac{1}{12}n + \frac{1}{24})d^2 + (-\frac{1}{6}n - \frac{1}{36})d + (-\frac{1}{36}n^3 + \frac{1}{24}n^2 + \frac{5}{72}n - \frac{1}{24}) & \text{if } n \leq d, \\ & d \text{ odd.} \end{cases}$$

$$\text{Cov}(\mathcal{X}_{O_{\leq d}}, \mathcal{X}_{O_{\leq d}}) = \frac{1}{4}d \quad \text{if } d \leq n.$$

According to Theorem 3.2.1, the covariance of \mathcal{X}_β and \mathcal{X}_γ is dependent of $\text{ord}(\beta, \gamma)$. For these, we recall that reflections in type B_n are given by the following transpositions:

$$s_{[ij]} = (i, j)(-i, -j), \quad s_{[i]} = (i, -i), \quad s_{[\tilde{i}j]} = (i, -j)(-i, j).$$

Hence, the order of two reflections is

$$\text{ord}(s_{[ij]}s_{[k\ell]}) = \begin{cases} 1 & \text{if } |\{i, j\} \cap \{k, \ell\}| = 2, \\ 2 & \text{if } |\{i, j\} \cap \{k, \ell\}| = 0, \\ 3 & \text{if } |\{i, j\} \cap \{k, \ell\}| = 1. \end{cases} \quad \text{ord}(s_{[\tilde{i}j]}s_{[\tilde{k}\ell]}) = \begin{cases} 1 & \text{if } |\{i, j\} \cap \{k, \ell\}| = 2, \\ 2 & \text{if } |\{i, j\} \cap \{k, \ell\}| = 0, \\ 3 & \text{if } |\{i, j\} \cap \{k, \ell\}| = 1. \end{cases}$$

$$\text{ord}(s_{[i]}s_{[k\ell]}) = \begin{cases} 2 & \text{if } |\{i\} \cap \{k, \ell\}| = 0, \\ 4 & \text{if } |\{i\} \cap \{k, \ell\}| = 1. \end{cases} \quad \text{ord}(s_{[i]}s_{[\tilde{k}\ell]}) = \begin{cases} 2 & \text{if } |\{i\} \cap \{k, \ell\}| = 0, \\ 4 & \text{if } |\{i\} \cap \{k, \ell\}| = 1. \end{cases}$$

$$\text{ord}(s_{[ij]}s_{[\tilde{k}\ell]}) = \begin{cases} 2 & \text{if } |\{i, j\} \cap \{k, \ell\}| \in \{0, 2\}, \\ 3 & \text{if } |\{i, j\} \cap \{k, \ell\}| = 1. \end{cases} \quad \text{ord}(s_{[i]}s_{[j]}) = \begin{cases} 1 & \text{if } i = j, \\ 2 & \text{if } i \neq j. \end{cases}$$

Using Theorem 3.2.1 now leads to the following combinations of roots N_a, P_b, O_c with non-zero covariance to investigate. In what follows, we write $X \sim Y$ to describe interactions between roots of type X and Y . We have

$$\begin{aligned} N \sim N : \quad & \text{Cov}(\mathcal{X}_{[ij]}, \mathcal{X}_{[ik]}) = \frac{1}{12} \text{ for } j \neq k, & \text{Cov}(\mathcal{X}_{[ij]}, \mathcal{X}_{[ki]}) = -\frac{1}{12} \text{ for } j \neq k, \\ & \text{Cov}(\mathcal{X}_{[ij]}, \mathcal{X}_{[jk]}) = -\frac{1}{12} \text{ for } i \neq k, & \text{Cov}(\mathcal{X}_{[ij]}, \mathcal{X}_{[kj]}) = \frac{1}{12} \text{ for } i \neq k. \\ N \sim O : \quad & \text{Cov}(\mathcal{X}_{[ij]}, \mathcal{X}_{[i]}) = -\frac{1}{8}, & \text{Cov}(\mathcal{X}_{[ij]}, \mathcal{X}_{[j]}) = \frac{1}{8}. \\ N \sim P : \quad & \text{Cov}(\mathcal{X}_{[ij]}, \mathcal{X}_{[\tilde{i}k]}) = -\frac{1}{12} \text{ for } j \neq k, & \text{Cov}(\mathcal{X}_{[ij]}, \mathcal{X}_{[\tilde{k}i]}) = -\frac{1}{12} \text{ for } j \neq k, \\ & \text{Cov}(\mathcal{X}_{[ij]}, \mathcal{X}_{[\tilde{j}k]}) = \frac{1}{12} \text{ for } i \neq k, & \text{Cov}(\mathcal{X}_{[ij]}, \mathcal{X}_{[\tilde{k}j]}) = \frac{1}{12} \text{ for } i \neq k. \\ P \sim O : \quad & \text{Cov}(\mathcal{X}_{[\tilde{i}j]}, \mathcal{X}_{[i]}) = \frac{1}{8}, & \text{Cov}(\mathcal{X}_{[\tilde{i}j]}, \mathcal{X}_{[j]}) = \frac{1}{8}. \\ P \sim P : \quad & \text{Cov}(\mathcal{X}_{[\tilde{i}j]}, \mathcal{X}_{[\tilde{i}k]}) = \frac{1}{12}, \quad \text{if } j \neq k, & \text{Cov}(\mathcal{X}_{[\tilde{i}j]}, \mathcal{X}_{[\tilde{k}i]}) = \frac{1}{12} \quad \text{if } j \neq k, \\ & \text{Cov}(\mathcal{X}_{[\tilde{i}j]}, \mathcal{X}_{[\tilde{j}k]}) = \frac{1}{12}, \quad \text{if } i \neq k, & \text{Cov}(\mathcal{X}_{[\tilde{i}j]}, \mathcal{X}_{[\tilde{k}j]}) = \frac{1}{12} \quad \text{if } i \neq k. \end{aligned}$$

We use case-by-case analysis to investigate the number of non-zero covariances. The first part of the interaction between N_a and P_b is proved in quite detail whereas other interactions are stated without proof since they work analogously.

Proposition 3.3.8 ([21, Proposition 4.8]) *We consider the two sets N_a and P_b for type B_n with $1 \leq a \leq n$ and $3 \leq b \leq 2n - 1$. The four cases with non-zero covariance for $N_a \sim P_b$ above are as follows:*

$$\begin{aligned} \left| \{[ij], [\tilde{k}\ell] \in N_a \times P_b \mid i = k, j \neq \ell\} \right| &= \begin{array}{c|c|c} & \parallel & \\ & n - a \leq \lfloor \frac{b-1}{2} \rfloor & \lfloor \frac{b-1}{2} \rfloor \leq n - a \\ \hline 1 \leq b - n & 2n - (a + b) + 1 & \lfloor \frac{1}{2}(2n - b + 1) \rfloor \\ \hline b - n \leq 1 & n - a & \lfloor \frac{b-1}{2} \rfloor \end{array} \\ \\ \left| \{[ij], [\tilde{k}\ell] \in N_a \times P_b \mid i = \ell, j \neq k\} \right| &= \begin{array}{c|c|c} & \parallel & \\ & b - 1 \leq n - a & n - a \leq b - 1 \\ \hline \lceil \frac{b+1}{2} \rceil & \lfloor \frac{b-1}{2} \rfloor & \lfloor \frac{1}{2}(2n - 2a - b + 1) \rfloor \\ \hline & & \end{array} \\ \\ \left| \{[ij], [\tilde{k}\ell] \in N_a \times P_b \mid j = k, i \neq \ell\} \right| &= \begin{array}{c|c|c} & \parallel & \\ & \lfloor \frac{b-1}{2} \rfloor & \\ \hline a + 1 \leq b - n & \lfloor \frac{1}{2}(2n - b + 1) \rfloor & \\ \hline b - n \leq a + 1 & \lfloor \frac{1}{2}(b - 2a - 1) \rfloor & \end{array} \end{aligned}$$

$$\left| \{[ij], [\tilde{k}\ell] \in N_a \times P_b \mid j = \ell, i \neq k\} \right| = \begin{array}{c|c|c} & n \leq b-1 & b-1 \leq n \\ \hline a+1 \leq \lceil \frac{b+1}{2} \rceil & \lceil \frac{1}{2}(2n-b+1) \rceil & \lfloor \frac{b-1}{2} \rfloor \\ \hline \lceil \frac{b+1}{2} \rceil \leq a+1 & n-a & b-a-1 \end{array}$$

Proof. We only give a proof for the first counting formula. For that, more explicit descriptions of N_a and P_b are

$$\begin{aligned} N_a &= \{[i, i+a] \mid 1 \leq i \leq n-a\}, \\ P_b &= \{[k, \widetilde{b-k}] \mid \max\{1, b-n\} \leq k \leq \lfloor \frac{b-1}{2} \rfloor\}. \end{aligned}$$

Combining these for $i = k$, we obtain

$$\max(1, b-n) \leq i = k \leq \min(n-a, \lfloor \frac{b-1}{2} \rfloor),$$

which leads to the stated cardinalities in the first table. \square

Given all cardinalities, we can prove the stated covariances between the roots of N_a and P_b .

Proof of Proposition 3.3.7. Again, we will only give a proof for the first case of this proposition since the others follow analogously. Let $a, b \leq d \leq \frac{n}{2}$ and d be even. We investigate the tables in Proposition 3.3.8 and extract the relevant cases under this restriction. For the first table, the only relevant case is $b-n \leq 1$ and $\lfloor \frac{b-1}{2} \rfloor \leq n-a$. We obtain

$$\sum_{1 \leq a, b \leq d} \left| \{[ij], [\tilde{k}\ell] \in N_a \times P_b \mid i = k\} \right| = \sum_{a=1}^d \sum_{b=1}^d \lfloor \frac{b-1}{2} \rfloor = \frac{1}{4}d^2(d-2).$$

Similarly, investigation of the second table reveals the only relevant case $b-1 \leq n-a$. This leads to

$$\sum_{1 \leq a, b \leq d} \left| \{[ij], [\tilde{k}\ell] \in N_a \times P_b \mid i = \ell\} \right| = \sum_{a=1}^d \sum_{b=1}^d \lfloor \frac{b-1}{2} \rfloor = \frac{1}{4}d^2(d-2).$$

Investigating the third table, the only relevant case is $b-n \leq a+1$. Since it is $a+1 \leq j = k \leq \lfloor \frac{b-1}{2} \rfloor$, we obtain an additional restriction $b \geq 2a+3$, and thus

$$\sum_{1 \leq a, b \leq d} \left| \{[ij], [\tilde{k}\ell] \in N_a \times P_b \mid j = k\} \right| = \sum_{a=1}^{\frac{d-4}{2}} \sum_{b=2a+3}^d \lfloor \frac{1}{2}(b-2a-1) \rfloor = \frac{1}{24}d(d^2-6d+8).$$

Investigating the last table, both cases with $b - 1 \leq n$ are relevant, yielding

$$\begin{aligned} \sum_{1 \leq a, b \leq d} \left| \{[ij], [\tilde{k}\ell] \in N_a \times P_b \mid j = \ell\} \right| = \\ \sum_{a=1}^{d-2} \sum_{b=a+2}^{\min(2a+1, d)} (b - a - 1) + \sum_{a=1}^{\frac{d-2}{2}} \sum_{b=2a+2}^d \lfloor \frac{b-1}{2} \rfloor = \frac{1}{8}(d-2)d(d-1). \end{aligned}$$

Lastly, one combines these numbers of interactions with the right value of their covariances, which yields to

$$\begin{aligned} \text{Cov}(\mathcal{X}_{P_{\leq d}}, \mathcal{X}_{N_{\leq d}}) &= \frac{1}{12} \left(\frac{1}{24}d(d^2 - 6d + 8) + \frac{1}{8}(d-2)d(d-1) - \frac{1}{4}d^2(d-2) - \frac{1}{4}d^2(d-2) \right) \\ &= -\frac{1}{36}d^3 + \frac{1}{32}d^2 + \frac{7}{144}d. \quad \square \end{aligned}$$

The calculations for the other cases stated in Proposition 3.3.7 follow analog considerations about interactions between the sets N_a , P_b and O_c . The results will be given without proofs.

Proposition 3.3.9 ([21, Proposition 4.9]) *Let N_a and O_b be sets of negative and neutral roots for type B_n with $1 \leq a, b \leq n$. Depending on relations between n, a and b , the cardinalities of the two relevant cases for $N_a \sim O_b$ are as follows:*

$$\begin{aligned} \left| \{[ij], [k] \in N_a \times O_b \mid i = k\} \right| &= \begin{cases} 1 & 1 \leq b \leq n - a, \\ 0 & \text{else.} \end{cases} \\ \left| \{[ij], [k] \in N_a \times O_b \mid j = k\} \right| &= \begin{cases} 1 & a + 1 \leq b \leq n, \\ 0 & \text{else.} \end{cases} \end{aligned}$$

Proposition 3.3.10 ([21, Proposition 4.10]) *Let P_a and O_b be sets of positive and neutral roots for type B_n with $3 \leq a \leq 2n - 1$ and $1 \leq b \leq n$. Depending on relations between n, a and b , the cardinalities of the two relevant cases for $P_a \sim O_b$ are as follows:*

$$\begin{aligned} \left| \{[\tilde{i}j], [k] \in P_a \times O_b \mid i = k\} \right| &= \begin{cases} 1 & \max(1, a - n) \leq b \leq \lfloor \frac{a-1}{2} \rfloor, \\ 0 & \text{else.} \end{cases} \\ \left| \{[\tilde{i}j], [k] \in P_a \times O_b \mid j = k\} \right| &= \begin{cases} 1 & \lfloor \frac{a+1}{2} \rfloor \leq b \leq \min(n, a - 1), \\ 0 & \text{else.} \end{cases} \end{aligned}$$

Proposition 3.3.11 ([21, Proposition 4.11]) *Let P_a and P_b be sets of positive roots for type B_n with $3 \leq a, b \leq 2n - 1$. Depending on relations between n, a and b , the cardinalities of the two relevant cases for $P_a \sim P_b$ are as follows:*

$$\left| \{[\tilde{i}\tilde{j}], [\tilde{k}\tilde{\ell}] \in P_a \times P_b \mid i = k\} \right| =$$

	$\lfloor \frac{a-1}{2} \rfloor \leq \lfloor \frac{b-1}{2} \rfloor$	$\lfloor \frac{b-1}{2} \rfloor \leq \lfloor \frac{a-1}{2} \rfloor$
$a - n, b - n \leq 1$	$\lfloor \frac{a-1}{2} \rfloor$	$\lfloor \frac{b-1}{2} \rfloor$
$1, b - n \leq a - n$	$\lfloor \frac{1}{2}(2n - a + 1) \rfloor$	$\lfloor \frac{1}{2}(2n - 2a + b + 1) \rfloor$
$1, a - n \leq b - n$	$\lfloor \frac{1}{2}(2n - 2b + a + 1) \rfloor$	$\lfloor \frac{1}{2}(2n - b + 1) \rfloor$

$$\left| \{[\tilde{i}\tilde{j}], [\tilde{k}\tilde{\ell}] \in P_a \times P_b \mid i = \ell\} \right| =$$

	$\lfloor \frac{a-1}{2} \rfloor \leq n, b - 1$	$n \leq \lfloor \frac{a-1}{2} \rfloor, b - 1$	$b - 1 \leq \lfloor \frac{a-1}{2} \rfloor, n$
$a - n, \lceil \frac{b+1}{2} \rceil \leq 1$	$\lfloor \frac{a-1}{2} \rfloor$	n	$b - 1$
$1, \lceil \frac{b+1}{2} \rceil \leq a - n$	$\lfloor \frac{1}{2}(2n - a + 1) \rfloor$	$2n - a + 1$	$n + b - a$
$1, a - n \leq \lceil \frac{b+1}{2} \rceil$	$\lfloor \frac{a-1}{2} \rfloor - \lceil \frac{b+1}{2} \rceil + 1$	$\lfloor \frac{1}{2}(2n - b + 1) \rfloor$	$\lfloor \frac{1}{2}(b - 1) \rfloor$

$$\left| \{[\tilde{i}\tilde{j}], [\tilde{k}\tilde{\ell}] \in P_a \times P_b \mid j = k\} \right| =$$

	$\lfloor \frac{b-1}{2} \rfloor \leq n, a - 1$	$n \leq \lfloor \frac{b-1}{2} \rfloor, a - 1$	$a - 1 \leq \lfloor \frac{b-1}{2} \rfloor, n$
$1, b - n \leq \lceil \frac{a+1}{2} \rceil$	$\lfloor \frac{b-1}{2} \rfloor - \lceil \frac{a+1}{2} \rceil + 1$	$\lfloor \frac{1}{2}(2n - a + 1) \rfloor$	$\lfloor \frac{1}{2}(a - 1) \rfloor$
$\lceil \frac{a+1}{2} \rceil, b - n \leq 1$	$\lfloor \frac{b-1}{2} \rfloor$	n	$a - 1$
$1, \lceil \frac{a+1}{2} \rceil \leq b - n$	$\lfloor \frac{1}{2}(2n - b + 1) \rfloor$	$2n - b + 1$	$n + a - b$

$$\left| \{[\tilde{i}\tilde{j}], [\tilde{k}\tilde{\ell}] \in P_a \times P_b \mid i = k\} \right| =$$

	$n \leq a - 1, b - 1$	$a - 1 \leq n, b - 1$	$b - 1 \leq n, b - 1$
$\lceil \frac{b+1}{2} \rceil \leq \lceil \frac{a+1}{2} \rceil$	$\lfloor \frac{1}{2}(2n - a + 1) \rfloor$	$\lfloor \frac{1}{2}(a - 1) \rfloor$	$\lfloor \frac{1}{2}(2b - a - 1) \rfloor$
$\lceil \frac{a+1}{2} \rceil \leq \lceil \frac{b+1}{2} \rceil$	$\lfloor \frac{1}{2}(2n - b + 1) \rfloor$	$\lfloor \frac{1}{2}(2a - b - 1) \rfloor$	$\lfloor \frac{1}{2}(b - 1) \rfloor$

Proposition 3.3.12 ([21, Proposition 4.12]) *Let O_a and O_b be sets of neutral roots for type B_n with $1 \leq a, b \leq n$. The relevant interactions of $O_a \sim O_b$ are as follows:*

$$\left| \{[i], [j] \in O_a \times O_b \mid i = j\} \right| = \begin{cases} 1 & a = b \\ 0 & \text{else.} \end{cases}$$

Given the number of non-zero covariances for all tuples of roots of different kind, we can deduce the variance by summing according given restrictions. Again, we will only provide explicit calculations for the first case of Theorem 3.3.5.

Proof of Theorem 3.3.5. Consider the first case with $d \leq \frac{n}{2}$ and d even. Using Lemma 3.3.2

together with Propositions 3.3.8, 3.3.9, 3.3.10, 3.3.11, and 3.3.12 gives

$$\begin{aligned}
 \mathbb{V}[\mathcal{X}_{\Phi_{\text{inv}}^{(d)}}] &= \text{Cov}(\mathcal{X}_{N \leq d}, \mathcal{X}_{N \leq d}) + 2 \text{Cov}(\mathcal{X}_{P \leq d}, \mathcal{X}_{N \leq d}) + 2 \text{Cov}(\mathcal{X}_{N \leq d}, \mathcal{X}_{O \leq d}) + \\
 &\quad 2 \text{Cov}(\mathcal{X}_{P \leq d}, \mathcal{X}_{O \leq d}) + \text{Cov}(\mathcal{X}_{P \leq d}, \mathcal{X}_{P \leq d}) + \text{Cov}(\mathcal{X}_{O \leq d}, \mathcal{X}_{O \leq d}) \\
 &= \left[\frac{1}{72}d(4d^2 + 3d + 6n - 1) \right] + \left[-\frac{1}{18}d^3 + \frac{1}{16}d^2 + \frac{7}{72}d \right] + \left[-\frac{1}{8}d^2 - \frac{1}{8}d \right] + \\
 &\quad \left[\frac{1}{8}d^2 - \frac{1}{4}d \right] + \left[\frac{1}{36}d^3 - \frac{1}{12}d^2 + \frac{1}{18}d \right] + \frac{1}{4}d \\
 &= \frac{1}{36}d^3 + \frac{1}{48}d^2 + \left(\frac{1}{12}n + \frac{1}{72} \right)d. \quad \square
 \end{aligned}$$

3.3.3 Type C_n

In this section, we provide the variances for d -descents and d -inversions of type C_n . The explicit proofs are omitted since they are analogous to calculations before.

Theorem 3.3.13 ([21, Proposition 4.13]) *Let \mathcal{X}_{Ψ} as in (3.2) and $\Phi_{\text{des}}^{(d)}, \Phi_{\text{inv}}^{(d)}$ as in (3.1). For $1 \leq d \leq 2n - 1$, we have that*

$$\mathbb{V}[\mathcal{X}_{\Phi_{\text{des}}^{(d)}}] = \begin{cases} \frac{1}{24}d + \frac{1}{12}n & \text{if } d \leq \frac{2n}{3}, \\ & d \text{ even,} \\ \frac{1}{24}d + \frac{1}{12}n + \frac{1}{24} & \text{if } d \leq \frac{2n}{3}, \\ & d \text{ odd,} \\ \frac{1}{24}d + \frac{1}{12}n & \text{if } \frac{2n}{3} \leq d \leq n, \\ & d \text{ even,} \\ \frac{1}{24}d + \frac{1}{12}n + \frac{1}{8} & \text{if } \frac{2n}{3} < d \leq n, \\ & d \text{ odd,} \\ -\frac{1}{8}d + \frac{1}{4}n & \text{if } n \leq d, \\ & d \text{ even,} \\ -\frac{1}{8}d + \frac{1}{4}n + \frac{1}{8} & \text{if } n \leq d, \\ & d \text{ odd.} \end{cases}$$

$$\mathbb{V}[\mathcal{X}_{\Phi_{\text{inv}}^{(d)}}] = \begin{cases} \frac{1}{36}d^3 + \frac{1}{48}d^2 + (\frac{1}{12}n + \frac{1}{72})d & \text{if } d \leq \frac{2n}{3}, \\ & d \text{ even,} \\ \frac{1}{36}d^3 + \frac{1}{48}d^2 + (\frac{1}{12}n + \frac{1}{72})d + \frac{1}{48} & \text{if } d \leq \frac{2n}{3}, \\ & d \text{ odd,} \\ \frac{1}{36}d^3 + \frac{11}{96}d^2 + (-\frac{1}{24}n + \frac{11}{144})d + (\frac{1}{24}n^2 - \frac{1}{24}) & \text{if } \frac{2n}{3} \leq d \leq n, \\ & d \text{ even,} \\ \frac{1}{36}d^3 + \frac{11}{96}d^2 + (-\frac{1}{24}n + \frac{5}{36})d + (\frac{1}{24}n^2 - \frac{1}{12}n + \frac{5}{96}) & \text{if } \frac{2n}{3} < d \leq n, \\ & d \text{ odd,} \\ -\frac{1}{12}d^3 + (\frac{1}{3}n - \frac{13}{96})d^2 + (-\frac{1}{3}n^2 + \frac{11}{24}n - \frac{1}{16})d + (\frac{1}{9}n^3 - \frac{5}{24}n^2 + \frac{7}{72}n) & \text{if } n \leq d, \\ & d \text{ even,} \\ -\frac{1}{12}d^3 + (\frac{1}{3}n - \frac{13}{96})d^2 + (-\frac{1}{3}n^2 + \frac{11}{24}n - \frac{1}{16})d + (\frac{1}{9}n^3 - \frac{5}{24}n^2 + \frac{1}{18}n + \frac{5}{96}) & \text{if } n \leq d, \\ & d \text{ odd.} \end{cases}$$

The case-by-case analysis for the interactions in type C_n only differs from type B_n in the heights of the roots. For positive roots in type C_n , the partition according their type and height is given by

$$\begin{aligned} N_a &= \{[ij] \mid 1 \leq i < j \leq n \mid j - i = a\}, \\ O_a &= \{[i] \mid 1 \leq i \leq n \mid 2i - 1 = a\}, \\ P_a &= \{[\tilde{ij}] \mid 1 \leq i < j \leq n \mid j + i - 1 = a\}. \end{aligned}$$

Then, the roots of height a are $N_a \cup O_a \cup P_a$. All considerations are completely analogous to those for type B_n , hence they will not be given here.

3.3.4 Type D_n

In this section, we provide the variances for d -descents and d -inversions of type D_n , again without proofs.

Theorem 3.3.14 ([21, Proposition 4.14]) *Let \mathcal{X}_{Ψ} as in (3.2) and $\Phi_{\text{des}}^{(d)}, \Phi_{\text{inv}}^{(d)}$ as in (3.1). We then have for $1 \leq d \leq 2n - 3$ that*

$$\mathbb{V}[\mathcal{X}_{\Phi_{\text{des}}^{(d)}}] = \left\{ \begin{array}{ll} \frac{1}{24}d + \frac{1}{12}n + \frac{1}{6} & \begin{array}{l} \text{if } d < \frac{n}{2}, \\ d \text{ even}, \end{array} \\ \frac{1}{24}d + \frac{1}{12}n + \frac{1}{8} & \begin{array}{l} \text{if } d < \frac{n}{2}, \\ d \text{ odd}, \end{array} \\ \frac{1}{24}d + \frac{1}{12}n + \frac{1}{3} & \begin{array}{l} \text{if } \frac{n}{2} \leq d < \frac{2n}{3}, \\ d \text{ even}, \end{array} \\ \frac{1}{24}d + \frac{1}{12}n + \frac{7}{24} & \begin{array}{l} \text{if } \frac{n}{2} \leq d \leq \frac{2n}{3}, \\ d \text{ odd}, \end{array} \\ \frac{1}{24}d + \frac{1}{12}n + \frac{1}{6} & \begin{array}{l} \text{if } \frac{2n}{3} \leq d < n, \\ d \text{ even}, \end{array} \\ \frac{1}{24}d + \frac{1}{12}n + \frac{7}{24} & \begin{array}{l} \text{if } \frac{2n}{3} \leq d < n, \\ d \text{ odd}, \end{array} \\ -\frac{1}{8}d + \frac{1}{4}n - \frac{1}{4} & \begin{array}{l} \text{if } n \leq d, \\ d \text{ even}, \end{array} \\ -\frac{1}{8}d + \frac{1}{4}n - \frac{1}{8} & \begin{array}{l} \text{if } n \leq d, \\ d \text{ odd}. \end{array} \end{array} \right.$$

$$\mathbb{V}[\mathcal{X}_{\Phi_{\text{inv}}^{(d)}}] = \left\{ \begin{array}{ll} \frac{1}{36}d^3 + \frac{1}{48}d^2 + \left(\frac{1}{12}n + \frac{1}{72}\right)d & \begin{array}{l} \text{if } d < \frac{n}{2}, \\ d \text{ even}, \end{array} \\ \frac{1}{36}d^3 + \frac{1}{48}d^2 + \left(\frac{1}{12}n + \frac{1}{18}\right)d + \frac{1}{16} & \begin{array}{l} \text{if } d < \frac{n}{2}, \\ d \text{ odd}, \end{array} \\ \frac{1}{36}d^3 + \frac{17}{48}d^2 + \left(-\frac{1}{4}n + \frac{5}{9}\right)d + \left(\frac{1}{12}n^2 - \frac{1}{4}n + \frac{1}{6}\right) & \begin{array}{l} \text{if } \frac{n}{2} \leq d < \frac{2n}{3}, \\ d \text{ even}, \end{array} \\ \frac{1}{36}d^3 + \frac{17}{48}d^2 + \left(-\frac{1}{4}n + \frac{5}{9}\right)d + \left(\frac{1}{12}n^2 - \frac{1}{4}n + \frac{11}{48}\right) & \begin{array}{l} \text{if } \frac{n}{2} \leq d < \frac{2n}{3}, \\ d \text{ odd}, \end{array} \\ \frac{1}{36}d^3 + \frac{1}{6}d^2 + \frac{13}{72}d & \begin{array}{l} \text{if } \frac{2n}{3} \leq d < n, \\ d \text{ even}, \end{array} \\ \frac{1}{36}d^3 + \frac{1}{6}d^2 + \frac{11}{36}d + \left(-\frac{1}{12}n - \frac{1}{6}\right) & \begin{array}{l} \text{if } \frac{2n}{3} \leq d < n, \\ d \text{ odd}, \end{array} \\ -\frac{1}{12}d^3 + \left(\frac{1}{3}n - \frac{5}{12}\right)d^2 + \left(-\frac{1}{3}n^2 + n - \frac{17}{24}\right)d + \left(\frac{1}{9}n^3 - \frac{5}{12}n^2 + \frac{13}{18}n - \frac{5}{12}\right) & \begin{array}{l} \text{if } n \leq d, \\ d \text{ even}, \end{array} \\ -\frac{1}{12}d^3 + \left(\frac{1}{3}n - \frac{5}{12}\right)d^2 + \left(-\frac{1}{3}n^2 + n - \frac{7}{12}\right)d + \left(\frac{1}{9}n^3 - \frac{5}{12}n^2 + \frac{23}{36}n - \frac{1}{4}\right) & \begin{array}{l} \text{if } n \leq d, \\ d \text{ odd}. \end{array} \end{array} \right.$$

Recall that the roots of D_n are a subset of the roots of Type B_n , which we already considered. They just differ in their heights. The partition of positive roots according their type and height in type D_n is given by

$$N_a = \{[ij] \mid 1 \leq i < j \leq n \mid j - i = a\}, \quad P_a = \{[\tilde{i}j] \mid 1 \leq i < j \leq n \mid j + i - 2 = a\}.$$

Then roots of height a are $N_a \cup P_a$.

Again, all considerations are completely analogous to those for type B_n , and are thus suppressed.

3.4 Central limit theorems

This final section of the chapter will combine the Coxeter-theoretic properties from Section 3.2 and the dependency graph method to conclude the stated central limit theorem. Bounds on the rates of convergence are provided where the method is applicable. The result for d -inversions will make use of a lower bound on their variance, which is deduced from the concrete variances given in Section 3.3.

3.4.1 The dependency graph method

Let $\{\mathcal{X}^{(n,j)}\}$ with $n \geq 0$ and $1 \leq j \leq k_n$ be a triangular array of random variables. For a fixed n , we define $G_n = (V, E)$ with

$$V = \{1, \dots, k_n\} \quad \text{and} \quad E = \{\{i, j\} \mid i \neq j, \mathcal{X}^{(n,i)} \text{ and } \mathcal{X}^{(n,j)} \text{ are dependent}\}.$$

If moreover for any disjoint subsets $I, L \subseteq V$ with no edges between I and J , the corresponding sets of random variables $\{\mathcal{X}^{(n,i)}\}_{i \in I}$ and $\{\mathcal{X}^{(n,\ell)}\}_{\ell \in L}$ are independent, the graph is called the n -th *dependency graph* of $\{\mathcal{X}^{(n,\ell)}\}$. In this case, G_n is a dependency graph in the sense of [13] and its *dependency degree* δ_n is the maximal vertex degree of G_n .

We present the following theorem due to Janson [13] in a slightly adapted version.

Theorem 3.4.1 [13, Theorem 2] *Let $\{\mathcal{X}^{(n,j)}\}$ with $n \geq 0$ and $1 \leq j \leq k_n$ be a triangular array of Bernoulli random variables, admitting the conditions of a dependency graph with dependency degree $(\delta_n)_{n \geq 0}$. Then the sequence $\mathcal{X}^{(n)} = \mathcal{X}^{(n,1)} + \dots + \mathcal{X}^{(n,k_n)}$ is asymptotically normal if there exists an $m \in \mathbb{N}$ such that*

$$\frac{k_n \cdot \delta_n^{m-1}}{\mathbb{V}[\mathcal{X}^{(n)}]^{m/2}} \longrightarrow 0.$$

Corollary 3.4.2 [11, Corollary 4.3 & Theorem 4.7] *If the assertion in the previous theorem is satisfied for $m = 3$, we obtain a bound for the rate of convergence given by*

$$\sup_{x \in \mathbb{R}} \left| \mathbb{P}[\mathcal{X}^{(n)} \leq x] - \mathbb{P}[\mathcal{N}(0, 1) \leq x] \right| \leq k_n \cdot \delta_n^2 \cdot \mathbb{V}[\mathcal{X}^{(n)}]^{-3/2} \longrightarrow 0.$$

In the following sections, Theorem 3.4.1 is used as the main tool to prove asymptotic normality for antichains, stated in Theorem 3.1.3, which directly implies the result for d -descents given in Corollary 3.1.4. To provide the proof for d -inversions in Theorem 3.1.5, we first provide a lower bound on the variance, deduced from the concrete calculations in Section 3.3.

For the following proofs, we introduce three notation about limiting behavior of functions. For functions $f, g : \mathbb{N}_+ \rightarrow \mathbb{R}_{\geq 0}$, we write $f \lesssim g$, if there exists $\varepsilon > 0$ and an $N \in \mathbb{N}$ such that for all $n \geq N$, it holds that $f(n) \leq \varepsilon g(n)$. We moreover write $f \ll g$, if for all $\varepsilon > 0$ there exists an $N \in \mathbb{N}$ with this property. We finally write

$$f \approx g \text{ for } f \lesssim g \lesssim f.$$

3.4.2 Central limit theorems for antichains in root posets and d -descents

For this subsections, let $\{\Phi^{(n)}\}_{n \geq 1}$ be a sequence of finite crystallographic root systems and let $\{\Psi^{(n)}\}_{n \geq 1}$ be a sequence of antichains in the respective root posets. We will investigate the random variable $\mathcal{X}_{\Psi^{(n)}}$ as given in (3.2) and proof asymptotic normality along with the stated bounds on the rate of convergence using the dependency graph method from above.

We start with stating some properties of roots in antichains and their corresponding random variables.

Lemma 3.4.3 ([21, Lemma 5.4]) *Let $\Psi \subset \Phi^+$ be an antichain. Then the following holds:*

- $\langle \beta, \gamma \rangle \leq 0$ for all $\beta \neq \gamma$ in Ψ ,
- there are at most $|\Psi| - 1$ many pairs of dependent random variables $\mathcal{X}_\beta, \mathcal{X}_\gamma$ for $\beta, \gamma \in \Psi$,
- the dependency degree δ is at most 3.

Proof. First consider $\Psi \subset \Delta$. For any two simple roots, the inner product is less or equal to zero, thus the first statement is satisfied. The dependency graph of \mathcal{X}_Ψ then equals the Coxeter graph of the parabolic subsystem generated by Ψ . These graphs are known to satisfy the second and third statement. In the case of Ψ being a general antichain, the roots may be send to a subset of simple roots by an element in W , as proved in [31]. Since the three properties are invariant under such a group action on Φ , the statements are satisfied for general antichains. \square

Proposition 3.4.4 ([21, Proposition 5.5]) *The variance of $\mathcal{X}_{\Psi^{(n)}}$ grows linearly with the cardinality of the antichain, i.e.,*

$$\mathbb{V}[\mathcal{X}_{\Psi^{(n)}}] \approx |\Psi^{(n)}|.$$

Proof. Given Theorem 3.2.1, we may rewrite $\mathbb{V}[\mathcal{X}_{\Psi^{(n)}}]$ as

$$\mathbb{V}[\mathcal{X}_{\Psi^{(n)}}] = \sum_{\beta \in \Psi^{(n)}} \mathbb{V}[\mathcal{X}_\beta] + \sum_{\substack{\beta, \gamma \in \Psi^{(n)} \\ \beta \neq \gamma}} \text{Cov}(\mathcal{X}_\beta, \mathcal{X}_\gamma) = \frac{1}{4} \left(|\Psi^{(n)}| - \sum_{\substack{\beta, \gamma \in \Psi^{(n)} \\ \beta \neq \gamma}} \left(1 - \frac{2}{\text{ord}(\beta, \gamma)} \right) \right).$$

Since $\beta \neq \gamma$, it is $\text{ord}(\beta, \gamma) \in \{2, 3, 4, 6\}$. We immediately obtain $\mathbb{V}[\mathcal{X}_{\Psi^{(n)}}] \leq \frac{|\Psi^{(n)}|}{4}$ under the assumption that $\text{ord}(\beta, \gamma) = 2$ for all (β, γ) .

Now we aim to find a lower bound for $\mathbb{V}[\mathcal{X}_{\Psi^{(n)}}]$ by showing that

$$\sum_{\substack{\beta, \gamma \in \Psi^{(n)} \\ \beta \neq \gamma}} \left(1 - \frac{2}{\text{ord}(\beta, \gamma)} \right) \leq \frac{2}{3} |\Psi^{(n)}|.$$

As in the proof of Lemma 3.4.3, roots of $\Psi^{(n)}$ can be transferred to simple roots of a parabolic subsystem, which is not necessary irreducible. Therefore, we use $\Psi^{(n)} = \Delta_1 \cup \dots \cup \Delta_k$ as decomposition in such a way that Δ_i consists of simple roots of an irreducible root system. Before proceeding, we note that if $\beta \in \Delta_i$ and $\gamma \in \Delta_j$ with $i \neq j$, they are independent, i.e., $\text{ord}(\beta, \gamma) = 2$. Second, for $\beta, \gamma \in \Delta_i$, there are exactly $2(|\Delta_i| - 1)$ pairs $(\beta, \gamma) \in \Delta_i^2$ with order greater or equal to three, and at most two pairs (β', γ') and (γ', β') with $\text{ord}(\beta', \gamma') > 3$. We then obtain

$$\sum_{\substack{\beta, \gamma \in \Psi^{(n)} \\ \beta \neq \gamma}} \left(1 - \frac{2}{\text{ord}(\beta, \gamma)} \right) = \sum_{i=1}^k \sum_{\substack{\beta, \gamma \in \Delta_i \\ \beta \neq \gamma}} \left(1 - \frac{2}{\text{ord}(\beta, \gamma)} \right) \leq \sum_{i=1}^k \left(\frac{2}{3} (|\Delta_i| - 2) + \frac{4}{3} \right) = \frac{2}{3} |\Psi^{(n)}|.$$

This summarizes to $\frac{|\Psi^{(n)}|}{12} \leq \mathbb{V}[\mathcal{X}_{\Psi^{(n)}}] \leq \frac{|\Psi^{(n)}|}{4}$. \square

Proof of Theorem 3.1.3. We need to check that Theorem 3.4.1 applies in this setting. First, $\mathcal{X}_{\Psi^{(n)}}$ is a sum of Bernoulli random variables. Second, Theorem 3.2.7 proved that the corresponding triangular array forms a dependency graphs. Third, Lemma 3.4.3 showed that δ_n is globally bounded by 3. Finally, by Proposition 3.4.4 it was shown that the variance grows linearly with $|\Psi^{(n)}| = k_n$. Investigation of the term in Theorem 3.4.1 with these assumption leads to

$$\frac{k_n \cdot \delta_n^{m-1}}{\mathbb{V}[\mathcal{X}_{\Psi^{(n)}}]^{m/2}} \approx |\Psi^{(n)}|^{\frac{2-m}{2}} \rightarrow 0$$

for any $m \geq 3$. Therefore, $\mathcal{X}_{\Psi^{(n)}}$ is asymptotically normal by Theorem 3.4.1, and with

Corollary 3.4.2, the bound on the rate of convergence is $|\Psi^{(n)}|^{-1/2}$. \square

Remark 3.4.5 The central limit for antichains in root posets, as stated in Theorem 3.1.3, can be derived by combining arguments from [14] and [31]. As already mentioned, any antichain may be sent to a set of simple roots by an element in W [31]. Thus, the situation is now stated in terms of some simple roots $\Delta^{(n)}$ of the root system $\Phi^{(n)}$. As Corollary 3.2.5 showed, the random variable $\mathcal{X}_{\Psi}^{(n)}$ may be considered in a parabolic subgroup $W_{\Delta^{(n)}}$. For this setup, a central limit was already proven in [14, Theorem 6.2]. However, the given approach using the dependency method extends the result by bounds on the rate of convergence.

3.4.3 Central limit theorems for d -inversions

In this section, let $\{\Phi^{(n)}\}_{n \geq 1}$ be a sequence of finite crystallographic root systems, and let $\{d_n\}_{n \geq 1}$ be a sequence of integers. We recall the random variable counting d -inversions

$$\mathcal{X}_{\Phi_{\text{inv}}^{(d_n)}} = \sum_{\beta \in \Phi_{\text{inv}}^{(d_n)}} \mathcal{X}_{\beta} \quad \text{with} \quad \Phi_{\text{inv}}^{(d_n)} = \{\beta \in \Phi^+ \mid \text{ht } \beta \leq d_n\}$$

and use the dependency graph method to prove asymptotic normality. Whenever applicable, we provide bounds on the rate of convergence. To avoid a case-by-case analysis for all classical types, we start with a lemma in which we deduce a lower bound for the variance, based on the concrete variances in Section 3.3.

Lemma 3.4.6 ([21, Lemma 5.7]) *There exists a global constant $\varepsilon > 0$ such that for any irreducible root system Φ of rank r and any parameter d , we have*

$$\mathbb{V}[\mathcal{X}_{\Phi_{\text{inv}}^{(d+1)}}] \geq \mathbb{V}[\mathcal{X}_{\Phi_{\text{inv}}^{(d)}}] > \begin{cases} \varepsilon \cdot r^3 & \text{if } r \leq d, \\ \varepsilon \cdot d^3 & \text{if } d \leq r \leq d^2, \\ \varepsilon \cdot r \cdot d & \text{if } d^2 \leq r. \end{cases}$$

Proof. The first property that the variance (weakly) increases in d can be checked by investigating the derivative in d for all concrete polynomials in Section 3.3 and noticing that these are nonnegative. Alternatively, one takes the difference between two variances for consecutive parameters in d .

Several uses of the first inequality result in

$$\mathbb{V}[\mathcal{X}_{\Phi_{\text{inv}}^{(d)}}] \geq \mathbb{V}[\mathcal{X}_{\Phi_{\text{inv}}^{(k)}}]$$

with $k = \min\{d, r/2\}$. We therefore only need to consider the concrete variances for cases with $2d \leq r$. In all classical types, the variance of this case includes terms with positive

coefficients for both rd and d^3 . We will analyze each case separately and provide an lower bound for each using the parameter $\varepsilon > 0$. While the optimal bounds may differ for each case, we can find a global parameter that satisfies all cases for all classical types and exceptional groups.

First, we consider $r \leq d$. With $k = r/2$, we can find an $\varepsilon > 0$ such that

$$\mathbb{V}[\mathcal{X}_{\Phi_{\text{inv}}^{(d)}}] \geq \mathbb{V}[\mathcal{X}_{\Phi_{\text{inv}}^{(r/2)}}] > \varepsilon \cdot r^3.$$

Secondly, we will consider the case where $d \leq r \leq d^2$ and divide it into two subcases. If $d \leq r/2$, it is $k = d$ and we can find an $\varepsilon > 0$ such that

$$\mathbb{V}[\mathcal{X}_{\Phi_{\text{inv}}^{(d)}}] > \varepsilon \cdot d^3.$$

If $d \geq r/2$, it is $k = r/2$. We can find an $\varepsilon > 0$ such that

$$\mathbb{V}[\mathcal{X}_{\Phi_{\text{inv}}^{(d)}}] \geq \mathbb{V}[\mathcal{X}_{\Phi_{\text{inv}}^{(r/2)}}] > \varepsilon \cdot r^3 \geq \varepsilon \cdot d^3,$$

where the last inequality uses the assumption of $r \geq d$.

Finally, we consider the case where $d^2 \leq r$. If $d > 1$, we have $2d \leq d^2 \leq r$ and $k = d$. Then, there exists some $\varepsilon > 0$ such that

$$\mathbb{V}[\mathcal{X}_{\Phi_{\text{inv}}^{(d)}}] > \varepsilon \cdot rd.$$

For the case $d = 1$, this bound holds trivially. □

For further analysis, we decompose the given root system $\Phi = \Phi^{(n)}$ into irreducible components

$$\Phi = \Phi_A \cup \Phi_B \cup \Phi_C = \bigcup_{i \in A} \Phi_i \cup \bigcup_{i \in B} \Phi_i \cup \bigcup_{i \in C} \Phi_i,$$

where the sets are chosen according to Lemma 3.4.6 as

$$A = \{i \mid r_i < d\}, \quad B = \{i \mid d \leq r_i \leq d^2\}, \quad C = \{i \mid d^2 < r_i\}, \quad (3.5)$$

with $r_i = \text{rk}(\Phi_i)$. One notes that different irreducible components Φ_i and Φ_j for $i \neq j$ live in orthogonal subspaces. We set $r_A = \sum_{i \in A} r_i = \text{rk}(\Phi_A)$ and r_B and r_C analogously, and observe that $r_n = \text{rk}(\Phi^{(n)}) = r_A + r_B + r_C$.

Since Theorem 3.1.5 requires $|\Phi_{\text{inv}}^{(d_n)}| \rightarrow \infty$, it is $r_n \rightarrow \infty$ as well. Without loss of generality, we further assume that there exists at least one positive root in $\Phi^{(n)}$ of height d_n . Otherwise, we set $\Phi^{(d_n)} = \Phi^{(d_n-1)}$ and replace d_n with $d_n - 1$ without modifying the random variable. The union of the root posets of $\{\Phi_i^{(n)} \mid i \in A \cup B \cup C\}$ is the root poset of $\Phi^{(n)}$. We use

notation from Theorem 3.4.1 and write δ_n for the n -th dependency degree.

Proposition 3.4.7 ([21, Proposition 5.8]) *We have*

$$|\Phi_{\text{inv}}^{(d_n)}| \lesssim r_n \cdot d_n \quad \text{and} \quad \delta_n \lesssim d_n.$$

Proof. The first property follows from the observation that the number of roots of a given height is bounded by the rank.

For the second statement we count the maximal number of dependencies. In general, two roots can only be dependent if they are in the same irreducible component. We will distinguish between exceptional and classical type. Let $\beta \in \Phi_{\text{inv}}^{(d_n)}$. First, suppose that β is an element of an irreducible component of exceptional type. Then the number of roots dependent to β is globally bounded. Second, consider β, γ as two elements of the same irreducible component of classical type A, B, C or D . Then β, γ are of the following form $e_j - e_i, e_i, e_j + e_i$. We have seen that $\beta \in \{e_j - e_i, e_i, e_j + e_i\}$ and $\gamma \in \{e_k - e_\ell, e_k, e_k + e_\ell\}$ are dependent if and only if they share one of their indices. This implies that there are at most $4d_n$ roots dependent of β . \square

Proof of Theorem 3.1.5 & Corollary 3.1.6. For easier readability, we write $\sigma_n^2 = \mathbb{V}[\mathcal{X}_{\Phi_{\text{inv}}^{(d_n)}}]$ and σ_i^2 for the variance of the corresponding random variable of the irreducible component Φ_i .

Due to independency of random variables of different irreducible components, we can write

$$\sigma_n^2 = \sigma_A^2 + \sigma_B^2 + \sigma_C^2 = \sum_{i \in A} \sigma_i^2 + \sum_{i \in B} \sigma_i^2 + \sum_{i \in C} \sigma_i^2$$

with the same sets A, B and C used for the decomposition $\Phi^{(n)} = \Phi_A \cup \Phi_B \cup \Phi_C$ in Equation (3.5).

By Lemma 3.4.6, we conclude

$$\sigma_A^2 = \sum_{i \in A} \sigma_i^2 > \varepsilon \cdot r_A^3, \quad \sigma_B^2 = \sum_{i \in B} \sigma_i^2 > \varepsilon \cdot |B| \cdot d^3, \quad \sigma_C^2 = \sum_{i \in C} \sigma_i^2 > \varepsilon \cdot d \cdot r_C.$$

with a global constant ε . For the first inequality, we used $\sum_{i \in A} r_i^3 \approx (\sum_{i \in A} r_i)^3 = r_A^3$. The others follow directly from the lemma.

We can finally start investigating the asymptotic normality of d -inversions by using Theorem 3.4.1. With Proposition 3.4.7, this theorem simplifies to finding an $m \in \mathbb{N}$ such that

$$\frac{|\Phi_{\text{inv}}^{(d_n)}| \cdot \delta_n^{m-1}}{\sigma_n^m} \lesssim \frac{r_n \cdot d_n^m}{\sigma_n^m} \longrightarrow 0.$$

We will distinguish between the limiting behavior of r_n , which we have seen to satisfy

$$r_n = r_A + r_B + r_C.$$

Suppose $r_n \approx r_A$: Then $\sigma_n^2 \approx \sigma_A^2 \gtrsim r_n^3$. Thus,

$$\frac{r_n \cdot d_n^m}{\sigma_n^m} \lesssim r_n^{1-\frac{3m}{2}} \cdot d_n^m \lesssim r_n^{1-\frac{m}{2}} \longrightarrow 0 \text{ for } m = 3,$$

where the second step uses that the height of a root poset is at most linear in its rank, *i.e.*, $d_n \lesssim r_n$.

Suppose $r_n \approx r_C$: Then $\sigma_n^2 \gtrsim r_n \cdot d_n$, and from (3.5) it is $d_n^2 \lesssim r_n$. Thus,

$$\frac{r_n \cdot d_n^m}{\sigma_n^m} \lesssim r_n^{1-\frac{m}{2}} \cdot d_n^{\frac{m}{2}} \lesssim r_n^{1-\frac{m}{4}} \longrightarrow 0 \text{ for } m = 5.$$

This proves the asymptotic normality without a bound on the rate of convergence. However, if we strengthen our assumption to $d_n^3 \ll r_n$, we obtain

$$r_n^{1-\frac{m}{2}} \cdot d_n^{\frac{m}{2}} \ll r_n^{1-\frac{m}{2}+\frac{m}{6}} = r_n^{1-\frac{2m}{6}},$$

and thus

$$\frac{r_n \cdot d_n^m}{\sigma_n^m} \lesssim r_n^{1-\frac{2m}{6}} \longrightarrow 0 \text{ for } m = 3$$

in this case.

Suppose $r_n \approx r_B$: Then $\sigma_n^2 \gtrsim |B| \cdot d_n^3$, and thus

$$\frac{r_n \cdot d_n^m}{\sigma_n^m} \lesssim r_n \cdot d_n^{-\frac{m}{2}} |B|^{-\frac{m}{2}}.$$

From (3.5), it is $r_i \leq d_n^2$ for $i \in B$. Thus, we can compute

$$r_n \approx r_B = \sum_{i \in B} r_i \leq \sum_{i \in B} d_n^2 = d_n^2 \cdot |B|. \quad (3.6)$$

With $r_n \rightarrow \infty$, we conclude that either $|B| \rightarrow \infty$ or $d_n^2 \rightarrow \infty$. This gives

$$r_n \cdot d_n^{-\frac{m}{2}} |B|^{-\frac{m}{2}} \lesssim d_n^{2-\frac{m}{2}} |B|^{1-\frac{m}{2}} \longrightarrow 0 \text{ for } m = 5.$$

If we even assume $r_n^2 \ll d_n^3$, we obtain

$$r_n \cdot d_n^{-\frac{m}{2}} |B|^{-\frac{m}{2}} \longrightarrow 0 \text{ for } m = 3. \quad \square$$

Chapter 4

Background on STIT tessellations

This chapter introduces necessary definitions and notations of probability theory, which are being used throughout the Chapter 5 and 6. We start by giving information about random measures and random tessellations in Section 4.1 before describing the construction of a STIT tessellation in Section 4.2. Lastly, important properties of STIT tessellations are given in Section 4.3.

4.1 Probability measures and tessellations

Let \mathcal{P} be a locally compact space with a countable base and $\mathfrak{B}(\mathcal{P})$ the Borel- σ -algebra of \mathbb{X} . The set of all Borel measures on \mathcal{P} is given by $M = M(\mathcal{P})$. It contains in particular all η with $\eta(C) < \infty$ for all compact subsets $C \subseteq \mathcal{P}$. The set M is equipped with the σ -algebra \mathcal{M} , which is generated by evaluation maps $\Phi_A : M \rightarrow \mathbb{R} \cup \{\infty\}$ and $\Phi_A(\eta) = \eta(A)$ for every $A \in \mathfrak{B}(\mathcal{P})$. Further let $N = \{\eta \in M \mid \eta(A) \in \mathbb{N}_0 \cup \{\infty\}, \forall A \in \mathfrak{B}\}$ be the set of all counting measures on \mathbb{E} . We use $\stackrel{D}{=}$ to denote equality in distribution.

Definition 4.1.1 A random measure X is a measurable map from some probability space $(\Omega, \mathbf{A}, \mathbb{P})$ into the measurable space (M, \mathcal{M}) of locally finite measures. It is called a *point process* in \mathcal{P} if it is concentrated on N almost surely. Its distribution is given by the image measure of \mathbb{P} under X . In symbols, this is $\mathbb{P}_X = X(\mathbb{P})$. The *intensity measure* γ of this random point process X is given by $\gamma(A) := \mathbb{E}X(A)$ for all $A \in \mathfrak{B}(\mathcal{P})$.

Throughout most parts of this thesis, we consider random measures on \mathbb{R}^d with $d = 2$. Whenever this applies, we will refer to this as *planar*. In some cases we will adapt definitions and properties in varying degree of scope to this special case.

Definition 4.1.2 A random measure X on \mathbb{R}^d is *stationary* if $X \stackrel{D}{=} X + x$ for all $x \in \mathbb{R}^d$. It

is called *isotropic* if $X \stackrel{D}{=} \vartheta X$ for all $\vartheta \in SO_d$.

A distribution often used in random measure theory and the theory of point processes is the Palm distribution. Following [27, Section 3.3], let X be a stationary random measure on \mathbb{R}^d with intensity $\gamma > 0$. Given a Borel set $B \in \mathcal{B}$ and $A \in \mathcal{M}$, the *Palm distribution* of X is

$$\mathbb{P}^0(A) = \frac{\mathbb{E} \int_B \mathbf{1}_A(X - x) X(dx)}{\mathbb{E} X(B)}.$$

In Chapter 5, we use the Palm distribution with respect to the random vertex process of a tessellation and with respect to the edge length measure concentrated on the skeleton. Intuitively, it describes the conditional distribution of a random measure, given that 0 is a typical point. In this definition, the typical point itself is considered. One might omit this point and consider $\varphi \setminus \{0\}$. This yields to the *reduced Palm distribution*.

Definition 4.1.3 (see [32]) Let \mathbb{C} be the set of compact and convex polygons in \mathbb{R}^2 . A (planar) tessellation is a subset $\mathcal{C} \subset \mathbb{C}$ with the following properties:

1. $\text{int}(c_1) \cap \text{int}(c_2) = \emptyset$ for $c_1, c_2 \in \mathcal{C}$ with $c_1 \neq c_2$,
2. $\bigcup_{c \in \mathcal{C}} c = \mathbb{R}^2$,
3. $|\{c \in \mathcal{C} \mid C \cap B \neq \emptyset\}| < \infty$ for any bounded $B \subset \mathbb{R}^2$.

In words, this means given the two-dimensional Euclidean space, a tessellation is a division into a set of non-overlapping cells, whose union covers the whole plane and which is locally finite. Note that a tessellation can alternatively be interpreted as the union of the boundaries of the polygons, called the skeleton of the tessellation, and denoted by $\mathcal{S}_{\mathcal{C}}$.

Let \mathbb{T} be the set of all planar tessellations and \mathfrak{T} the σ -algebra of \mathbb{T} generated by

$$\{\mathcal{C} \in \mathbb{T} : \mathcal{S}_{\mathcal{C}} \cap [-r, r]^2 \neq \emptyset\}$$

for all $r > 0$. A *random* planar tessellation is then given by a random variable Γ in $[\mathbb{T}, \mathfrak{T}]$. The properties of stationarity and isotropy can be defined analogously to their definitions for random measures. A random tessellation Γ is called *stationary* if it is invariant under shifts. More formally, for all $x \in \mathbb{R}^2$ it yields

$$\Gamma \stackrel{D}{=} \Gamma + x.$$

Moreover, it is called *isotropic* if

$$\Gamma \stackrel{D}{=} \vartheta \Gamma$$

for all rotations $\vartheta \in SO_2$.

4.2 Construction of a STIT tessellation

STIT tessellations were introduced by Nagel and Weiß [24] for the d -dimensional Euclidean space. We give a simplified description of its construction for the case of \mathbb{R}^2 , which is sufficient for the content of this thesis.

Imagine the 2-dimensional Euclidean space and a window of observation $W = [-r, r]^2, r > 0$. This window is given a lifetime, which is exponentially distributed. After its lifetime has passed, the window is divided by a random line L into two cells, say $W_+ = W \cap L^+$ and $W_- = W \cap L^-$ where L^+ and L^- denote the two half-planes induced by L . This process can be repeated by associating independent lifetimes to W_+ and W_- after which these cells are cut by a random line again. At a given observation time t this process is stopped. At that time, W is divided into a random number of non-intersecting random polygons. This state is called the realization of the tessellation within W and is denoted by $Y(t, W)$. A picture of such a process is shown in Figure 4.1.

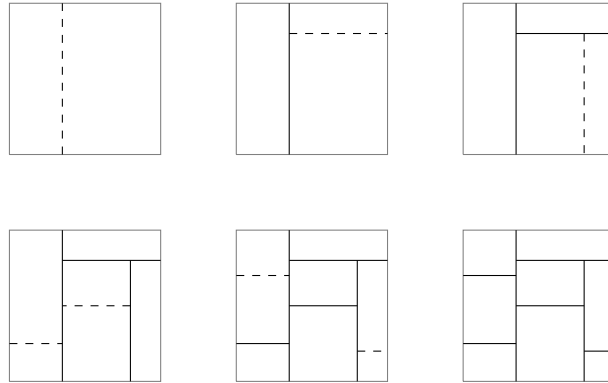


FIGURE 4.1: Schematic construction of a planar STIT tessellation within a square observation window with only two directions of cutting at different times.

More precise, we give a description for the lifetimes and the distribution of the random lines used in this construction. Let $[\mathbb{R}^2]$ be the space of lines in \mathbb{R}^2 and $[\mathbb{R}^2]_0$ the lines passing through the origin. These spaces come with natural Borel σ -fields. Note that each line in \mathbb{R}^2 is completely determined by its angle α to the x -axis and their minimal signed distance r towards the origin (see Figure 4.2).

One may identify $[\mathbb{R}^2]$ as the product of $[0, \pi) \times \mathbb{R}$ and define a locally finite and translation-invariant probability measure $\Lambda = \vartheta \times \ell$ on this product. In this setting, ϑ is called the directional measure and ℓ is the Lebesgue measure on \mathbb{R} . For any polygon A , we write $[A]$

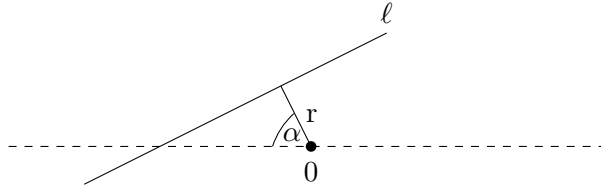


FIGURE 4.2: Visualization of a line ℓ in \mathbb{R}^2 being parameterized by its angle α and distance from the origin r .

for all lines $g \in [\mathbb{R}^2]$ intersecting with A , *i.e.*,

$$[A] = \{g \in [\mathbb{R}^2] \mid g \cap A \neq \emptyset\} \in \mathfrak{B}([\mathbb{R}^2]).$$

With these ideas how to describe lines and their intersection with polygons we will complete the construction of a STIT tessellation by giving information about the life-time of cells and the distribution of lines added to this process.

Given a cell $c \subset \mathbb{R}^2$, we set $\Lambda([c])$ as parameter, with which its lifetime is exponentially distributed. Moreover, $\Lambda(\cdot \cap [c])/\Lambda([c])$ is the distribution according to which a cell c is split by a line. Further restrictions on the probability measure Λ are widely known and often used whenever general computations become too complicated. In this thesis, two restrictive sub-classes of STITs are of importance.

Isotropic STIT: Tessellations which are invariant under rotation are called isotropic. The definition of Λ given in the construction above will result in such an isotropic STIT tessellation if and only if ϑ is the uniform distribution on $[0, \pi)$. This class is studied extensively in a number of publications, see for example [17, 18, 19, 28, 29].

Mondrian tessellations: Reminiscent of the famous painting by Piet Mondrian, the Mondrian tessellations are restricted to axis-parallel line segments, which can be equipped with equal or non-equal weights. For this, let $\{e_1, e_2\}$ be the standard orthonormal basis of \mathbb{R}^2 and $E_i = \text{span}(e_i)$ for $i \in \{1, 2\}$. A weighted planar Mondrian tessellation is given by a STIT tessellation $Y(t, W)$ for which

$$\Lambda_p(\cdot) = p \int_{\mathbb{R}} \mathbf{1}(E_1 + \tau e_2 \in \cdot) d\tau + (1-p) \int_{\mathbb{R}} \mathbf{1}(E_2 + \tau e_1 \in \cdot) d\tau \quad (4.1)$$

is chosen as the driving measure on the space $[\mathbb{R}^2]$ for some weight parameter $p \in (0, 1)$ and time parameter $t > 0$. One may rewrite this measure in terms of the product space $[0, \pi) \times \mathbb{R}$ with the Dirac measure on 0 and $\pi/2$ and the Lebesgue measure on \mathbb{R} .

A visualization of an planar isotropic STIT tessellation and a planar weighted Mondrian tessellation with weight $p = 0.5$ is given in Figure 1.1.

Since these set-ups will appear in different chapters of this thesis, we are going to use $Y(t, W)$ as a general notation for Mondrian tessellations in Chapter 5 and for isotropic STIT tessellation in Chapter 6.

4.3 Properties of STIT tessellations

In the remainder of this section, we will explain important properties of tessellations needed for the results in Chapter 5 and Chapter 6.

First, one might question the effect of W used in the construction of a STIT tessellation. It is well known by [18] that STIT tessellations can be extended to the whole plane, thus the choice of W does not matter. This property is due to their consistency which means that the intersection of a given tessellation in W , *i.e.*, $Y(t, W)$ and a set V with $V \subseteq W$, is equal in distribution to a tessellation of V . More formally, this is

$$Y(t, W) \cap V \stackrel{D}{=} Y(t, V).$$

This property implies that there exists a global and stationary tessellation $Y(t)$ such that

$$Y(t) \cap W \stackrel{D}{=} Y(t, W)$$

for all compact and convex $W \subset \mathbb{R}^2$. STIT tessellations satisfy this condition. Nagel and Biehler [4] even proved that the measure Λ used for the construction of a STIT tessellation is the only suitable measure which allows a consistent extension.

Already emphasized by their name, another important property of STIT tessellations is their stability under iteration. The idea of a single iteration is described as follows. Let $\{c_{0,k} | k \in \mathbb{N}_{\geq 1}\}$ be the set of cells in Y_0 and define $\{Y_1^{c_{0,k}} | c_{0,k} \in Y_0\}$ as the set of independent but identically distributed copies of Y_1 . Thus, there is one copy of Y_1 for each cell in Y_0 . The iteration of Y_0 with Y_1 is then given by

$$Y_0 \boxtimes Y_1 = \{c_{0,k} \cap c_{k,i} \mid c_{0,k} \in Y_0, c_{k,i} \in Y_1^{c_{0,k}} \text{ with } \text{int}(c_{0,k}) \cap \text{int}(c_{k,i}) \neq \emptyset\}.$$

A picture of such an iteration is seen in Figure 4.3. This idea of iterating two tessellation can be extended to multiple iterations.

Definition 4.3.1 A random stationary tessellation Y is called *stable under iteration* (or STIT) if

$$Y \stackrel{D}{=} \underbrace{n(Y \boxtimes \dots \boxtimes Y)}_{\text{n-times}}$$

for all $n \in \mathbb{N}$.

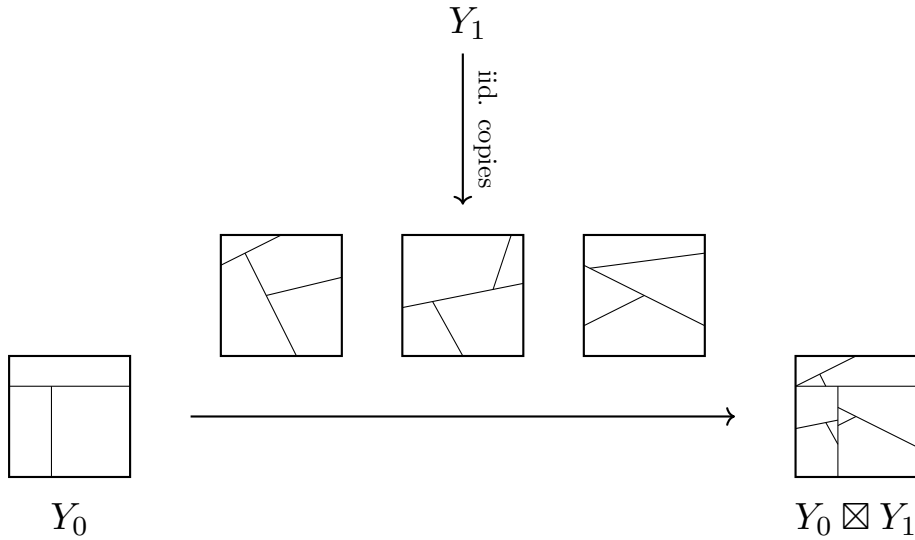


FIGURE 4.3: Schematic visualization of an iteration of Y_0 with Y_1 . The three iid copies of Y_1 are iterated in the upper, lower left, and lower right cell (from left to right) of Y_0 .

Another interesting property of a STIT tessellation is given by the point process induced by certain intersection points. Given a STIT tessellation $Y(t)$ and a fixed line $g \in [\mathbb{R}^2]$, Nagel and Weiß showed in [23, Lemma 5] that the process induced by the intersection points of g and the skeleton of $Y(t)$ is a stationary Poisson point process on g . This is that given an interval where g intersects W , the number of intersection points of g with the skeleton of $Y(t)$ is Poisson distributed. Whats more, for a collection of non overlapping intervals, the random variables counting the number of points in each interval are independent.

Chapter 5

Probabilistic analysis of Mondrian tessellations

This chapter is based on research together with Betken, Kaufmann and Thäle in [3]. Throughout this chapter, a tessellation $Y(t, W)$ is understood as a planar Mondrian tessellation with time parameter $t > 0$ and within an observation window $W \subset \mathbb{R}^2$ being a convex polygon. The main results will be stated in Section 5.1. Concrete formulas for the (co-)variances for the number of maximal edges in $Y(t, W)$ and the weighted total edge length of $Y(t, W)$ will be presented in Section 5.2. A somehow modified version of the known pair- and cross-correlation functions will be given in Section 5.3.

5.1 Main results

5.1.1 Set-up

Given a square $W = [-r, r]^2 \subset \mathbb{R}^2$ with $r > 0$, a time parameter $t > 0$ and a Mondrian tessellation $Y(t, W)$. We follow [28] and define $\Sigma_\phi(Y)$ and $A_\phi(Y)$ for some bounded and measurable functional ϕ on line segments, *i.e.*, on $[\mathbb{R}^2] \cap W$. Let Y be a realization of $Y(t, W)$ for some $t > 0$. We define

$$\Sigma_\phi(Y) := \sum_{e \in \text{MaxEdges}(Y)} \phi(e), \quad (5.1)$$

and

$$A_\phi(Y) = \int_{[W]} \sum_{e \in \text{Segments}(Y \cap L)} \phi(e) \Lambda_p(dL), \quad (5.2)$$

with $L \in [W]$ and where $MaxEdges(Y)$ are the cell splitting edges, which are referred to as I-segments later in Chapter 6.

There are two explicit functionals ϕ of interest in this chapter.

1. Let $\phi \equiv 1$. Then $\Sigma_\phi(Y)$ simply counts the number of maximal edges in Y .
2. Let $\phi(e) = \Lambda_p([e])$ as given in Equation (4.1). Then $\Sigma_\phi(Y)$ is the weighted total edge length of Y , where all maximal edges parallel to e_1 are weighted by p and those parallel to e_2 are weighted with $1 - p$. This follows from the fact that for any measurable set $A \subset \mathbb{R}^2$, the expression $\Lambda_p([A])$ simplifies to

$$\begin{aligned} \Lambda_p([A]) &= p \int_{\mathbb{R}} \mathbf{1}(E_1 + \tau e_2 \in [A]) d\tau + (1 - p) \int_{\mathbb{R}} \mathbf{1}(E_2 + \tau e_1 \in [A]) d\tau \quad (5.3) \\ &= p \ell_1(\Pi_{E_2} A) + (1 - p) \ell_1(\Pi_{E_1} A), \end{aligned}$$

where $\Pi_{E_i}(A)$ denotes the orthogonal projection of A onto E_i for $i \in \{1, 2\}$.

5.1.2 Variances

This section states the results about the variances of Σ_{Λ_p} and Σ_1 and their covariance. We start by giving an easier result of their expected values known from [28, Section 2.3] as a proposition.

Proposition 5.1.1 ([3, Proposition 2.1]) *Consider a Mondrian tessellation $Y(t, W)$ with weight $p \in (0, 1)$. Then, for any compact and convex $W \subset \mathbb{R}^2$,*

$$\mathbb{E}[\Sigma_{\Lambda_p}(Y(t, W))] = 2tp(1 - p)\ell_2(W)$$

and

$$\mathbb{E}[\Sigma_1(Y(t, W))] = t^2 p(1 - p) \ell_2(W) + t(p \ell_1(\Pi_{E_2} W) + (1 - p) \ell_1(\Pi_{E_1} W)).$$

If $W = [-a, a] \times [-b, b]$, with $a, b > 0$, these expressions specify to

$$\mathbb{E}[\Sigma_{\Lambda_p}(Y(t, W))] = 8tp(1 - p)ab \quad \text{and} \quad \mathbb{E}[\Sigma_1(Y(t, W))] = 4t^2 p(1 - p)ab + 2t(pb + (1 - p)a).$$

We now turn to second-order properties of these functionals and remark that for general planar STIT tessellations, results are known from [28, Theorem 1]. These quite abstract formulas for the variance and covariance of Σ_1 and Σ_{Λ_p} have been specified to isotropic STIT tessellations using integral geometry (see for instance [28, Section 3.4]). It turned out that specifying them to Mondrian tessellations isn't a trivial task.

Theorem 5.1.2 [28, Theorem 2.3] *Let $W = [-a, a] \times [-b, b]$, with $a, b > 0$, be an observation window, and let $Y(t, W)$ be a Mondrian tessellation with weight $p \in (0, 1)$.*

(i) *The variance of the weighted total edge length Σ_{Λ_p} of $Y(t, W)$ is given by*

$$\mathbb{V}[\Sigma_{\Lambda_p}(Y(t, W))] = -8abp(1-p) \left((1-p)g_1(2at(1-p)) + pg_1(2btp) \right)$$

with $g_1(x) = \sum_{k=1}^{\infty} (-1)^k \frac{x^k}{k(k+1)!}$ non-positive and monotonically decreasing on $[0, \infty)$.

(ii) *The variance of the number of maximal edges Σ_1 of $Y(t, W)$ is given by*

$$\begin{aligned} \mathbb{V}[\Sigma_1(Y(t, W))] &= 2tbp + 2ta(1-p) + 12abt^2p(1-p) \\ &\quad - 16abt^2p(1-p) \left((1-p)g_2(2a(1-p)t) + pg_2(2btp) \right) \end{aligned}$$

with $g_2(x) = \sum_{k=1}^{\infty} (-1)^k \frac{x^k}{k(k+1)(k+2)!}$.

(iii) *The covariances of Σ_1 and Σ_{Λ_p} for $Y(t, W)$ is given by*

$$\begin{aligned} \text{Cov}(\Sigma_{\Lambda_p}(Y(t, W)), \Sigma_1(Y(t, W))) \\ = 8tabp(1-p) \left(1 - [(1-p)g_3(2at(1-p)) + pg_3(2btp)] \right) \end{aligned}$$

with $g_3(x) = \sum_{k=1}^{\infty} (-1)^k \frac{x^k}{k(k+1)(k+1)!}$.

We can specialize these results by choosing a square as the window of observation, *i.e.*, $W = Q_r = [-r, r]^2$ with $r > 0$. Moreover, we will examine the behavior of the variance as r approaches infinity. We write $f(x) \asymp g(x)$ if for two functions $f, g : [0, \infty) \mapsto \mathbb{R}$, it is $\frac{f(x)}{g(x)} \mapsto 1$ as $x \mapsto \infty$.

Corollary 5.1.3 ([3, Corollary 2.4]) *Let $Q_r = [-r, r]^2$ with $r > 0$ be a square and $Y(t, Q_r)$ be a Mondrian tessellation with weight $p \in (0, 1)$. Then, as $r \rightarrow \infty$,*

$$\mathbb{V}[\Sigma_{\Lambda_p}(Y(t, Q_r))] \asymp 8p(1-p)r^2 \log(r), \quad \mathbb{V}[\Sigma_1(Y(t, Q_r))] \asymp 8t^2p(1-p)r^2 \log(r)$$

and

$$\text{Cov}(\Sigma_{\Lambda_p}(Y(t, Q_r)), \Sigma_1(Y(t, Q_r))) \asymp 8tp(1-p)r^2 \log(r).$$

Remark 5.1.4 ([3, Remark 2.5]) Since asymptotic formulas are also known for isotropic planar STIT tessellations and rectangular Poisson line processes, it seems reasonable to compare their results with the one for weighted Mondrians. By Λ_{iso} we denote the isometric invariant measure on the space of lines in \mathbb{R}^2 and normalize the measure in such a way that its value for lines passing the square $[0, 1]^2$ equals $\frac{4}{\pi}$. More formally, this is $\Lambda_{\text{iso}}([0, 1]^2) = \frac{4}{\pi}$.

It is also used in literature like [27].

- (i) For the isotropic STIT tessellation, we combine results from [28, Sections 3.4] and [29, Theorem 3] to obtain

$$\mathbb{V}[\Sigma_{\Lambda_{\text{iso}}}(Y(t, B_r^2))] \asymp \frac{16}{\pi} r^2 \log(r) \quad \text{and} \quad \mathbb{V}[\Sigma_1(Y(t, B_r^2))] \asymp \frac{16}{\pi} t^2 r^2 \log(r),$$

where B_r^2 is a disc of radius $r > 0$ and $r \mapsto \infty$. For the covariance, it can be deduced from [28, Theorem 1] that

$$\text{Cov}(\Sigma_{\Lambda_{\text{iso}}}(Y(t, B_r^2)), \Sigma_1(Y_t(B_r^2))) \asymp \frac{16}{\pi} t r^2 \log(r).$$

- (ii) For the rectangular Poisson line process we consider the stationary planar Poisson line process, η_p with intensity measure $t\Lambda_p$ for $t > 0$ and a square $Q_r = [-r, r]^2$ with $r > 0$. The variances for the weighted edge length and the number of maximal edges are given by

$$\mathbb{V}[\Sigma_{\Lambda_p}(Q_r)] = 4tp(1-p)r^3 \quad \text{and} \quad \mathbb{V}[\Sigma_1(Q_r)] \asymp 2t^3p(1-p)r^3,$$

respectively.

5.1.3 Correlation Function

In case of isotropic planar STIT tessellations, explicit formulas for the pair-correlations function of the vertex point process and the random edge length measure were derived in [28] and [29], respectively. Moreover, the cross-correlation function between the point process and the random length measure is given in [28]. To find analogues of these correlation functions, their concepts need to be adapted to the setting of planar Mondrian tessellations in a suitable way. For that, let $Y(t)$ be a weighted planar Mondrian tessellation with $t > 0$ and weight $p \in (0, 1)$. Let $R_p = [0, 1-p] \times [0, p]$ be a rectangle depending on the weight parameter p and $R_{r,p} = rR_p$ be a rescaled version with $r > 0$. In order to obtain analogues of Ripley's K-function, we may consider $Y(t)$ under the Palm distribution with respect to the random edge length measure \mathcal{E}_t concentrated on its skeleton. Then, following [32], we let $t^2 K_{\mathcal{E}}(r)$ be the total edge length of $Y(t)$ in $R_{r,p}$. Similarly, we may consider $Y(t)$ under the Palm distribution with respect to the random vertex point process \mathcal{V}_t . With $\lambda_{\mathcal{V}} = t^2 p(1-p)$ denoting the intensity of the vertex process in $Y(t)$, we let $\lambda_{\mathcal{V}}^2 K_{\mathcal{V}}(r)$ be the total number of vertices of $Y(t)$ in $R_{r,p}$ again. Whereas usually a ball of radius $r > 0$ is considered in Ripley's K-function, when the driving measure is isotropic, we consider $R_{r,p}$ instead, because Λ_p is non-isotropic. More precisely, the ball is the associated zonoid related to an isotropic directional distribution (see [27, Section 4.6]), whereas the rectangle with side length p and $1-p$ is the one related to the directional distribution used in the Mondrian case.

Since these functions are still quite complicated, we will provide their normalized derivatives, which in our cases exist. A suitable normalization is

$$g_{\mathcal{E}}(r) = \frac{1}{2p(1-p)r} \frac{dK_{\mathcal{E}}(r)}{dr} \quad \text{and} \quad g_{\mathcal{V}}(r) = \frac{1}{2p(1-p)r} \frac{dK_{\mathcal{V}}(r)}{dr}, \quad (5.4)$$

where the dependence on $t > 0$ is suppressed for better readability. Since these modified functions are based on a rectangular $R_{r,p}$ instead of a ball of radius r , we use $2p(1+p)r$ instead of $2\pi r$ for normalization. This means that instead of $\Lambda_{\text{iso}}([B_r^2]) = 2\pi r$, one uses $\Lambda_p([R_{r,p}]) = 2p(1+p)r$ for normalization. Given these little distinctions, we refer to these functions as *Mondrian pair-correlation function* of \mathcal{E}_t and \mathcal{V}_t , respectively. Following similar thoughts, we define the *Mondrian cross-correlation function* of \mathcal{E}_t and \mathcal{V}_t , based on the known definition of the cross K-function for the isotropic case, by

$$g_{\mathcal{E},\mathcal{V}}(r) = \frac{1}{2p(1-p)r} \frac{dK_{\mathcal{E},\mathcal{V}}(r)}{dr}. \quad (5.5)$$

The dependence on $t > 0$ is suppressed again.

For stationary and isotropic STIT tessellations, Schreiber and Thäle provided the edge-pair-correlation function in [29, Theorem 7.1], as well as the vertex-pair-correlation and cross-correlation function in [28, Corollary 4 & 3]. We now state their Mondrian analogue.

Theorem 5.1.5 ([3, Theorem 2.6]) *Let $Y(t)$ be a Mondrian tessellation with weight $p \in (0, 1)$ and time parameter $t > 0$. Then*

$$g_{\mathcal{E}}(r) = 1 + \frac{1}{2t^2r^2} \left(\frac{1}{p^2} + \frac{1}{(1-p)^2} - \frac{e^{-trp^2}}{p^2} - \frac{e^{-tr(1-p)^2}}{(1-p)^2} \right).$$

Theorem 5.1.6 ([3, Theorem 2.7]) *Let $Y(t)$ be a Mondrian tessellation with weight $p \in (0, 1)$ and time parameter $t > 0$. Then*

$$g_{\mathcal{E},\mathcal{V}}(r) = 1 + \frac{1}{t^2r^2p(1-p)} \left[\frac{1}{p} + \frac{1}{1-p} - \frac{1}{2tr(1-p)^3} - \frac{1}{2trp^3} - e^{-tr(1-p)^2} \left(\frac{1}{2(1-p)} - \frac{1}{2tr(1-p)^3} \right) - e^{-trp^2} \left(\frac{1}{2p} - \frac{1}{2trp^3} \right) \right].$$

Theorem 5.1.7 ([3, Theorem 2.8]) *Let Y_t be a Mondrian tessellation with weight $p \in (0, 1)$ and time parameter $t > 0$. Then*

$$g_{\mathcal{V}}(r) = 1 + \frac{1}{t^2r^2p^2(1-p)^2} \left[4 - \frac{2}{trp^2} + \frac{1}{t^2r^2p^4} - \frac{2}{tr(1-p)^2} + \frac{1}{t^2r^2(1-p)^4} \right]$$

$$\left. -e^{-trp^2} \left(\frac{1}{2} - \frac{1}{trp^2} + \frac{1}{t^2r^2p^4} \right) - e^{-tr(1-p)^2} \left(\frac{1}{2} - \frac{1}{tr(1-p)^2} + \frac{1}{t^2r^2(1-p)^4} \right) \right].$$

For $t = 1$, the dependence of $g_{\mathcal{E}}(r)$, $g_{\mathcal{E},\mathcal{V}}(r)$ and $g_{\mathcal{V}}(r)$ on r is shown in Figure 5.1 for different weights $p \in \{0.5, 0.75, 0.9\}$.

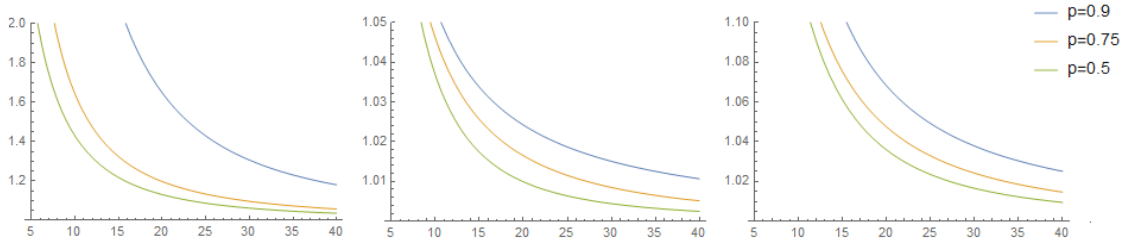


FIGURE 5.1: Let $t = 1$. From left to right: $g_{\mathcal{E}}(r)$, $g_{\mathcal{E},\mathcal{V}}(r)$, and $g_{\mathcal{V}}(r)$.

Remark 5.1.8 ([3, Remark 2.9]) As before, one might compare these results to their equivalent statements for the planar isotropic STIT tessellations and the rectangular Poisson line process.

- (i) For the isotropic case, it is shown by Schreiber and Thäle in [30] that the pair-correlation function of the random edge length measure \mathcal{E}_t has the form

$$g_{\mathcal{E}}(r) = 1 + \frac{1}{2t^2r^2} \left(1 - e^{-\frac{2}{\pi}tr} \right).$$

The same authors have shown in [29] that the pair-correlation function of the vertex point process \mathcal{V}_t and the cross-correlation function of the random edge length measure and the vertex point process are given as follows:

$$g_{\mathcal{E},\mathcal{V}}(r) = 1 + \frac{1}{t^2r^2} - \frac{\pi}{4t^3r^3} - \frac{e^{-\frac{2}{\pi}tr}}{2t^2r^2} \left(1 - \frac{\pi}{2tr} \right)$$

and

$$g_{\mathcal{V}}(r) = 1 + \frac{2}{t^2r^2} - \frac{\pi}{t^3r^3} + \frac{\pi^2}{4t^4r^4} - \frac{e^{-\frac{2}{\pi}tr}}{2t^2r^2} \left(1 - \frac{\pi}{tr} + \frac{\pi^2}{2t^2r^2} \right).$$

- (ii) For the rectangular Poisson line process, which was defined in more detail in Remark 5.1.4, one uses the theorem of Slivnyak-Mecke (see for example [33, Example 4.3]) to conclude that the cross- and pair-correlation functions in this setting are given by

$$g_{\mathcal{E}}(r) = 1 + \frac{1}{tr}, \quad g_{\mathcal{E},\mathcal{V}}(r) = 1 + \frac{1}{4trp(1-p)} \quad \text{and} \quad g_{\mathcal{V}}(r) = 1 + \frac{1}{2trp^2(1-p)^2}.$$

5.2 Expected value and variance for Mondrian tessellations

In order to obtain first and second order properties, one usually makes use of the functionals Σ_ϕ and A_ϕ along with some martingale results already proven in [28, Proposition 1]. In Section 5.2.1, we start by introducing the point intersection measure and then prove the stated expected values for Σ_1 and Σ_{Λ_p} . The definition of the segment intersection measure and the proof of the variances for these functionals are given in Section 5.2.2.

5.2.1 The point intersection measure and expected values

We start with the definition of the *point intersection measure* on \mathbb{R}^2 , which will be our main tool for proving first order properties. It is given by

$$\llcorner \Lambda_p \cap \Lambda_p \gg (\cdot) := \int_{[\mathbb{R}^2]} \int_{[L]} \mathbf{1}(L \cap L' \in \cdot) \Lambda_p(dL') \Lambda_p(dL).$$

Applied to our setting of planar Mondrian tessellations, L and L' are restricted to axis-parallel lines, *i.e.* $L = E_i + \tau e_j$ and $L' = E_j + \sigma e_i$ for $i, j \in \{1, 2\}$ and $i \neq j$. Together with their weights, we can conclude for a measurable set $A \subset \mathbb{R}^2$ that

$$\begin{aligned} \llcorner \Lambda_p \cap \Lambda_p \gg (A) &= \int_{[\mathbb{R}^2]} \int_{[L]} \mathbf{1}(L \cap L' \cap A \neq \emptyset) \Lambda_p(dL') \Lambda_p(dL) \\ &= 2p(1-p) \int_{\mathbb{R}} \int_{\mathbb{R}} \mathbf{1}((E_2 + \tau e_1) \cap (E_1 + \sigma e_2) \cap A \neq \emptyset) d\sigma d\tau \\ &= 2p(1-p) \int_{\mathbb{R}} \ell_1((E_2 + \tau e_1) \cap A) d\tau \\ &= 2p(1-p) \ell_2(A). \end{aligned} \tag{5.6}$$

Together with results from [28], we can prove the stated expectations.

Proof of Proposition 5.1.1. General expressions for the expected values are given in [28, Equations (8) and (9)] by

$$\mathbb{E}[\Sigma_{\Lambda_p}(Y(t, W))] = t \llcorner \Lambda_p \cap \Lambda_p \gg (W) \tag{5.7}$$

$$\text{and } \mathbb{E}[\Sigma_1(Y(t, W))] = t\Lambda_p([W]) + \frac{t^2}{2} \llcorner \Lambda_p \cap \Lambda_p \gg (W). \tag{5.8}$$

For Σ_{Λ_p} we combine (5.6) and (5.7) to conclude that

$$\mathbb{E}[\Sigma_{\Lambda_p}(Y(t, W))] = 2tp(1-p)\ell_2(W)$$

and for $W = [-a, a] \times [-b, b]$ with $a, b > 0$, it is

$$\mathbb{E}[\Sigma_{\Lambda_p}(Y(t, W))] = 8abt p(1-p).$$

For Σ_1 , we combine (5.3) and (5.8) to conclude that

$$\mathbb{E}[\Sigma_1(Y(t, W))] = t(p\ell_1(\Pi_{E_2}W) + (1-p)\ell_1(\Pi_{E_1}W)) + \frac{t^2}{2}2p(1-p)\ell_2(W)$$

and for $W = [-a, a] \times [-b, b]$ $a, b > 0$, it is

$$\mathbb{E}[\Sigma_1(Y(t, W))] = 4t^2p(1-p)ab + 2t(pb + (1-p)a).$$

□

5.2.2 The segment intersection measure and variances

In order to calculate the variances, we introduce the *segment intersection measure*, which is defined on the space of all line segments in \mathbb{R}^2 , denoted by $\mathcal{S}(\mathbb{R}^2)$. It is given by

$$\ll (\Lambda_p \times \Lambda_p) \cap \Lambda_p \gg (\cdot) := \int_{[\mathbb{R}^2]} \int_{[L]} \int_{[L]} \delta_{L(L_1, L_2)}(\cdot) \Lambda_p(dL_1) \Lambda_p(dL_2) \Lambda_p(dL), \quad (5.9)$$

where δ_x is the Dirac measure for a point $x \in \mathbb{R}^2$. This measure will be used for proving the properties of second order. Given a measurable set $A \subset \mathbb{R}^2$ and $\mathcal{S}(A)$ as the space of all line segments completely lying in A , one get

$$\begin{aligned} \ll (\Lambda_p \times \Lambda_p) \cap \Lambda_p \gg (\mathcal{S}(A)) &= \int_{[\mathbb{R}^2]} \int_{[L]} \int_{[L]} \delta_{L(L_1, L_2)}(\mathcal{S}(A)) \Lambda_p(dL_1) \Lambda_p(dL_2) \Lambda_p(dL) \\ &= \int_{[\mathbb{R}^2]} \int_{[L]} \int_{[L]} \mathbf{1}\{L(L_1, L_2) \subset A\} \Lambda_p(dL_1) \Lambda_p(dL_2) \Lambda_p(dL), \end{aligned}$$

where we recall that for a line L intersecting with L_1, L_2 , we write $L(L_1, L_2)$ for the segment between the intersection points. We will continue this consideration with a case distinction.

We first consider $L = E_1 + \sigma e_2$, and since lines of this direction appear with weight p , part of the integral can be written as

$$p \int_{\mathbb{R}} \int_{[E_1 + \sigma e_2]} \int_{[E_1 + \sigma e_2]} \mathbf{1}\{\overline{(E_1 + \sigma e_2) \cap L_1, (E_1 + \sigma e_2) \cap L_2} \subset A\} \Lambda_p(dL_1) \Lambda_p(dL_2) d\sigma. \quad (5.10)$$

In order to have $(E_1 + \sigma e_2) \cap L_i \neq \emptyset$ for $i \in \{1, 2\}$, the lines $(E_1 + \sigma e_2)$ and L_1, L_2 have to be perpendicular. Thus, in this case it is $L_1 = E_2 + \tau_1 e_1$ and $L_2 = E_2 + \tau_2 e_1$ for some $\tau_1, \tau_2 \in \mathbb{R}$. It easily follows that their intersection points are given as (τ_1, σ) and (τ_2, σ) which leads to (5.10) being equal to

$$= p(1-p)^2 \int_{\mathbb{R}} \int_{\mathbb{R}} \int_{\mathbb{R}} \mathbf{1}\{\overline{(\tau_1, \sigma), (\tau_2, \sigma)} \subset A\} d\tau_1 d\tau_2 d\sigma. \quad (5.11)$$

We now consider $L = E_2 + \sigma e_1$. With similar deliberations as before, it is

$$\begin{aligned} & (1-p) \int_{\mathbb{R}} \int_{[E_2 + \sigma e_1]} \int_{[E_2 + \sigma e_1]} \mathbf{1}\{\overline{(E_2 + \sigma e_1) \cap L_1, (E_2 + \sigma e_1) \cap L_2} \subset A\} \Lambda_p(dL_1) \Lambda_p(dL_2) d\sigma \\ &= (1-p)p^2 \int_{\mathbb{R}} \int_{\mathbb{R}} \int_{\mathbb{R}} \mathbf{1}\{\overline{(\sigma, \tau_1), (\sigma, \tau_2)} \subset A\} d\tau_1 d\tau_2 d\sigma. \end{aligned} \quad (5.12)$$

At this point, we can finally give a more explicit formula for the segment intersection measure in our setting by adding (5.11) and (5.12). We obtain

$$\begin{aligned} \ll (\Lambda_p \times \Lambda_p) \cap \Lambda_p \gg (\mathcal{S}(A)) &= p(1-p)^2 \int_{\mathbb{R}} \int_{\mathbb{R}} \int_{\mathbb{R}} \mathbf{1}\{\overline{(\tau_1, \sigma), (\tau_2, \sigma)} \subset A\} d\tau_1 d\tau_2 d\sigma \\ &+ (1-p)p^2 \int_{\mathbb{R}} \int_{\mathbb{R}} \int_{\mathbb{R}} \mathbf{1}\{\overline{(\sigma, \tau_1), (\sigma, \tau_2)} \subset A\} d\tau_1 d\tau_2 d\sigma. \end{aligned} \quad (5.13)$$

We are now able to combine this formula of the segment intersection measure with known results from [28] to prove the stated variances for Σ_{Λ_p} and Σ_1 .

Proof of Theorem 5.1.2. First, we combine [28, Theorem 1] and Equations (13) and (14) in [28] to obtain

$$\begin{aligned} \mathbb{V}[\Sigma_{\Lambda_p}(Y(t, W))] &= \int_0^t \int_{[W]} \int_{[L \cap W]} \int_{[L \cap W]} \exp(-u \Lambda_p([L(L_1, L_2)])) \Lambda_p(dL_2) \Lambda_p(dL_1) \Lambda_p(dL) du \\ &= \int_{[W]} \int_{[L \cap W]} \int_{[L \cap W]} \frac{1}{\Lambda_p([L(L_1, L_2)])} \left(\exp(-t \Lambda_p([L(L_1, L_2)])) - 1 \right) \\ &\quad \times \Lambda_p(dL_2) \Lambda_p(dL_1) \Lambda_p(dL) \end{aligned}$$

by Fubini's theorem. As already discussed before, it is necessary that L is perpendicular to

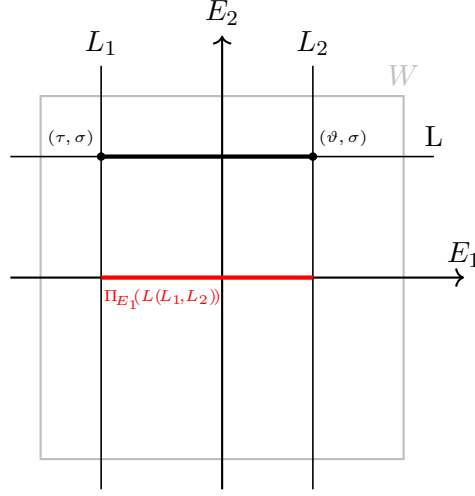


FIGURE 5.2: Visualization of the projection $\Pi_{E_1}(L(L_1, L_2))$ of $L(L_1, L_2)$ with $L_1 = E_2 + \tau e_1$, $L_2 = E_2 + \vartheta e_1$ and $L = E_1 + \sigma e_2$.

L_1, L_2 to ensure $L(L_1, L_2) \neq \emptyset$. Thus, we consider

$$L = E_i + \sigma e_j, \quad L_1 = E_j + \tau e_i, \quad \text{and} \quad L_2 = E_j + \vartheta e_i$$

for some $\sigma, \tau, \vartheta \in \mathbb{R}$ and $i, j \in \{1, 2\}$ with $i \neq j$.

For $i = 1, j = 2$, it is $L = E_1 + \sigma e_2$, $L_1 = E_2 + \tau e_1$ and $L_2 = E_2 + \vartheta e_1$. Using the definition of $\Lambda_p(\cdot)$ as in (5.3), we have

$$\Lambda_p([L(L_1, L_2)]) = (1 - p) |\tau - \vartheta| \mathbf{1}\{(\tau, \sigma) \in W\} \mathbf{1}\{(\vartheta, \sigma) \in W\}.$$

The situation is visualized in Figure 5.2.

For $i = 2, j = 1$, we get by using analog considerations that

$$\Lambda_p([L(L_1, L_2)]) = p |\tau - \vartheta| \mathbf{1}\{(\sigma, \tau) \in W\} \mathbf{1}\{(\sigma, \vartheta) \in W\}.$$

Hence, these two cases are considered to conclude

$$\begin{aligned} \mathbb{V}[\Sigma_{\Lambda_p}(Y(t, W))] &= - \int_{[W]} \int_{[L \cap W]} \int_{[L \cap W]} \frac{1}{\Lambda_p([L(L_1, L_2)])} \left(\exp(-t \Lambda_p([L(L_1, L_2)])) - 1 \right) \\ &\quad \times \Lambda_p(dL_2) \Lambda_p(dL_1) \Lambda_p(dL) \\ &= - \left(p(1 - p)^2 \int_{-b}^b \int_{-a}^a \int_{-a}^a \frac{1}{|\tau - \vartheta|} \left(\exp(-t(1 - p)|\tau - \vartheta|) - 1 \right) d\vartheta d\tau d\sigma \right) \end{aligned}$$

$$\begin{aligned}
 & + (1-p)p^2 \int_{-a}^a \int_{-b}^b \int_{-b}^b \frac{1}{|\tau - \vartheta|} \left(\exp(-tp|\tau - \vartheta|) - 1 \right) d\vartheta d\tau d\sigma \\
 & = -2 \left(p(1-p)^2 \int_{-b}^b \int_{-a}^a \int_{-a}^{\tau} \frac{1}{\tau - \vartheta} \left(\exp(-t(1-p)(\tau - \vartheta)) - 1 \right) d\vartheta d\tau d\sigma \right. \\
 & \quad \left. + (1-p)p^2 \int_{-a}^a \int_{-b}^b \int_{-b}^{\tau} \frac{1}{\tau - \vartheta} \left(\exp(-tp(\tau - \vartheta)) - 1 \right) d\vartheta d\tau d\sigma \right)
 \end{aligned}$$

by Fubini's theorem. For the inner integrals, we use the description of $\exp(x)$ by its formal power series and obtain

$$\begin{aligned}
 & \int_{-a}^{\tau} \frac{1}{\tau - \vartheta} \left(\exp(-t(1-p)(\tau - \vartheta)) - 1 \right) d\vartheta = \int_0^{\tau+a} \frac{1}{\vartheta} \left(\exp(-t(1-p)\vartheta) - 1 \right) d\vartheta \\
 & = \int_0^{\tau+a} \frac{1}{\vartheta} \sum_{k=1}^{\infty} (-1)^k \frac{(t(1-p)\vartheta)^k}{k!} d\vartheta = \sum_{k=1}^{\infty} (-1)^k \frac{(t(1-p))^k}{k!} \frac{(\tau+a)^k}{k}
 \end{aligned}$$

and

$$\int_{-b}^{\tau} \frac{1}{\tau - \vartheta} \left(\exp(-tp(\tau - \vartheta)) - 1 \right) d\vartheta = \sum_{k=1}^{\infty} (-1)^k \frac{(tp)^k}{k!} \frac{(\tau+b)^k}{k},$$

respectively. Continuing with the two integrals and using integration by substitution, it is

$$\int_{-b}^b \int_{-a}^a \sum_{k=1}^{\infty} (-1)^k \frac{(t(1-p))^k}{k!} \frac{(\tau+a)^k}{k} d\tau d\sigma = 4ab \sum_{k=1}^{\infty} (-1)^k \frac{(2at(1-p))^k}{(k+1)!k}$$

and

$$\int_{-a}^a \int_{-b}^b \sum_{k=1}^{\infty} (-1)^k \frac{(tp)^k}{k!} \frac{(\tau+b)^k}{k} d\tau d\sigma = 4ab \sum_{k=1}^{\infty} (-1)^k \frac{(2btp)^k}{(k+1)!k}.$$

Together with $g_1(x)$ as stated in Theorem 5.1.2(i), the result is proven.

Continuing with Theorem 5.1.2(ii), we combine Proposition 5.1.1 and Equation (12) from [28] to obtain

$$\mathbb{V}[\Sigma_1(Y(t, W))] = t\Lambda_p([W]) + 3 \int_0^t \mathbb{E}[\Sigma_{\Lambda_p}(Y(s, W))] ds + 2 \int_0^t \int_0^s \mathbb{V}[\Sigma_{\Lambda_p}(Y(u, W))] du.$$

Starting with the first expression, we use the definition of Λ_p as in (5.3) to conclude

$$t\Lambda_p([W]) = 2tbp + 2ta(1 - p).$$

For the second expression, we use Equation (8) in [28], which states that

$$3 \int_0^t \mathbb{E}[\Sigma_{\Lambda_p}(Y(s, W))] ds = \frac{3t^2}{2} \ll \Lambda_p \cap \Lambda_p \gg (W), \quad (5.14)$$

and which simplifies with (5.6) to

$$\frac{3}{2}t^2 \ll \Lambda_p \cap \Lambda_p \gg (W) = 12t^2abp(1 - p).$$

For the last term, we use Theorem 5.1.2 (i) to obtain

$$\begin{aligned} & 2 \int_0^t \int_0^s \mathbb{V}[\Sigma_{\Lambda_p}(Y(u, W))] du ds \\ &= -16abp(1 - p) \int_0^t \int_0^s \left((1 - p)g_1(2a(1 - p)u) + pg_1(2bpu) \right) du ds. \end{aligned}$$

Now, by using the definition of $g_1(x)$ as stated in Theorem 5.1.2(i), we get

$$\begin{aligned} \int_0^t \int_0^s g_1(2a(1 - p)u) du ds &= \sum_{k=1}^{\infty} (-1)^k \frac{(2a(1 - p))^k}{k(k + 1)!} \int_0^t \int_0^s u^k du ds \\ &= t^2 \sum_{k=1}^{\infty} (-1)^k \frac{(2a(1 - p)t)^k}{k(k + 1)(k + 2)!}, \end{aligned}$$

and similarly

$$\int_0^t \int_0^s g_1(2bpu) du ds = t^2 \sum_{k=1}^{\infty} (-1)^k \frac{(2bpt)^k}{k(k + 1)(k + 2)!}.$$

Adding all three terms and setting $g_2(x) = \sum_{k=1}^{\infty} (-1)^k \frac{x^k}{k(k+1)(k+2)!}$, the stated variance for Σ_1 follows.

Last, we prove the covariance stated in Theorem 5.1.2 (iii). We use Equations (11) and (8)

in [28] to see that

$$\text{Cov}(\Sigma_{\Lambda_p}(Y(t, W)), \Sigma_1(Y(t, W))) = t \ll \Lambda_p \cap \Lambda_p \gg (W) + \int_0^t \mathbb{V}[\Sigma_{\Lambda_p}(Y(s, W))] ds.$$

For the first term, one simply uses (5.6) to obtain

$$t \ll \Lambda_p \cap \Lambda_p \gg (W) = 8tabp(1-p).$$

For the integral, we conclude, using the definitions of Σ_{Λ_p} and $g_1(x)$, that

$$\begin{aligned} \int_0^t \mathbb{V}[\Sigma_{\Lambda_p}(Y_s(W))] ds &= -8abp(1-p) \int_0^t (1-p)g_1(2a(1-p)s) + pg_1(2bps) ds \\ &= -8abp(1-p) \sum_{k=1}^{\infty} (-1)^k \frac{(1-p)(2a(1-p))^k + p(2bp)^k}{k(k+1)!} \int_0^t s^k ds \\ &= -8tabp(1-p) \sum_{k=1}^{\infty} (-1)^k \frac{(1-p)(2at(1-p))^k + p(2btp)^k}{k(k+1)(k+1)!} \\ &= -8tabp(1-p) \left((1-p)g_3(2at(1-p)) + pg_3(2btp) \right), \end{aligned}$$

which in combination with the first term yields the result. \square

Proof of Corollary 5.1.3. One can check that $g_1(x) \asymp \log(x)$, $g_2(x) \asymp -\frac{1}{2}\log(x)$ and that $g_3(x) \asymp -\log(x)$, as $x \rightarrow \infty$. For example, by [6, Equation 1.1.3] one may rewrite

$$g_1(x) = 1 - \gamma - \Gamma(0, x) - \log(x) - \frac{1}{x} + \frac{\exp(-x)}{x}$$

where γ denotes the Euler-Mascheroni constant and $\Gamma(0, x)$ the upper incomplete Gamma-function, for which

$$\frac{\exp(-x)}{x} \left(1 - \frac{1}{x} \right) \leq \Gamma(0, x) \leq \frac{\exp(-x)}{x} \left(1 - \frac{1}{x} + \frac{1}{x^2} \right)$$

for $x \rightarrow \infty$ is satisfied by [6]. Thus, we conclude

$$g_1(x) \asymp -\log(x)$$

for $x \rightarrow \infty$. With Theorem 5.1.2, the results then follow. \square

5.3 Pair- and cross-correlations

The goal of this section is to establish the pair- and cross-correlation functions for Mondrian tessellations, as stated in Theorem 5.1.5, 5.1.6, and Theorem 5.1.7. To accomplish this, we will utilize results from [28, Section 3], which are stated in a more general setting than that of Mondrian tessellations. Therefore, we will need to perform certain computations to adapt these results to our specific case. We begin by collecting all relevant definitions and heavy computations of integrals in Section 5.3.1, which will be used later in the specific calculations for the edge pair correlation (Section 5.3.2), edge-vertex cross-correlation (Section 5.3.3) and vertex pair correlation (Section 5.3.4). All the subsections 5.3.2 - 5.3.4, follow a similar structure, which can be described in five steps.

Firstly, we adapt the concrete formula for the covariance measure directly from [28] to the Mondrian setting, or derive such a formula in case of the edge length measure using similar considerations. Secondly, we use some results from Section 5.3.1 to transfer these terms to a suitable form, such that the reduced covariance measure can be deduced as a third step. This can be achieved by utilizing [9, Equations (8.1.1a) and (8.1.7)], which states that given some measurable product $A \times B \subset \mathbb{R}^2 \times \mathbb{R}^2$, the reduced covariance measure can be defined by

$$\text{Cov}(\mathcal{X})(A \times B) = \int_A \int_{B-x} \widehat{\text{Cov}}(\mathcal{X})(dy) \ell_2(dx), \quad (5.15)$$

for \mathcal{X} being the random edge length measure \mathcal{E}_t , the total number of vertices \mathcal{V}_t or the combined process $(\mathcal{E}_t, \mathcal{V}_t)$ in our cases. Fourthly, we obtain the reduced second moment measure as an interim result by [9, Equation (8.1.6)], from which we deduce the Mondrian analogue of Ripley's K-function. Lastly, we take the derivative and normalization as described in (5.4) and (5.5) to obtain the correlation functions.

5.3.1 Preparatory calculations

First, we start with relevant definitions which we adopt from [28, Section 3]. Given two edge functionals

$$J^f(e) := \int_e f(x)dx \quad \text{and} \quad \eta^f(e) := \sum_{x \in \text{Vertices}(e)} f(x)$$

for some bounded and measurable functions $f : \mathbb{R}^2 \mapsto \mathbb{R}$ with bounded support. By $\text{Vertices}(e)$ we denote the set of inner points in a maximal edge, *i.e.*, splitting edges of the tessellation. We can define the covariance measures by choosing a pair of these functionals.

We obtain the covariance measure for the random edge length measure \mathcal{E}_t by

$$\int_{(\mathbb{R}^2)^2} (f \otimes g)(x) \text{Cov}(\mathcal{E}_t)(dx) = \text{Cov}(\Sigma_{J^f}(Y(t)), \Sigma_{J^g}(Y(t))),$$

for the cross-covariance of the vertex process \mathcal{V}_t and the random edge length measure \mathcal{E}_t by

$$\int_{(\mathbb{R}^2)^2} (f \otimes g)(x) \text{Cov}(\mathcal{V}_t, \mathcal{E}_t)(dx) = \text{Cov}(\Sigma_{\eta^f}(Y(t)), \Sigma_{J^g}(Y(t))),$$

and for the vertex process \mathcal{V}_t by

$$\int_{(\mathbb{R}^2)^2} (f \otimes g)(x) \text{Cov}(\mathcal{V}_t)(dx) = \text{Cov}(\Sigma_{\eta^f}(Y(t)), \Sigma_{\eta^g}(Y(t))).$$

We will use more precise formulas for the cases of the cross-covariance and the vertex process given in [28, Theorem 2 & 3]. Additionally, we will obtain a concrete formula for the covariance measure of the random edge length measure. In our setting, we will use the notation

$$\Delta^e := \sum_{x \in \text{Vertices}(e)} \delta_x \quad \text{and} \quad \ell_1(\cdot \cap e)(A) := \ell_1(A \cap e) \quad (5.16)$$

for some $A \subseteq \mathbb{R}^2$ for η^f and J^f , respectively. Moreover, we define

$$(\Lambda_p[\cdot \cap e])(A) := \Lambda_p([A \cap e]) \quad (5.17)$$

for segments $e \in Y(t)$.

We can give more concrete descriptions of Δ^e and $\Lambda_p[\cdot \cap e]$ by using the fact that every segment e in a Mondrian tessellation is either parallel to E_1 or to E_2 . This implies that either the second or the first coordinate of its endpoints coincide. To make it more precise, given a segment e which is parallel to E_1 , its endpoints can be given as (τ, σ) and (ω, σ) for some $\sigma, \tau, \omega \in \mathbb{R}$. Equivalently, if e is parallel to E_2 , its endpoints can be given as (σ, τ) and (σ, ω) . To simplify notation, we will describe segments using their endpoints and write $\overline{(\tau\omega)}_\sigma$ for segments parallel to E_1 and $\overline{\sigma(\tau\omega)}$ for those parallel to E_2 . With this distinction between the two kinds of segments, we can conclude

$$\Delta^e = \begin{cases} \delta_{(\tau,\sigma)} + \delta_{(\omega,\sigma)} & \text{for } e = \overline{(\tau\omega)}_\sigma, \\ \delta_{(\sigma,\tau)} + \delta_{(\sigma,\omega)} & \text{for } e = \overline{\sigma(\tau\omega)}, \end{cases} \quad (5.18)$$

and

$$\Lambda_p([\cdot \cap \overline{(\tau\omega)_\sigma}]) = (1-p) \ell_1(\cdot \cap \overline{(\tau\omega)_\sigma}), \quad \Lambda_p([\cdot \cap_\sigma \overline{(\tau\omega)}]) = p \ell_1(\cdot \cap_\sigma \overline{(\tau\omega)}). \quad (5.19)$$

For simplification of notation, we define the two integrals for bounded measurable functions $f : \mathbb{R}^2 \rightarrow \mathbb{R}$ with bounded support and $t > 0$ as

$$\mathcal{I}^1(f(s); t) := \int_0^t f(s) ds, \quad (5.20)$$

and

$$\mathcal{I}^n(f(s); t) := \int_0^t \int_0^{s_1} \dots \int_0^{s_{n-1}} f(s) ds ds_{n-1} \dots ds_1 = \frac{1}{(n-1)!} \int_0^t (t-s)^{n-1} f(s) ds, \quad (5.21)$$

for integers $n \geq 2$.

Proofs for the Mondrian pair and cross correlations are based on more general results in [28], which include a number of integrals for which simplifications can be given in case of Mondrian tessellations. This section provides several lemmas transferring those integrals either to a simpler form or calculating their concrete values.

We start with a lemma simplifying the expression in [28, Theorem 3]. It concerns integrals over a product measures of dirac measure and 1-dimensional Lebesgue measures. This lemma prepares a later use of a diagonal shift argument in the sense of [9, Corollary 8.1.III].

Lemma 5.3.1 [28, Lemma 4.1] *Let $A, B \in \mathcal{B}(\mathbb{R}^2)$. For any $q \in [0, 1]$ and $j \in \mathbb{N}$, we simplify the following integrals over different product measures.*

(i) *Product of a dirac measure with 1-dimensional Lebesgue measure*

$$\begin{aligned} & \int_{\mathbb{R}} \int_{\mathbb{R}} \int_{\mathbb{R}} (\delta_{(\tau, \sigma)} \otimes \ell_1(\cdot \cap \overline{(\tau\vartheta)_\sigma})(A \times B) \mathcal{I}^j(s^2 \exp(-sq|\tau - \vartheta|); t) d\vartheta d\tau d\sigma \\ &= \int_{\mathbb{R}^2} \delta_w(A) \int_{\mathbb{R}} \ell_1(B - w \cap \overline{(0z)_0}) \mathcal{I}^j(s^2 \exp(-sq|z|); t) dz dw \end{aligned}$$

and

$$\begin{aligned} & \int_{\mathbb{R}} \int_{\mathbb{R}} \int_{\mathbb{R}} (\delta_{(\sigma, \tau)} \otimes \ell_1(\cdot \cap_\sigma \overline{(\tau\vartheta)})(A \times B) \mathcal{I}^j(s^2 \exp(-sq|\tau - \vartheta|); t) d\vartheta d\tau d\sigma \\ &= \int_{\mathbb{R}^2} \delta_w(A) \int_{\mathbb{R}} \ell_1(B - w \cap_0 \overline{(0z)}) \mathcal{I}^j(s^2 \exp(-sq|z|); t) dz dw. \end{aligned}$$

(ii) *Product of two 1-dimensional Lebesgue measures*

$$\begin{aligned} & \int_{\mathbb{R}} \int_{\mathbb{R}} \int_{\mathbb{R}} (\ell_1(\cdot \cap \overline{(\tau\vartheta)})_{\sigma} \otimes \ell_1(\cdot \cap \overline{(\tau\vartheta)})_{\sigma})(A \times B) \mathcal{I}^j(s^2 \exp(-sq|\tau - \vartheta|); t) \, d\vartheta \, d\tau \, d\sigma \\ &= \int_{\mathbb{R}^2} \delta_w(A) \int_{\mathbb{R}} \left(\int_{\overline{(0z)_0}} \int_{\overline{(0z)_0}} \delta_{y-x}(B - w) \, dx \, dy \right) \mathcal{I}^j(s^2 \exp(-sq|z|); t) \, dz \, dw \end{aligned}$$

and

$$\begin{aligned} & \int_{\mathbb{R}} \int_{\mathbb{R}} \int_{\mathbb{R}} (\ell_1(\cdot \cap_{\sigma} \overline{(\tau\vartheta)}) \otimes \ell_1(\cdot \cap_{\sigma} \overline{(\tau\vartheta)}))(A \times B) \mathcal{I}^j(s^2 \exp(-sq|\tau - \vartheta|); t) \, d\vartheta \, d\tau \, d\sigma \\ &= \int_{\mathbb{R}^2} \delta_w(A) \int_{\mathbb{R}} \left(\int_{\mathbb{R}} \int_{\mathbb{R}} \delta_{y-x}(\cdot) \, dx \, dy \right) \mathcal{I}^j(s^2 \exp(-sq|z|); t) \, dz \, dw. \end{aligned}$$

(iii) *Product of two dirac measure*

$$\begin{aligned} & \int_{\mathbb{R}} \int_{\mathbb{R}} \int_{\mathbb{R}} (\delta_{(\tau,\sigma)} \otimes \delta_{(\tau,\sigma)})(A \times B) \mathcal{I}^j(s^2 \exp(-sq|\tau - \vartheta|); t) \, d\vartheta \, d\tau \, d\sigma \\ &= \int_{\mathbb{R}^2} \delta_w(A) \int_{\mathbb{R}} \delta_{\mathbf{0}}(B - w) \mathcal{I}^j(s^2 \exp(-sq|z|); t) \, dz \, dw, \end{aligned}$$

where $\mathbf{0} := (0, 0)$. Furthermore,

$$\begin{aligned} & \int_{\mathbb{R}} \int_{\mathbb{R}} \int_{\mathbb{R}} (\delta_{(\tau,\sigma)} \otimes \delta_{(\vartheta,\sigma)})(A \times B) \mathcal{I}^j(s^2 \exp(-sq|\tau - \vartheta|); t) \, d\vartheta \, d\tau \, d\sigma \\ &= \int_{\mathbb{R}^2} \delta_w(A) \int_{\mathbb{R}} \delta_{(z,0)}(B - w) \mathcal{I}^j(s^2 \exp(-sq|z|); t) \, dz \, dw \end{aligned}$$

and

$$\begin{aligned} & \int_{\mathbb{R}} \int_{\mathbb{R}} \int_{\mathbb{R}} (\delta_{(\sigma,\tau)} \otimes \delta_{(\sigma,\vartheta)})(A \times B) \mathcal{I}^j(s^2 \exp(-sq|\tau - \vartheta|); t) \, d\vartheta \, d\tau \, d\sigma \\ &= \int_{\mathbb{R}^2} \delta_w(A) \int_{\mathbb{R}} \delta_{(0,z)}(B - w) \mathcal{I}^j(s^2 \exp(-sq|z|); t) \, dz \, dw. \end{aligned}$$

Proof. In each part of this lemma, results are stated for vertical and horizontal line segments. Since the proofs are similar, we will only provide the proof for one version of (i) and (ii) each. In (iii), we will restrain from proving the third equality.

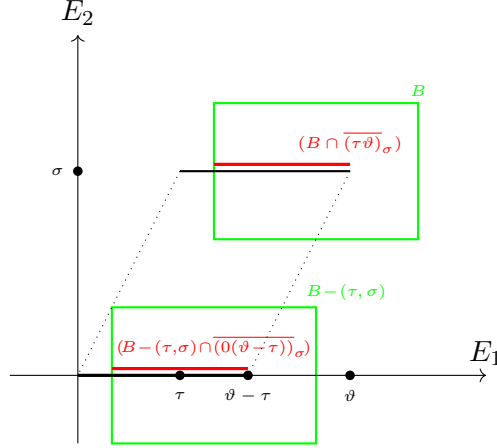


FIGURE 5.3: Visualization of the equality of the Lebesgue measure when shifting a line segment by (τ, σ) .

We start with the first equality in (i), we note that shifting a line segment $(\tau, \vartheta)_\sigma$ to start at the origin will not change the Lebesgue measure if B is shifted by (τ, σ) , *i.e.*, $\ell_1(B \cap \overline{(\tau\vartheta)}_\sigma) = \ell_1(B - (\tau, \sigma) \cap \overline{(0(\vartheta - \tau))_0})$ for any $\tau, \vartheta, \sigma \in \mathbb{R}$, see Figure 5.3. We can conclude

$$\begin{aligned} & \int_{\mathbb{R}} \int_{\mathbb{R}} \int_{\mathbb{R}} \delta_{(\tau, \sigma)}(A) \ell_1(B \cap \overline{(\tau\vartheta)}_\sigma) \mathcal{I}^j(s^2 \exp(-sq|\tau - \vartheta|); t) d\vartheta d\tau d\sigma \\ &= \int_{\mathbb{R}} \int_{\mathbb{R}} \delta_{(\tau, \sigma)}(A) \int_{\mathbb{R}} \ell_1(B - (\tau, \sigma) \cap \overline{(0(\vartheta - \tau))_0}) \mathcal{I}^j(s^2 \exp(-sq|\tau - \vartheta|); t) d\vartheta d\tau d\sigma. \end{aligned}$$

Substituting $z = \vartheta - \tau$, one may rewrite the given integral as

$$\int_{\mathbb{R}} \int_{\mathbb{R}} \delta_{(\tau, \sigma)}(A) \int_{\mathbb{R}} \ell_1(B - (\tau, \sigma) \cap \overline{(0z)_0}) \mathcal{I}^j(s^2 \exp(-sq|z|); t) dz d\tau d\sigma,$$

which proves the first equality of (i) if $\omega = (\tau, \sigma)$. Continuing with (ii), we replace the Lebesgue measure by integrals of Dirac measures and use a similar shift of the subsets A and B to obtain

$$\begin{aligned} & \int_{\mathbb{R}} \int_{\mathbb{R}} \int_{\mathbb{R}} \ell_1(A \cap \overline{(\tau\vartheta)}_\sigma) \ell_1(B \cap \overline{(\tau\vartheta)}_\sigma) \mathcal{I}^j(s^2 \exp(-sq|\tau - \vartheta|); t) d\tau d\vartheta d\sigma \\ &= \int_{\mathbb{R}} \int_{\mathbb{R}} \int_{\mathbb{R}} \left(\int_{\overline{(\tau\vartheta)}_\sigma} \int_{\overline{(\tau\vartheta)}_\sigma} \delta_x(A) \delta_y(B) dx dy \right) \mathcal{I}^j(s^2 \exp(-sq|\tau - \vartheta|); t) d\tau d\vartheta d\sigma \\ &= \int_{\mathbb{R}} \int_{\mathbb{R}} \int_{\mathbb{R}} \left(\int_{\overline{(0(\vartheta - \tau))_0}} \int_{\overline{(0(\vartheta - \tau))_0}} \delta_x(A - (\tau, \sigma)) \delta_y(B - (\tau, \sigma)) dx dy \right) \\ & \quad \times \mathcal{I}^j(s^2 \exp(-sq|\tau - \vartheta|); t) d\tau d\vartheta d\sigma \end{aligned}$$

$$= \int_{\mathbb{R}^2} \int_{\mathbb{R}} \left(\int_{\overline{(0z)_0}} \int_{\overline{(0z)_0}} \delta_{w+x}(A) \delta_y(B-w) \mathcal{I}^j(s^2 \exp(-sq|z|); t) dx dy \right) dz dw,$$

where we again substituted $z = \vartheta - \tau$ and set $(\tau, \sigma) = w$. With another substitution $\tilde{w} = w+x$, we conclude

$$\begin{aligned} & \int_{\mathbb{R}^2} \int_{\mathbb{R}} \left(\int_{\overline{(0z)_0}} \int_{\overline{(0z)_0}} \delta_{w+x}(A) \delta_y(B-w) dx dy \right) \mathcal{I}^j(s^2 \exp(-sq|z|); t) dz dw \\ &= \int_{\mathbb{R}^2} \delta_{\tilde{w}}(A) \int_{\mathbb{R}} \left(\int_{\overline{(0z)_0}} \int_{\overline{(0z)_0}} \delta_{y-x}(B-\tilde{w}) dx dy \right) \mathcal{I}^j(s^2 \exp(-sq|z|); t) dz d\tilde{w}, \end{aligned}$$

which proves the first equality in (ii). We proceed with the first and second term of (iii) in a similar way. By substitution of $z = \vartheta - \tau$ and putting $w = (\tau, \sigma)$, we conclude

$$\begin{aligned} & \int_{\mathbb{R}} \int_{\mathbb{R}} \int_{\mathbb{R}} \delta_{(\tau,\sigma)}(A) \delta_{(\tau,\sigma)}(B) \mathcal{I}^j(s^2 \exp(-sq|\tau - \vartheta|); t) d\vartheta d\tau d\sigma \\ &= \int_{\mathbb{R}^2} \delta_w(A) \int_{\mathbb{R}} \delta_{\mathbf{0}}(B-w) \mathcal{I}^j(s^2 \exp(-sq|z|); t) dz dw. \end{aligned}$$

for the first, and

$$\begin{aligned} & \int_{\mathbb{R}} \int_{\mathbb{R}} \int_{\mathbb{R}} \delta_{(\tau,\sigma)}(A) \delta_{(\vartheta,\sigma)}(B) \mathcal{I}^j(s^2 \exp(-sq|\tau - \vartheta|); t) d\vartheta d\tau d\sigma \\ &= \int_{\mathbb{R}^2} \delta_w(A) \int_{\mathbb{R}} \delta_{(z,0)}(B-w) \mathcal{I}^j(s^2 \exp(-sq|z|); t) dz dw \end{aligned}$$

for the second term in (iii). □

The next lemma explicitly takes into account that our tessellation is considered in a growing window $rR_p = [0, r(1-p)] \times [0, rp]$. In this situation, the Dirac and Lebesgue measure of line segments is specified as follows. For $z > 0$,

$$\delta_{(z,0)}(rR_p) = \mathbf{1}_{[0,(1-p)r]}(z), \quad \ell_1(rR_p \cap \overline{(0z)_0}) = \begin{cases} z & \text{for } z \in (0, r(1-p)], \\ (1-p)r & \text{for } z > r(1-p), \end{cases} \quad (5.22)$$

$$\delta_{(0,z)}(rR_p) = \mathbf{1}_{[0,rp]}(z), \quad \ell_1(rR_p \cap \overline{0(0z)}) = \begin{cases} z & \text{for } z \in (0, rp], \\ pr & \text{for } z > rp. \end{cases} \quad (5.23)$$

Moreover, if $z \leq 0$ it is $\ell_1(rR_p \cap \overline{(0z)}_0) = \ell_1(rR_p \cap \overline{0(0z)}) = 0$.

Lemma 5.3.2 ([3, Lemma 4.2]) *Let $u_1, u_2 : (0, \infty) \times [0, 1] \rightarrow (0, \infty)$ and set $R_{r,p} = [0, u_1(r, p)] \times [0, u_2(r, p)]$. It holds that*

$$\int_{\overline{(0z)}_0} \int_{\overline{(0z)}_0} \delta_{y-x}(R_{r,p}) \, dx \, dy = \begin{cases} zu_1(r, p) - \frac{u_1(r,p)^2}{2} & \text{for } |z| \geq u_1(r, p), \\ \frac{z^2}{2} & \text{for } 0 < |z| < u_1(r, p), \end{cases}$$

and

$$\int_{\overline{0(0z)}} \int_{\overline{0(0z)}} \delta_{y-x}(R_{r,p}) \, dx \, dy = \begin{cases} zu_2(r, p) - \frac{u_2(r,p)^2}{2} & \text{for } |z| \geq u_2(r, p), \\ \frac{z^2}{2} & \text{for } 0 < |z| < u_2(r, p). \end{cases}$$

Proof. Once again, we constrain ourselves to proving the first statement, since the other works analogously. We first note that for any $z \in \mathbb{R}^+$ and $x, y \in \overline{(0z)}_0$

$$\delta_{y-x}(R_{r,p}) = \delta_{(y,0)}(R_{r,p} + (x, 0)) = 1 \quad \text{if and only if} \quad y \in [x, x + u_1(r, p)].$$

We will first assume $z \geq 0$ and $z \geq u_1(r, p)$. We then have

$$\begin{aligned} \int_{\overline{(0z)}_0} \int_{\overline{(0z)}_0} \delta_{y-x}(R_{r,p}) \, dy \, dx &= \int_0^z \int_x^{(x+u_1(r,p)) \wedge z} 1 \, dy \, dx \\ &= \int_0^{z-u_1(r,p)} \int_x^{x+u_1(r,p)} 1 \, dy \, dx + \int_{z-u_1(r,p)}^z \int_x^z 1 \, dy \, dx \\ &= u_1(r, p)(z - u_1(r, p)) + \int_{z-u_1(r,p)}^z (z - x) \, dx \\ &= u_1(r, p)(z - u_1(r, p)) + \frac{u_1(r, p)^2}{2} \\ &= zu_1(r, p) - \frac{u_1(r, p)^2}{2}, \end{aligned}$$

and for $0 \leq z \leq u_1(r, p)$, we get

$$\int_{\overline{0(0z)}} \int_{\overline{0(0z)}} \delta_{y-x}(R_{r,p}) \, dy \, dx = \int_0^z \int_x^z 1 \, dx \, dy = \int_0^z (z - x) \, dx = \frac{z^2}{2}.$$

Proofs for $z \leq 0$ and for the second claim work analogously. □

Since stating the Mondrian pair- and cross-correlation functions involves taking derivatives of analogs of Ripley's K-function, we will provide a lemma about differentiation of integrals needed in the following subsections.

Lemma 5.3.3 *Let $u_1, u_2 : \mathbb{R} \times [0, 1] \mapsto \mathbb{R}^+$ be two differentiable functions and $R_{r,p} = [0, u_1(r, p)] \times [0, u_2(r, p)]$. It then holds that*

$$\begin{aligned} & \frac{d}{dr} \left[\int_{\mathbb{R}} \left(\int_{(0z)_0} \int_{(0z)_0} \delta_{y-x}(R_{r,p}) \, dy \, dx \right) \mathcal{I}^j(s^2 \exp(-sqz); t) \, dz \right] \\ &= 2u_1'(r, p) \int_{u_1(r,p)}^{\infty} (z - u_1(r, p)) \mathcal{I}^j(s^2 \exp(-sqz); t) \, dz \end{aligned} \quad (5.24)$$

and

$$\begin{aligned} & \frac{d}{dr} \left[\int_{\mathbb{R}} \left(\int_{o(0z)} \int_{o(0z)} \delta_{y-x}(R_{r,p}) \, dy \, dx \right) \mathcal{I}^j(s^2 \exp(-sqz); t) \, dz \right] \\ &= 2u_2'(r, p) \int_{u_2(r,p)}^{\infty} (z - u_2(r, p)) \mathcal{I}^j(s^2 \exp(-sqz); t) \, dz. \end{aligned} \quad (5.25)$$

Before starting with the proof, we notice that given a differentiable function $u : \mathbb{R} \times [0, 1] \rightarrow \mathbb{R}^+$ and $k \in \mathbb{N}$, it is

$$\begin{aligned} & \frac{d}{dr} \left[u(r, p)^k \int_0^{u(r,p)} f(z) \mathcal{I}^j(s^2 \exp(-sqz); t) \, dz \right] \\ &= k u(r, p)^{k-1} u'(r, p) \int_0^{u(r,p)} f(z) \mathcal{I}^j(s^2 \exp(-sqz); t) \, dz \\ &\quad + u(r, p)^k u'(r, p) f(u(r, p)) \mathcal{I}^j(s^2 \exp(-squ(r, p)); t) \end{aligned} \quad (5.26)$$

and

$$\begin{aligned} & \frac{d}{dr} \left[u(r, p)^k \int_{u(r,p)}^{\infty} f(z) \mathcal{I}^j(s^2 \exp(-sqz); t) \, dz \right] \\ &= k u(r, p)^{k-1} u'(r, p) \int_{u(r,p)}^{\infty} f(z) \mathcal{I}^j(s^2 \exp(-sqz); t) \, dz \end{aligned}$$

$$- u(r, p)^k u'(r, p) f((u(r, p))) \mathcal{I}^j(s^2 \exp(-squ(r, p)); t), \quad (5.27)$$

where u' denotes the partial derivative of u with respect to the r -coordinate. This is easily given by the Leibniz product rule.

Proof of Lemma 5.3.3. We will provide proof for the second claim. First, by Lemma 5.3.2 we obtain

$$\begin{aligned} & \frac{d}{dr} \left[\int_{\mathbb{R}} \left(\int_{\frac{o(0z)}{o(0z)}} \int_{\frac{o(0z)}{o(0z)}} \delta_{y-x}(R_{r,p}) dy dx \right) \mathcal{I}^j(s^2 \exp(-sqz); t) dz \right] \\ &= \frac{d}{dr} \left[\int_0^{u_2(r,p)} z^2 \mathcal{I}^j(s^2 \exp(-sqz); t) dz + 2 \int_{u_2(r,p)}^{\infty} \left(zu_2(r, p) - \frac{u_2(r, p)^2}{2} \right) \mathcal{I}^j(s^2 \exp(-sqz); t) dz \right] \\ &= \frac{d}{dr} \left[\int_0^{u_2(r,p)} z^2 \mathcal{I}^j(s^2 \exp(-sqz); t) dz \right. \\ & \quad \left. + 2u_2(r, p) \int_{u_2(r,p)}^{\infty} z \mathcal{I}^j(s^2 \exp(-sqz); t) dz \right. \\ & \quad \left. - u_2(r, p)^2 \int_{u_2(r,p)}^{\infty} \mathcal{I}^j(s^2 \exp(-sqz); t) dz \right] \end{aligned}$$

For the first summand, we use (5.26) with $k = 0$ and $f(z) = z^2$ and obtain

$$\frac{d}{dr} \left[\int_0^{u_2(r,p)} z^2 \mathcal{I}^j(s^2 \exp(-sqz); t) dz \right] = u_2(r, p)^2 u_2'(r, p) \mathcal{I}^j(s^2 \exp(-squ_2(r, p)); t).$$

For the second summand, we use (5.27) with $k = 1$ and $f(z) = z$ to obtain

$$\begin{aligned} & \frac{d}{dr} \left[2u_2(r, p) \int_{u_2(r,p)}^{\infty} z \mathcal{I}^j(s^2 \exp(-sqz); t) dz \right] \\ &= 2u_2'(r, p) \int_{u_2(r,p)}^{\infty} z \mathcal{I}^j(s^2 \exp(-sqz); t) dz - 2u_2(r, p)^2 u_2'(r, p) \mathcal{I}^j(s^2 \exp(-squ_2(r, p)); t). \end{aligned}$$

Lastly, the third summand simplifies by (5.27) with $k = 2$ and $f(z) = 1$ to

$$\begin{aligned} & \frac{d}{dr} \left[u_2(r, p)^2 \int_{u_2(r, p)}^{\infty} \mathcal{I}^j(s^2 \exp(-sqz); t) \right] \\ &= 2u_2(r, p) u_2'(r, p) \int_{u_2(r, p)}^{\infty} \mathcal{I}^j(s^2 \exp(-s(1-p)z); t) dz \\ & \quad + u_2(r, p)^2 u_2'(r, p) \mathcal{I}^j(s^2 \exp(-squ_2(r, p)); t). \end{aligned}$$

Putting these terms back together finishes the proof for the second claim. \square

Since the integrals $\mathcal{I}^j(s^2 \exp(-sqz); t)$ for $j \in \{1, 2, 3\}$ will appear several times in the following calculations for the Mondrian correlations, we will provide explicit formulas for the most relevant terms without proofs.

Lemma 5.3.4 ([3, Lemma 4.3]) *Let $q \in [0, 1], t \in [0, \infty), s \in [0, t], j \in \{1, 2, 3\}$ and \mathcal{I}^j as defined in (5.20) and (5.21). Then it holds that*

$$\begin{aligned} & \mathcal{I}^j(s^2 \exp(-sq); t) \\ &= q^{-(j+2)} \left(\sum_{r=0}^{j-1} \left[(-1)^{r+j+1} (qt)^r \frac{(j+1-r)!}{(j-1-r)! r!} \right] - \exp(-qt) (qt(qt+2j) + \frac{(j+1)!}{(j-1)!}) \right) \end{aligned}$$

and, for $y \geq 0$,

$$\begin{aligned} & \int_y^{\infty} z \mathcal{I}^j(s^2 \exp(-sqz); t) dz \\ &= y^{-j} q^{-(2+j)} \left((-1)^{j+1} \sum_{r=0}^{j-1} (-1)^r \frac{1+j-r}{r!} (yqt)^r + (-1)^j \exp(-yqt) \left((1+j) + yqt \right) \right). \end{aligned}$$

5.3.2 Edge pair-correlations for Mondrian tessellations

This section now takes the relevant statements from before and will prove the edge pair-correlation for Mondrian tessellations.

Proof of Theorem 5.1.5. As a first step, we adapt calculations from [28, Section 3.3] and martingale arguments given in [28, Equation (3)] to our setting. By Equation (5.2), one can

conclude that

$$\int_{(\mathbb{R}^2)^2} (f \otimes g)(x) \text{Cov}(\mathcal{E}_t)(dx) = \int_0^t \mathbb{E} A_{J^f, J^g}(Y(s)) ds,$$

which can be simplified, using [28, Equation (24)] with driving measure Λ_p , to

$$= \frac{1}{2} \int_{\mathcal{S}(\mathbb{R}^2)} J^f(e) J^g(e) \int_0^t s^2 \exp(-s\Lambda_p([e])) ds \ll (\Lambda_p \times \Lambda_p) \cap \Lambda_p \gg (de).$$

By shortening the notation of the second integral by (5.20), and by applying the segment intersection measure as in Equation (5.9) and the explicit edge functional for J^f , yields

$$\begin{aligned} & \text{Cov}(\mathcal{E}_t)(\cdot \times \cdot) \\ &= \frac{1}{2} \int_{\mathcal{S}(\mathbb{R}^2)} \ell_1(\cdot \cap e) \otimes \ell_1(\cdot \cap e)(\cdot \times \cdot) \mathcal{I}^1(s^2 \exp(-s\Lambda_p([e])); t) \times \ll (\Lambda_p \times \Lambda_p) \cap \Lambda_p \gg (de) \\ &= \frac{1}{2} \int_{[\mathbb{R}^2] [L] [L]} \int \int \ell_1(\cdot \cap L(L_1, L_2)) \otimes \ell_1(\cdot \cap L(L_1, L_2))(\cdot \times \cdot) \mathcal{I}^1(s^2 \exp(-s\Lambda_p([L(L_1, L_2)])); t) \\ & \quad \times \Lambda_p(dL_1) \Lambda_p(dL_2) \Lambda_p(dL) \\ &= \frac{1}{2} p(1-p)^2 \int_{\mathbb{R}} \int_{\mathbb{R}} \int_{\mathbb{R}} \ell_1(\cdot \cap \overline{(\tau\vartheta)_\sigma}) \otimes \ell_1(\cdot \cap \overline{(\tau\vartheta)_\sigma})(\cdot \times \cdot) \\ & \quad \mathcal{I}^1(s^2 \exp(-s(1-p)|\tau - \vartheta|); t) d\tau d\vartheta d\sigma \\ & \quad + \frac{1}{2} p^2(1-p) \int_{\mathbb{R}} \int_{\mathbb{R}} \int_{\mathbb{R}} \ell_1(\cdot \cap_\sigma \overline{(\tau\vartheta)}) \otimes \ell_1(\cdot \cap_\sigma \overline{(\tau\vartheta)})(\cdot \times \cdot) \\ & \quad \mathcal{I}^1(s^2 \exp(-sp|\tau - \vartheta|); t) d\tau d\vartheta d\sigma. \end{aligned} \quad (5.28)$$

As for the second step of this proof, we prepare Equation (5.28) such that the reduced covariance measure can be deduced by (5.15). For this, we use Lemma 5.3.1 and obtain

$$\begin{aligned} & \frac{1}{2} p(1-p)^2 \int_{\mathbb{R}} \int_{\mathbb{R}} \int_{\mathbb{R}} \ell_1(A \cap \overline{(\tau\vartheta)_\sigma}) \ell_1(B \cap \overline{(\tau\vartheta)_\sigma}) \mathcal{I}^1(s^2 \exp(-s(1-p)|\tau - \vartheta|); t) d\tau d\vartheta d\sigma \\ & \quad + \frac{1}{2} p^2(1-p) \int_{\mathbb{R}} \int_{\mathbb{R}} \int_{\mathbb{R}} \ell_1(A \cap_\sigma \overline{(\tau\vartheta)}) \otimes \ell_1(B \cap_\sigma \overline{(\tau\vartheta)}) \mathcal{I}^1(s^2 \exp(-sp|\tau - \vartheta|); t) d\tau d\vartheta d\sigma \\ &= \frac{1}{2} p(1-p)^2 \int_{\mathbb{R}^2} \delta_w(A) \int_{\mathbb{R}} \int_{\overline{(0z)_0} \overline{(0z)_0}} \delta_{y-x}(B-w) dx dy \mathcal{I}^1(s^2 \exp(-s(1-p)|z|); t) dz dw \end{aligned}$$

$$+ \frac{1}{2} p^2 (1-p) \int_{\mathbb{R}^2} \delta_w(A) \int_{\mathbb{R}} \int_{\frac{o(0z)}{o(0z)}} \delta_{y-x}(B-w) dx dy \mathcal{I}^1(s^2 \exp(-sp|z|); t) dz dw. \quad (5.29)$$

Finally able to deduce the reduced covariance measure in a third step by Equation (5.15), we conclude

$$\begin{aligned} \widehat{\text{Cov}}(\mathcal{E}_t)(\cdot) &= \frac{1}{2} p (1-p)^2 \int_{\mathbb{R}} \int_{\frac{(0z)_o}{(0z)_o}} \int_{\frac{(0z)_o}{(0z)_o}} \delta_{y-x}(\cdot) dx dy \mathcal{I}^1(s^2 \exp(-s(1-p)|z|); t) dz \\ &\quad + \frac{1}{2} p^2 (1-p) \int_{\mathbb{R}} \int_{\frac{o(0z)}{o(0z)}} \int_{\frac{o(0z)}{o(0z)}} \delta_{y-x}(\cdot) dx dy \mathcal{I}^1(s^2 \exp(-sp|z|); t) dz. \end{aligned}$$

As fourth step of the proof, we use the coherence between the reduced covariance measure and the second moment measure $\widehat{\mathcal{K}}(\mathcal{E}_t)$ given in [9, Equation (8.1.6)]. We can conclude that

$$\widehat{\mathcal{K}}(\mathcal{E}_t)(\cdot) = \widehat{\text{Cov}}(\mathcal{E}_t)(\cdot) + t^2 \ell_2(\cdot).$$

In a more general sense, the factor t^2 represents the square of the intensity of \mathcal{E}_t , which is simply equal to t , as stated in [28, Equation (8)]. Using $\lambda_{\mathcal{E}} = t$ again, one can define the modified Ripley's K-function, which in our setting is applied to $R_{r,p}$. Thus, we get the Mondrian analogue as

$$K_{\mathcal{E}}(r) := \frac{1}{t^2} \widehat{\mathcal{K}}(\mathcal{E}_t)(R_{r,p}),$$

where $R_{r,p} = [0, r(1-p)] \times [0, rp]$. By these two coherences and the reduced covariance measure, we can finally conclude the Mondrian analogue of the K-function as

$$\begin{aligned} K_{\mathcal{E}}(r) &= r^2 p (1-p) + \frac{p(1-p)^2}{2t^2} \int_{\mathbb{R}} \int_{\frac{(0z)_o}{(0z)_o}} \int_{\frac{(0z)_o}{(0z)_o}} \delta_{y-x}(R_{r,p}) dx dy \mathcal{I}^1(s^2 \exp(-s(1-p)|z|); t) dz \\ &\quad + \frac{p^2(1-p)}{2t^2} \int_{\mathbb{R}} \int_{\frac{o(0z)}{o(0z)}} \int_{\frac{o(0z)}{o(0z)}} \delta_{y-x}(R_{r,p}) dx dy \mathcal{I}^1(s^2 \exp(-sp|z|); t) dz. \end{aligned}$$

As the fifth step, we use Lemma 5.3.3 which gives

$$\begin{aligned} \frac{d}{dr} K_{\mathcal{E}}(r) &= 2rp(1-p) + \frac{p(1-p)^3}{t^2} \int_{(1-p)r}^{\infty} (z - (1-p)r) \mathcal{I}^1(s^2 \exp(-s(1-p)z); t) dz \\ &\quad + \frac{p^3(1-p)}{t^2} \int_{rp}^{\infty} (z - rp) \mathcal{I}^1(s^2 \exp(-spz); t) dz. \end{aligned}$$

Finally, as the last step, the normalization of $K_{\mathcal{E}}(r)$ as described in (5.4) along with the

explicit calculations for the integrals in Lemma 5.3.4, results in the pair-correlation function stated in Theorem 5.1.5. \square

5.3.3 Edge-vertex cross-correlations for Mondrian tessellations

In this section, we collect all relevant results from previous sections and follow the same five steps to prove the Mondrian cross-correlation of the vertex process \mathcal{V}_t and the random edge length measure \mathcal{E}_t .

Proof of Theorem 5.1.6. As first step, we use the explicit formula for the cross-covariance measure from [28, Theorem 3] for general locally finite driving measures Λ together with some modification to match our settings. For this, we use the segments intersection measure given in (5.9) as well as concrete description of a line segments. This yields

$$\begin{aligned} & \text{Cov}(\mathcal{V}_t, \mathcal{E}_t)(\cdot \times \cdot) \\ &= \int_{[W]} \int_{[L \cap W]} \int_{[L \cap W]} \left[\frac{1}{2} \Delta^{L(L_1, L_2)} \otimes \ell_1(\cdot \cap L(L_1, L_2)) (\cdot \times \cdot) \mathcal{I}^1(s^2 \exp(-s\Lambda_p([L(L_1, L_2)])); t) \right. \\ & \quad \left. + \Lambda_p([\cdot \cap L(L_1, L_2)]) \otimes \ell_1(\cdot \cap L(L_1, L_2)) (\cdot \times \cdot) \mathcal{I}^2(s^2 \exp(-s\Lambda_p([L(L_1, L_2)])); t) \right] \\ & \quad \times \Lambda_p(dL_1) \Lambda_p(dL_2) \Lambda_p(dL). \end{aligned} \quad (5.30)$$

With the specific measure $\Lambda_p(\cdot)$ for Mondrian tessellations given in (5.3), and Equations (5.13), (5.18) and (5.19), we obtain

$$\begin{aligned} & \text{Cov}(\mathcal{V}_t, \mathcal{E}_t)(\cdot \times \cdot) \\ &= p(1-p)^2 \int_{\mathbb{R}} \int_{\mathbb{R}} \int_{\mathbb{R}} \left[\frac{1}{2} (\delta_{(\tau, \sigma)} + \delta_{(\vartheta, \sigma)}) \otimes \ell_1(\cdot \cap \overline{(\tau\vartheta)}_\sigma) (\cdot \times \cdot) \mathcal{I}^1(s^2 \exp(-s(1-p)|\tau - \vartheta|); t) \right. \\ & \quad \left. + (1-p) \left(\ell_1(\cdot \cap \overline{(\tau\vartheta)}_\sigma) \otimes \ell_1(\cdot \cap \overline{(\tau\vartheta)}_\sigma) \right) (\cdot \times \cdot) \mathcal{I}^2(s^2 \exp(-s(1-p)|\tau - \vartheta|); t) \right] d\tau d\vartheta d\sigma \\ & \quad + p^2(1-p) \int_{\mathbb{R}} \int_{\mathbb{R}} \int_{\mathbb{R}} \left[\frac{1}{2} (\delta_{(\sigma, \tau)} + \delta_{(\sigma, \vartheta)}) \otimes \ell_1(\cdot \cap \overline{(\tau\vartheta)}) (\cdot \times \cdot) \mathcal{I}^1(s^2 \exp(-sp|\tau - \vartheta|); t) \right. \\ & \quad \left. + p \left(\ell_1(\cdot \cap \overline{(\tau\vartheta)}) \otimes \ell_1(\cdot \cap \overline{(\tau\vartheta)}) \right) (\cdot \times \cdot) \mathcal{I}^2(s^2 \exp(-sp|\tau - \vartheta|); t) \right] d\tau d\vartheta d\sigma. \end{aligned} \quad (5.31)$$

For the second step, we apply Lemma 5.3.1(i) to the first summand of each integral and use

Lemma 5.3.1(ii) to simplify the second summands. For $A, B \in \mathcal{B}(\mathbb{R}^2)$, we obtain

$$\begin{aligned}
 & \frac{p(1-p)^2}{2} \int_{\mathbb{R}} \int_{\mathbb{R}} \int_{\mathbb{R}} (\delta_{(\tau, \sigma)} + \delta_{(\vartheta, \sigma)}) \otimes \ell_1(\cdot \cap \overline{(\tau\vartheta)}_{\sigma})(A \times B) \\
 & \qquad \qquad \qquad \mathcal{I}^1(s^2 \exp(-s(1-p)|\tau - \vartheta|); t) \, d\tau \, d\vartheta \, d\sigma \\
 & = p(1-p)^2 \int_{\mathbb{R}^2} \delta_w(A) \int_{\mathbb{R}} \ell_1(B - w \cap \overline{(0z)}_0) \mathcal{I}^1(s^2 \exp(-s(1-p)|z|); t) \, dz \, dw \quad (5.32)
 \end{aligned}$$

for the first term and

$$\begin{aligned}
 & p(1-p)^3 \int_{\mathbb{R}} \int_{\mathbb{R}} \int_{\mathbb{R}} \left(\ell_1(\cdot \cap \overline{(\tau\vartheta)}_{\sigma}) \otimes \ell_1(\cdot \cap \overline{(\tau\vartheta)}_{\sigma}) \right) (A \times B) \\
 & \qquad \qquad \qquad \mathcal{I}^2(s^2 \exp(-s(1-p)|\tau - \vartheta|); t) \, d\tau \, d\vartheta \, d\sigma \\
 & = p(1-p)^3 \int_{\mathbb{R}^2} \delta_w(A) \int_{\mathbb{R}} \left(\int_{\overline{(0z)}_0} \int_{\overline{(0z)}_0} \delta_{y-x}(B - w) \, dx \, dy \right) \\
 & \qquad \qquad \qquad \mathcal{I}^2(s^2 \exp(-s(1-p)|z|); t) \, dz \, dw \quad (5.33)
 \end{aligned}$$

for the second term of the first integral. The second term can be simplified similarly.

As a third step, we can proceed with the diagonal-shift argument as described in (5.15), as we have done previously. We can deduce the reduced covariance measure as follows:

$$\begin{aligned}
 & \widehat{\text{Cov}}_{\mathcal{V}, \mathcal{E}}(\cdot) \\
 & = p(1-p) \left((1-p) \int_{\mathbb{R}} \ell_1(\cdot \cap \overline{(0z)}_0) \mathcal{I}^1(s^2 \exp(-s(1-p)|z|); t) \, dz \right. \\
 & \quad + p \int_{\mathbb{R}} \ell_1(\cdot \cap \overline{(0z)}) \mathcal{I}^1(s^2 \exp(-sp|z|); t) \, dz \\
 & \quad + (1-p)^2 \int_{\mathbb{R}} \left(\int_{\overline{(0z)}_0} \int_{\overline{(0z)}_0} \delta_{y-x}(\cdot) \, dx \, dy \right) \mathcal{I}^2(s^2 \exp(-s(1-p)|z|); t) \, dz \\
 & \quad \left. + p^2 \int_{\mathbb{R}} \left(\int_{\overline{o(0z)}} \int_{\overline{o(0z)}} \delta_{y-x}(\cdot) \, dx \, dy \right) \mathcal{I}^2(s^2 \exp(-sp|z|); t) \, dz \right). \quad (5.34)
 \end{aligned}$$

Let $\lambda_{\mathcal{V}}$ and $\lambda_{\mathcal{E}}$ denote the intensities for the vertex and edge process, respectively. We can

deduce the reduced second moment measure as

$$\widehat{\mathcal{K}}_{\mathcal{V},\mathcal{E}}(\cdot) = \widehat{\text{Cov}}_{\mathcal{V},\mathcal{E}}(\cdot) + \lambda_{\mathcal{V}}\lambda_{\mathcal{E}}\ell_2(\cdot).$$

The Mondrian cross K-function of \mathcal{V}_t and \mathcal{E}_t is then defined as

$$K_{\mathcal{V},\mathcal{E}}(r) = \frac{1}{\lambda_{\mathcal{V}}\lambda_{\mathcal{E}}}\widehat{\mathcal{K}}_{\mathcal{V},\mathcal{E}}(R_{r,p}) = \frac{1}{\lambda_{\mathcal{V}}\lambda_{\mathcal{E}}}\widehat{\text{Cov}}_{\mathcal{V},\mathcal{E}}(R_{r,p}) + \ell_2(R_{r,p}). \quad (5.35)$$

The intensities are known as $\lambda_{\mathcal{V}} = t^2p(1-p)$ and $\lambda_{\mathcal{E}} = t$. For the reduced covariance measure given by Equation (5.34), we simplify notation by using $T_1(r), T_2(r), T_3(r)$ and $T_4(r)$ for the first, second, third and fourth summand, respectively. This yields

$$K_{\mathcal{V},\mathcal{E}}(R_{r,p}) = r^2p(1-p) + \frac{1}{t^3} \left[(1-p)T_1(r) + pT_2(r) + (1-p)^2T_3(r) + p^2T_4(r) \right]. \quad (5.36)$$

As a final step, we can obtain the cross-correlation function $g_{\mathcal{V},\mathcal{E}}(r)$ by taking the derivative and applying suitable normalization. With Equations (5.22) and (5.23), we can simplify $T_1(r)$ and $T_2(r)$, before using (5.26), (5.27) to conclude that

$$\begin{aligned} \frac{dT_1(r)}{dr} &= \frac{d}{dr} \left[\int_0^{r(1-p)} z \mathcal{I}^1(s^2 \exp(-s(1-p)z); t) dz \right. \\ &\quad \left. + r(1-p) \int_{r(1-p)}^{\infty} \mathcal{I}^1(s^2 \exp(-s(1-p)z); t) dz \right] \\ &= r(1-p)^2 \mathcal{I}^1(s^2 \exp(-s(1-p)^2r); t) + (1-p) \int_{r(1-p)}^{\infty} \mathcal{I}^1(s^2 \exp(-s(1-p)z); t) dz \\ &\quad - r(1-p)^2 \mathcal{I}^1(s^2 \exp(-s(1-p)^2r); t) \\ &= (1-p) \int_{r(1-p)}^{\infty} \mathcal{I}^1(s^2 \exp(-s(1-p)z); t) dz \end{aligned}$$

and

$$\begin{aligned} \frac{dT_2(r)}{dr} &= \frac{d}{dr} \left[\int_0^{rp} z \mathcal{I}^1(s^2 \exp(-spz); t) dz + rp \int_{rp}^{\infty} \mathcal{I}^1(s^2 \exp(-spz); t) dz \right] \\ &= p \int_{rp}^{\infty} \mathcal{I}^1(s^2 \exp(-spz); t) dz. \end{aligned}$$

For the third and fourth term, we use Lemma 5.3.3 to see that

$$\begin{aligned} \frac{dT_3(r)}{dr} &= \frac{d}{dr} \left[\int_{\mathbb{R}} \left(\int_{\overline{(0z)_0}} \int_{\overline{(0z)_0}} \delta_{y-x}(R_{r,p}) \, dx \, dy \right) \mathcal{I}^2(s^2 \exp(-s(1-p)|z|); t) \, dz \right] \\ &= 2(1-p) \int_{r(1-p)}^{\infty} (z - r(1-p)) \mathcal{I}^2(s^2 \exp(-s(1-p)z); t) \, dz \end{aligned}$$

and

$$\begin{aligned} \frac{dT_4(r)}{dr} &= \frac{d}{dr} \left[\int_{\mathbb{R}} \left(\int_{\overline{0(0z)_0}} \int_{\overline{0(0z)_0}} \delta_{y-x}(R_{r,p}) \, dx \, dy \right) \mathcal{I}^2(s^2 \exp(-sp|z|); t) \, dz \right] \\ &= 2p \int_{rp}^{\infty} (z - rp) \mathcal{I}^2(s^2 \exp(-spz); t) \, dz. \end{aligned}$$

By the explicit formula of the integrals given in Lemma 5.3.4, we obtain

$$\frac{dT_1(r)}{dr} = I_1(1-p), \quad \frac{dT_2(r)}{dr} = I_1(p), \quad \frac{dT_3(r)}{dr} = I_2(1-p), \quad \frac{dT_4(r)}{dr} = I_2(p)$$

with

$$I_1(q) = \frac{1 - \exp(-trq^2)(1 + trq^2)}{r^2q^5}$$

and

$$I_2(q) = \frac{2trq^2 - 3 + \exp(-trp^2)(3 + trq^2)}{r^2q^6} - \frac{trq^2 - 2 + \exp(-trq^2)(2 + trq^2)}{r^3q^7}.$$

Putting these expressions back together in (5.36) and finally normalizing by multiplication with $\frac{1}{2rp(1-p)}$, one obtains the cross-correlation function $g_{\nu, \mathcal{E}}(r)$. \square

5.3.4 Vertex pair-correlations for Mondrian tessellations

This sections aim is proving the Mondrian vertex pair-correlation as stated in Theorem 5.1.7. As in the previous section, we use the general result stated in [28, Theorem 2] and specialize this results to Mondrians. To finally obtain the pair-correlation function, we once more follow the same five steps.

Proof. As a first step, we use the explicit formula for the covariance measure given in [28,

Theorem 2] with Λ_p as driving measure. This yields to

$$\begin{aligned}
 & \text{Cov}(\mathcal{V}_t)(\cdot \times \cdot) \\
 &= \int_{\mathcal{S}(\mathbb{R}^2)} \frac{1}{2} (\Delta^e \otimes \Delta^e)(\cdot \times \cdot) \mathcal{I}^1(s^2 \exp(-s\Lambda_p([e])); t) \ll (\Lambda_p \times \Lambda_p) \cap \Lambda_p \gg (de) \\
 & \quad + \int_{\mathcal{S}(\mathbb{R}^2)} (\Delta^e \otimes \Lambda_p([\cdot \cap e]) + \Lambda_p([\cdot \cap e]) \otimes \Delta^e)(\cdot \times \cdot) \\
 & \quad \quad \quad \mathcal{I}^2(s^2 \exp(-s\Lambda_p([e])); t) \ll (\Lambda_p \times \Lambda_p) \cap \Lambda_p \gg (de) \\
 & \quad + 4 \int_{\mathcal{S}(\mathbb{R}^2)} (\Lambda_p([\cdot \cap e]) \otimes \Lambda_p([\cdot \cap e]))(\cdot \times \cdot) \\
 & \quad \quad \quad \mathcal{I}^3(s^2 \exp(-s\Lambda_p([e])); t) \ll (\Lambda_p \times \Lambda_p) \cap \Lambda_p \gg (de). \quad (5.37)
 \end{aligned}$$

We will investigate each summand separately and will give the explicit formulas for each step of the proof for the first summand. The Mondrian specific expressions of the segment intersection measure (5.9) and for line segments e together with (5.18) yields

$$\begin{aligned}
 & \int_{\mathcal{S}(\mathbb{R}^2)} \frac{1}{2} (\Delta^e \otimes \Delta^e)(\cdot \times \cdot) \mathcal{I}^1(s^2 \exp(-s\Lambda_p([e])); t) \ll (\Lambda_p \times \Lambda_p) \cap \Lambda_p \gg (de) \\
 &= \int_{[\mathbb{R}^2]} \int_{[L]} \int_{[L]} \frac{1}{2} (\Delta^{L(L_1, L_2)} \otimes \Delta^{L(L_1, L_2)})(\cdot \times \cdot) \\
 & \quad \quad \quad \mathcal{I}^1(s^2 \exp(-s\Lambda_p([L(L_1, L_2)])); t) \Lambda_p(dL_1) \Lambda_p(dL_2) \Lambda_p(dL) \\
 &= p(1-p)^2 \int_{\mathbb{R}} \int_{\mathbb{R}} \int_{\mathbb{R}} \frac{1}{2} \left((\delta_{(\tau, \sigma)} + \delta_{(\vartheta, \sigma)}) \otimes (\delta_{(\tau, \sigma)} + \delta_{(\vartheta, \sigma)}) \right) (\cdot \times \cdot) \\
 & \quad \quad \quad \mathcal{I}^1(s^2 \exp(-s(1-p)|\tau - \vartheta|); t) d\vartheta d\tau d\sigma \\
 &+ (1-p)p^2 \int_{\mathbb{R}} \int_{\mathbb{R}} \int_{\mathbb{R}} \frac{1}{2} \left((\delta_{(\sigma, \tau)} + \delta_{(\sigma, \vartheta)}) \otimes (\delta_{(\sigma, \tau)} + \delta_{(\sigma, \vartheta)}) \right) (\cdot \times \cdot) \\
 & \quad \quad \quad \mathcal{I}^1(s^2 \exp(-sp|\tau - \vartheta|); t) d\vartheta d\tau d\sigma. \quad (5.38)
 \end{aligned}$$

As a second step, we prepare for the diagonal shift argument to obtain the reduced covariance measure by (5.15) again. For this, let $A \times B$ be a measurable product. The first summand of Equation (5.38) simplifies to four products which are investigated separately. By Lemma 5.3.1(iii), we obtain

$$\int_{\mathbb{R}} \int_{\mathbb{R}} \int_{\mathbb{R}} \delta_{(\tau, \sigma)}(A) \delta_{(\tau, \sigma)}(B) \mathcal{I}^1(s^2 \exp(-s(1-p)|\tau - \vartheta|); t) d\vartheta d\tau d\sigma$$

$$\begin{aligned}
 &= \int_{\mathbb{R}} \int_{\mathbb{R}} \int_{\mathbb{R}} \delta_{(\vartheta, \sigma)}(A) \delta_{(\vartheta, \sigma)}(B) \mathcal{I}^1(s^2 \exp(-s(1-p)|\tau - \vartheta|); t) \, d\vartheta \, d\tau \, d\sigma \\
 &= \int_{\mathbb{R}^2} \delta_w(A) \int_{\mathbb{R}} \delta_{\mathbf{0}}(B - w) \mathcal{I}^1(s^2 \exp(-s(1-p)|z|); t) \, dz \, dw
 \end{aligned}$$

and

$$\begin{aligned}
 &\int_{\mathbb{R}} \int_{\mathbb{R}} \int_{\mathbb{R}} \delta_{(\tau, \sigma)}(A) \delta_{(\vartheta, \sigma)}(B) \mathcal{I}^1(s^2 \exp(-s(1-p)|\tau - \vartheta|); t) \, d\vartheta \, d\tau \, d\sigma \\
 &= \int_{\mathbb{R}} \int_{\mathbb{R}} \int_{\mathbb{R}} \delta_{(\vartheta, \sigma)}(A) \delta_{(\tau, \sigma)}(B) \mathcal{I}^1(s^2 \exp(-s(1-p)|\tau - \vartheta|); t) \, d\vartheta \, d\tau \, d\sigma \\
 &= \int_{\mathbb{R}^2} \delta_w(A) \int_{\mathbb{R}} \delta_{(z, 0)}(B - w) \mathcal{I}^1(s^2 \exp(-s(1-p)|z|); t) \, dz \, dw.
 \end{aligned}$$

The second summand in (5.37) can be simplified in the same way.

As third step, we use the diagonal shift argument from (5.15) again and obtain the reduced covariance measure of the vertex process as

$$\begin{aligned}
 \widehat{\text{Cov}}(\mathcal{V}_t)(\cdot) &= p(1-p) \left[(1-p) \left(\int_{\mathbb{R}} \delta_{\mathbf{0}}(\cdot) \mathcal{I}^1(s^2 \exp(-s(1-p)|z|); t) \, dz \right. \right. \\
 &\quad \left. \left. + \int_{\mathbb{R}} \delta_{(z, 0)}(\cdot) \mathcal{I}^1(s^2 \exp(-s(1-p)|z|); t) \, dz \right) \right. \\
 &\quad \left. + p \left(\int_{\mathbb{R}} \delta_{\mathbf{0}}(\cdot) \mathcal{I}^1(s^2 \exp(-sp|z|); t) \, dz + \int_{\mathbb{R}} \delta_{(0, z)}(\cdot) \mathcal{I}^1(s^2 \exp(-sp|z|); t) \, dz \right) \right. \\
 &\quad \left. + 4 \left((1-p)^2 \int_{\mathbb{R}} \ell_1(\cdot \cap \overline{(0z)_0}) \mathcal{I}^2(s^2 \exp(-s(1-p)|z|); t) \, dz \right. \right. \\
 &\quad \left. \left. + p^2 \int_{\mathbb{R}} \ell_1(\cdot \cap \overline{0(0z)}) \mathcal{I}^2(s^2 \exp(-sp|z|); t) \, dz \right. \right. \\
 &\quad \left. \left. + (1-p)^3 \int_{\mathbb{R}} \left(\int_{\overline{(0z)_0}} \int_{\overline{(0z)_0}} \delta_{y-x}(\cdot) \, dx \, dy \right) \mathcal{I}^3(s^2 \exp(-s(1-p)|z|); t) \, dz \right. \right. \\
 &\quad \left. \left. + p^3 \int_{\mathbb{R}} \left(\int_{\overline{0(0z)}} \int_{\overline{0(0z)}} \delta_{y-x}(\cdot) \, dx \, dy \right) \mathcal{I}^3(s^2 \exp(-sp|z|); t) \, dz \right) \right].
 \end{aligned}$$

As the fourth step, we use the intensity $\Lambda_{\mathcal{V}} = t^2 p(1-p)$ and the coherences of the reduced

covariance measure and Ripley's K-function to conclude

$$K_{\mathcal{V}}(r) = \frac{1}{\lambda_{\mathcal{V}}^2} \widehat{\mathcal{K}}(\mathcal{V}_t)(R_{r,p}) = \frac{1}{(t^2 p(1-p))^2} \widehat{\text{Cov}}(\mathcal{V}_t)(R_{r,p}) + \ell_2(R_{r,p}). \quad (5.39)$$

Simplifying notation, we write $S_1(r)$ for the first two integral expressions, $S_2(r)$ for the third and fourth integral, and $S_i(r)$ with $3 \leq i \leq 6$ for the last four integral expressions, respectively. We obtain

$$\begin{aligned} \mathcal{K}(\mathcal{V}_t)(R_{r,p}) = & \\ & r^2 p(1-p) + \frac{1}{t^2(1-p)} \left[(1-p)S_1(r) + pS_2(r) \right. \\ & \left. + 4 \left((1-p)^2 S_3(r) + p^2 S_4(r) + (1-p)^3 S_5(r) + p^3 S_6(r) \right) \right]. \end{aligned}$$

As a final step, we take the derivative of each summand separately before applying suitable normalization. For $S_1(r)$, we use Equation (5.26) after some simplification and obtain

$$\begin{aligned} \frac{dS_1(r)}{dr} &= \frac{d}{dr} \left[\int_{\mathbb{R}} \delta_{\mathbf{0}}(R_{r,p}) \mathcal{I}^1(s^2 \exp(-s(1-p)|z|); t) dz \right. \\ & \quad \left. + \int_{\mathbb{R}} \delta_{(z,0)}(R_{r,p}) \mathcal{I}^1(s^2 \exp(-s(1-p)|z|); t) dz \right] \\ &= \frac{d}{dr} \left[2 \int_0^{\infty} \mathcal{I}^1(s^2 \exp(-s(1-p)z); t) dz + \int_0^{(1-p)r} \mathcal{I}^1(s^2 \exp(-s(1-p)z); t) dz \right] \\ &= (1-p) \mathcal{I}^1(s^2 \exp(-s(1-p)^2 r); t). \end{aligned}$$

Likewise, $S_2(r)$ yields

$$\begin{aligned} \frac{dS_2(r)}{dr} &= \frac{d}{dr} \left[\int_{\mathbb{R}} \delta_{\mathbf{0}}(R_{r,p}) \mathcal{I}^1(s^2 \exp(-sp|z|); t) dz + \int_{\mathbb{R}} \delta_{(0,z)}(R_{r,p}) \mathcal{I}^1(s^2 \exp(-sp|z|); t) dz \right] \\ &= p \mathcal{I}^1(s^2 \exp(-sp^2 r); t). \end{aligned}$$

We obtain the derivatives of $S_3(r)$ and $S_4(r)$ in a similar way to those of $T_1(r)$ and $T_2(r)$. The derivatives of $S_5(r)$ and $S_6(r)$ follow similar considerations to those of $T_3(r)$ and $T_4(r)$.

Putting all derivatives back together and using concrete values for the integrals according to Lemma 5.3.4, we obtain the pair-correlation function as stated in Theorem 5.1.7.

□

Chapter 6

Probabilistic analysis of line segments

Different kinds of line segments appear in STIT tessellations. These are investigated under various aspects in several publications (see for example [8, 17, 34]). Topics of research often involves the distributions of their length, birth time or the number of internal vertices. We first describe the set-up and necessary notations, as well as known results including probability density functions for the length, birth time and number of internal vertices in Section 6.1. From these, we derive some refined results. In Section 6.2, we first give the probability density functions and expected values of these properties conditioned on the birth time of an I-segment. Another refinement concerns differently weighted I-segments and their density functions. In Section 6.3, we use some of these results to refine geometrical and metrical properties proven by Cowan [8] in a set-up without birth time dependencies.

6.1 Set-up

In this section, we introduce additional terms and notations necessary for this chapter and recall relevant results. The main focus for the third part of this thesis are different kinds of line segments within planar STIT tessellations, namely I-, J- and K-segments. A line segment between two vertices but without any internal vertices is called a *K-segment* or an *edge*. Line segments of a planar STIT tessellation which are sides of a cell are referred to as *J-segments* or *sides*. Lastly, an *I-segment* is the union of collinear edges which can not be lengthened by another edge. Therefore, they are also referred to as *maximal edges*.

For $X \in \{I, J, K\}$, we define \mathbb{X} to be the set of all segments of type X and $\gamma_{\mathbb{X}}$ as the intensity of segments of type X . For a given segment x , we denote its center by $m(x)$ and we write \mathcal{X} for the typical X -segment. For non-negative functions f on \mathbb{X} , the following identity may be

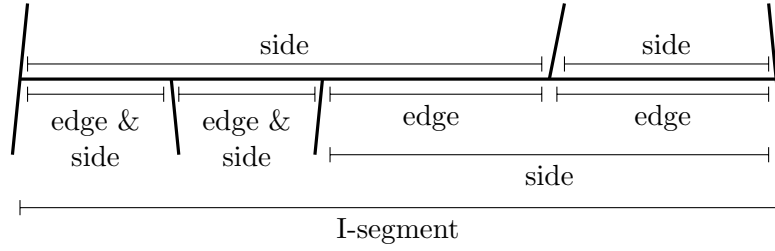


FIGURE 6.1: Snippet of a planar STIT tessellation with line segments labeled according their types.

used to define the *typical X-segment*:

$$\mathbb{E}f(\mathcal{X}) = \frac{1}{\gamma_{\mathbb{X}}} \mathbb{E} \sum_{\substack{x \in \mathbb{X} \\ m(x) \in [0,1]^2}} f(x - m(x)) .$$

Intuitively, \mathcal{X} is the line segment which is randomly chosen among all X -segments with their center in a bounded window. One might add a translation invariant weight function $w : \mathbb{X} \rightarrow \mathbb{R}_+$ to influence the probability with which an segments is chosen. A *typical w -weighted X -segment* is then defined by

$$\mathbb{E}f(\mathcal{X}^w) = \frac{1}{\mathbb{E} \sum_{\substack{x \in \mathbb{X} \\ m(x) \in [0,1]^2}} w(x)} \sum_{\substack{x \in \mathbb{X} \\ m(x) \in [0,1]^2}} f(x - m(x)) w(x) ,$$

where \mathcal{X}^w denotes the typical X -segments weighted with w . In what follows, we are interested in properties of typical I-segments. More precisely, we consider their length, birth time or number of internal vertices. Also, we use five different weight functions $w \in \{\ell, \beta, \xi, \xi_{+1}, \xi_{+2}\}$, which, defined on \mathbb{I} , refer to the length, birth time, number of internal vertices, number of internal edges and number of internal sides, respectively. The latter two notations suggest a description for the number of internal edges and sides in terms of the number of internal vertices, *i.e.*, the number of internal edges (sides) in an I-segment is given by its number of internal vertices plus one (two).

One main groundwork for the following results is the property of STIT tessellations inducing a stationary Poisson point process on a line g intersecting the skeleton of $Y(t)$ (see Section 4.3). One may think about g as a line, which covers an I-Segment of the tessellation. This Poisson point process may be considered as a superimposition of two marked Poisson processes. Two properties of these are of importance for the last section. First, consider the I-segment as a horizontal line. The probability for edges pointing upward or downward from the intersection points is $\frac{1}{2}$. Second, the points are distributed uniformly at random within a given interval. Based on these properties, Cowan deduced geometrical results concerning different line segments in [8], and since these are not dependent on the birth time of an

I-segment, we can adopt them to our analysis in Section 6.3.1.

6.2 Refined analysis of I-segments

Within planar STIT tessellations, I-segments are one of the most studied line segments when it comes to properties like distribution function of their length, birth time or number of internal vertices (see for example [20, 34]). The joint probability density function of these is given by

$$h_{\ell(\mathcal{I}),\beta(\mathcal{I}),\xi(\mathcal{I})}(x, s, m) = \frac{4s^2 \left(\frac{4}{\pi}x(t-s)\right)^m}{\pi t^2 m!} e^{-\frac{2}{\pi}x(2t-s)} \quad (6.1)$$

in [20, Equation (5.13)]. Integration and summation will lead to the probability density functions of a single mark. These and their expected values are:

$$\begin{aligned} h_{\ell(\mathcal{I})}(x) &= \frac{1}{t^2 x^3} \left(\pi^2 - (\pi^2 + 2\pi t x + 2t^2 x^2) \cdot e^{-\frac{2}{\pi} t x} \right), & \mathbb{E}[\ell(\mathcal{I})] &= \frac{\pi}{t}, \\ h_{\beta(\mathcal{I})}(s) &= \frac{2s}{t^2}, & \mathbb{E}[\beta(\mathcal{I})] &= \frac{2t}{3}, \\ p_m = h_{\xi(\mathcal{I})}(m) &= 2^{m+1} \int_0^1 \frac{(1-a)^2 a^m}{(1+a)^{m+1}} da, & \mathbb{E}[\xi(\mathcal{I})] &= 2. \end{aligned}$$

One may deduce other joint and conditional density functions from these results. Relevant density functions and expected values for this chapter are collected in the following corollary.

Corollary 6.2.1 *For the length $\ell(\mathcal{I})$, birth time $\beta(\mathcal{I})$ and number of internal vertices $\xi(\mathcal{I})$ for typical I-segments, some selected joint and conditional density functions are given as follows:*

$$\begin{aligned} p_{m|s} = h_{\xi(\mathcal{I})|\beta(\mathcal{I})=s}(m) &= \frac{s(2(t-s))^m}{(2t-s)^{m+1}} & \mathbb{E}[\xi(\mathcal{I}) | \beta(\mathcal{I}) = s] &= 2 \left(\frac{t}{s} - 1 \right) \\ h_{\ell(\mathcal{I})|\beta(\mathcal{I})=s, \xi(\mathcal{I})=m}(x) &= \frac{x^m (2(2t-s))^{m+1}}{\pi^{m+1} m!} e^{-\frac{2}{\pi} x(2t-s)} & \mathbb{E}[\ell(\mathcal{I}) | \beta(\mathcal{I}) = s, \xi(\mathcal{I}) = m] &= \frac{(m+1)\pi}{2(2t-s)} \\ h_{\ell(\mathcal{I})|\beta(\mathcal{I})=s}(x) &= \frac{2}{\pi} s e^{-\frac{2}{\pi} s x} & \mathbb{E}[\ell(\mathcal{I}) | \beta(\mathcal{I}) = s] &= \frac{\pi}{2s} \end{aligned}$$

The proof of this corollary simply uses integration of (6.1) and division of the probability density functions of a single mark.

Another refinement of I-segments may concern distributions for weighted versions of these segments.

Proposition 6.2.2 *For a given weight function $w \in \{\ell, \beta, \xi, \xi_{+1}, \xi_{+2}\}$ defined on \mathbb{I} , the joint probability density function of the length, birth time and number of internal vertices of a*

w -weighted I -segment is given by

$$h_{(\ell(\mathcal{I}), \beta(\mathcal{I}), \xi(\mathcal{I}))}(x, s, m) = \frac{1}{\mathbb{E}w(\mathcal{I})} \cdot w(I) \cdot h_{\ell(I), \beta(I), \xi(I)}(x, s, m).$$

Proof. We start with the probability

$$\begin{aligned} \mathbb{P}(\ell(\mathcal{I}^w) \leq x, \beta(\mathcal{I}^w) \leq s, \xi(\mathcal{I}^w) = m) &= \mathbb{E}[\mathbf{1}(\ell(\mathcal{I}^w) \leq x, \beta(\mathcal{I}^w) \leq s, \xi(\mathcal{I}^w) = m)] \\ &= \frac{1}{\mathbb{E}w(\mathcal{I})} \mathbb{E}[w(\mathcal{I}) \mathbf{1}(\ell(\mathcal{I}^w) \leq x, \beta(\mathcal{I}^w) \leq s, \xi(\mathcal{I}^w) = m)] \\ &= \frac{1}{\mathbb{E}w(\mathcal{I})} \int_0^s \int_0^x w(\mathcal{I}) h_{\ell(\mathcal{I}), \beta(\mathcal{I}), \xi(\mathcal{I})}(a, b, m) da db \end{aligned}$$

and obtain the density function by taking the derivative with respect to s and x , what concludes the proof. \square

In particular, we will attach weights which we can describe with the number of internal vertices. These are

$$\xi(I) = m, \quad \xi_{+1}(I) = m + 1, \quad \xi_{+2}(I) = m + 2,$$

for the number of internal vertices, number of internal edges and number of internal sides, respectively.

Lemma 6.2.3 *Let $\xi(I)$, $\xi_{+2}(I)$ and $\xi_{+1}(I)$ be the weight functions defined as before. The probability density functions for the birth time distribution of typical I -segments according their weight are given by*

$$h_{\beta(I^\xi)}(s) = \frac{2}{t} \left(1 - \frac{s}{t}\right), \quad h_{\beta(I^{\xi_{+1}})}(s) = \frac{2}{3t} \left(2 - \frac{s}{t}\right), \quad h_{\beta(I^{\xi_{+2}})}(s) = \frac{1}{t}.$$

Proof. We use Proposition 6.2.2 to deduce a joint probability density function followed by integration and summation to obtain the stated marginal distributions. For $(d, w) = (0, \xi)$ (respectively $(1, \xi_{+1})$, and $(2, \xi_{+2})$), we have

$$h_{\beta(I^w)}(s) = \int_0^\infty \sum_{m=0}^\infty \frac{1}{d+2} \cdot (m+d) \cdot h_{\ell(\mathcal{I}), \beta(\mathcal{I}), \xi(\mathcal{I})}(x, s, m) dx.$$

For example, for $(d, w) = (0, \xi)$ we have

$$h_{\beta(I^\xi)}(s) = \int_0^\infty \sum_{m=0}^\infty \frac{1}{2} \cdot m \cdot h_{\ell(\mathcal{I}), \beta(\mathcal{I}), \xi(\mathcal{I})}(x, s, m) dx$$

$$= \frac{4s^2}{2\pi t^2} \int_0^\infty e^{-\frac{2}{\pi}x(2t-s)} \sum_{m=0}^\infty \frac{(\frac{4}{\pi}x(t-s))^m}{(m-1)!} dx.$$

Using the power series of the real exponential function leads to

$$h_{\beta(I\xi)}(s) = \frac{8s^2(t-s)}{\pi^2 t^2} \int_0^\infty x e^{-\frac{2}{\pi}xs} ds = \frac{2}{t} \left(1 - \frac{s}{t}\right),$$

where the last step uses integration by parts. \square

6.3 Geometrical and metrical properties of line segments

In this section, we refine several results of Cowan [8]. Specifically, Cowan studied the probability of specific geometrical and metrical properties of line segments. Here, we refine his calculations by conditioning on the birth time of (covering) I-segments. In the first part, we focus on geometrical properties of side, whereas the second deals with the length distribution of different line segments.

6.3.1 Geometrical properties of sides

We write \mathcal{P} for a geometrical property, e.g. the position of a side on its covering I-segment, and define ρ as the probability that a side satisfies this property. The probability may be obtained by counting these sides in two different ways. First, one can consider the intensity of all sides within a tessellation and multiply with the probability for a side satisfying \mathcal{P} . This is $\rho \cdot \gamma_{\mathbb{I}}$ with $\gamma_{\mathbb{I}}$ being the intensity of sides. Second one may also multiply the intensity of I-segments with the expected number of sides fulfilling \mathcal{P} on a typical I-segment. For the latter, we write $\mathbb{E}n(\mathcal{P})$. Putting these together, one obtain

$$\begin{aligned} \rho \gamma_{\mathbb{I}} &= \gamma_{\mathbb{I}} \mathbb{E}n(\mathcal{P}) \\ \Rightarrow \quad \rho &= \frac{\gamma_{\mathbb{I}}}{\gamma_{\mathbb{J}}} \mathbb{E}n(\mathcal{P}) = \frac{1}{4} \sum_{m=0}^\infty h_{\xi(\mathcal{I})}(m) \mathbb{E}[n(\mathcal{P}) \mid m]. \end{aligned}$$

One may use similar considerations to ask for those probabilities under the condition that I-segments are chosen according to their birth time s . For this, we use the density function and side intensity conditioned on the birth time s , which yields the weighted probability

$$\rho_s = \frac{s}{2t} \sum_{m=0}^\infty h_{\xi(\mathcal{I})|\beta(\mathcal{I})=s}(m) \mathbb{E}[n(\mathcal{P}) \mid m]. \quad (6.2)$$



FIGURE 6.2: An I-segment with inner vertices all pointing in the same directions (left) or pointing in different directions (right) with sides adjacent to exactly one terminus highlighted in red.

Given this identity, we can investigate the first geometrical questions in [8] adapted to our setting of I-segments with birth time dependency.

Problem 1: Position of the typical side in the covering I-Segment

We can distinguish sides of a STIT tessellation by their position on the covering I-segment. For this problem we write $\rho_{a,s}$ for the probability that the typical side, lying on an I-segment with birth time s is adjacent to a termini.

a) *A typical side is adjacent to both termini*

This property emerges whenever all internal vertices within an I-segment are pointing in the same direction. As the probabilities for pointing up- or downwards are both $\frac{1}{2}$, the probability for m internal vertices pointing the same direction is $2 \cdot \left(\frac{1}{2}\right)^m$. Thus, the probability of a typical side being adjacent to both termini is

$$\rho_{2,s} = \frac{s}{2t} \cdot \sum_{m=0}^{\infty} \frac{s \cdot (2(t-s))^m}{(2t-s)^{m+1}} \cdot \left(\frac{1}{2}\right)^{m-1} = \frac{s^2}{t^2}.$$

b) *A typical side is adjacent to exactly one terminus*

We consider two different cases here. First, suppose all inner vertices are either pointing upwards or downwards. In this setting, there are exactly two sides with this property, one at each terminus (see Figure 6.2, left). The probability for this is given by $\frac{1}{2}$ as in a). For the second case, both directions of pointing occur. Thus, there are four sides with this property, two at each end of the I-segment (see Figure 6.2, right). We obtain

$$\rho_{1,s} = \frac{s}{2t} \cdot \sum_{m=1}^{\infty} \frac{s \cdot (2(t-s))^m}{(2t-s)^{m+1}} \cdot \left[2 \cdot \left(\frac{1}{2}\right)^{m-1} + 4 \cdot \left(1 - \left(\frac{1}{2}\right)^{m-1}\right) \right] = \frac{2s(t-s)}{t^2}.$$

c) *A typical side is adjacent to none terminus*

For this, we simply use complementary probability. We obtain

$$\rho_{0,s} = 1 - \left(\frac{s^2}{t^2}\right) - \left(\frac{2s(t-s)}{t^2}\right) = \frac{(t-s)^2}{t^2}.$$

The birth time dependency of these probabilities is shown in Figure 6.3. Former results by Cowan in [8] state that the probabilities, if I-segments are not conditioned on their birth

time, equal $\frac{1}{3}$ for all cases.

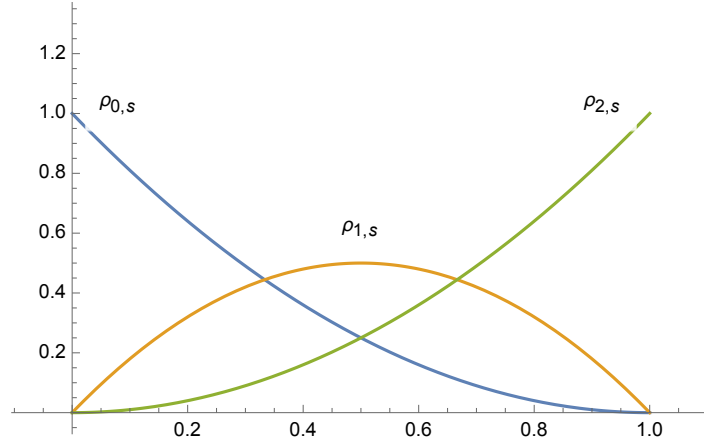


FIGURE 6.3: Let $t = 1$. The probability $\rho_{a,s}$ with $a \in \{0, 1, 2\}$.

Remark 6.3.1 One may recover results by Cowan in [8] by multiplying the probabilities above with the density function of the birth time distribution of I-segments conditioned on the number of sides and integrating over s . More formally, for $\rho_{2,s}$ we have

$$\int_0^t \frac{s^2}{t^2} \cdot \frac{1}{t} ds = \frac{1}{t^3} \int_0^t s^2 ds = \frac{1}{3}.$$

Problem 2: Number of internal vertices of a typical side

In this problem, we focus on the number of internal vertices within the interior of a typical side, which is covered by an I-segment with birth time s . In other words, this problem is about the number of consecutive vertices pointing in the same direction. We again use results from Cowan in [8] for the expected value, since these are not dependent on s . He concludes that for a internal vertices,

$$\mathbb{E}n(\mathcal{P}_a \mid m) = \begin{cases} 0 & \text{for } m < a, \\ \left(\frac{1}{2}\right)^{a-1} & \text{for } m = a, \\ (m - a + 3) \left(\frac{1}{2}\right)^{(a+1)} & \text{for } m > a. \end{cases}$$

Again using Equation (6.2), we get

$$\begin{aligned} \rho_{a,s} &= \frac{s}{2t} \cdot \left[\frac{s \cdot (2(t-s))^a}{(2t-s)^{a+1}} \cdot \left(\frac{1}{2}\right)^{a-1} + \sum_{m=a+1}^{\infty} \frac{s \cdot (2(t-s))^m}{(2t-s)^{m+1}} \cdot (m-a+3) \left(\frac{1}{2}\right)^{(a+1)} \right] \\ &= \frac{t \cdot (t-s)^a}{(2t-s)^{a+1}} \end{aligned}$$

where $\rho_{a,s}$ describes the probability of a typical side, lying on an I-segment with birth time s , contains a internal vertices. The expected number of internal vertices dependent on the birth time is $1 - \frac{s}{t}$. Fixing the number of internal vertices, Figure 6.4 shows the change of its probability dependent on s . Naturally, sides on I-segments born early tend to have a higher number of internal vertices than those appearing later.

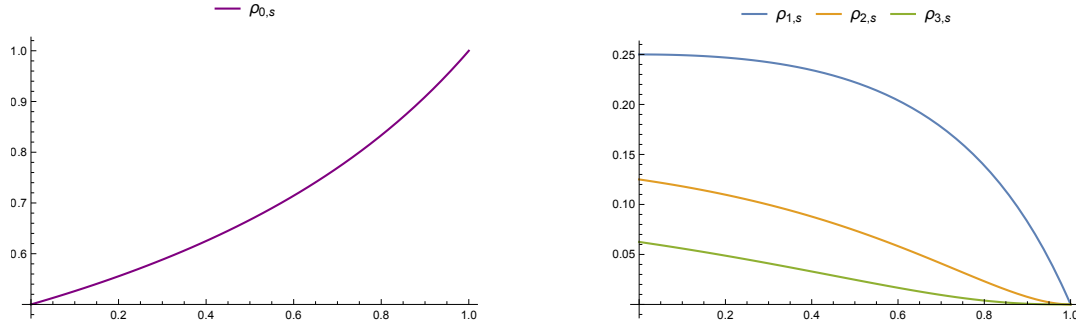


FIGURE 6.4: Let $t = 1$. The probability $\rho_{a,s}$ with $a = 0$ (left) and $a \in \{1, 2, 3\}$ (right).

Problem 3: Number of sides adjacent to a typical side

We say two sides J, J' are adjacent if $J \subseteq J'$ or $J' \subseteq J$. The calculation for the expected value in this situation is quite complicated, but as they are independent of s , we refer to [8] for more details. We write $\rho_{a,s}$ for the probability that a typical side, lying on an I-segment with birth time s , is adjacent to a sides. These are

$$\rho_{1,s} = \frac{s}{2t} \cdot \sum_{m=3}^{\infty} \frac{s \cdot (2(t-s))^m}{(2t-s)^{m+1}} \cdot \frac{m-2}{4} = \frac{(t-s)^3}{t(2t-s)^2},$$

$$\begin{aligned} \rho_{2,s} &= \frac{s}{2t} \cdot \left[2 \cdot h_{\xi(\mathcal{I})|\beta(\mathcal{I})=s}(0) + 2 \cdot h_{\xi(\mathcal{I})|\beta(\mathcal{I})=s}(1) \right. \\ &\quad \left. + \frac{7}{2} \cdot h_{\xi(\mathcal{I})|\beta(\mathcal{I})=s}(2) + \sum_{m=3}^{\infty} h_{\xi(\mathcal{I})|\beta(\mathcal{I})=s}(m) \cdot \left(4 + \frac{5}{8}(m-2)\right) \right] \\ &= \frac{5t^4 - 4st^3 - 3s^2t^2 + 4s^3t - s^4}{t(2t-s)^3}, \end{aligned}$$

and for $a \geq 3$

$$\rho_{a,s} = \frac{s}{2t} \cdot \left[\left(\frac{1}{2}\right)^{a-3} h_{\xi(\mathcal{I})|\beta(\mathcal{I})=s}(a-2) + \left(\frac{1}{2}\right)^{a-2} h_{\xi(\mathcal{I})|\beta(\mathcal{I})=s}(a) + \frac{7}{2} h_{\xi(\mathcal{I})|\beta(\mathcal{I})=s}(2) \right]$$

$$\begin{aligned}
 & \left. + \sum_{m=3}^{\infty} \left(4 + \frac{5}{8}(m-2) \right) \cdot h_{\xi(\mathcal{I})|\beta(\mathcal{I})=s}(m) \right] \\
 &= \frac{t^3 \cdot (t-s)^{a-2}}{(2t-s)^{a+1}}.
 \end{aligned}$$

Given these probabilities, we can again recover known results for non-weighted I-segments in Cowan [8] in the same manner as explained in Remark 6.3.1. The expected value for the number of internal vertices is $2 + s \left(\frac{1}{t} - \frac{1}{2t-s} \right)$. The probabilities for some concrete number of internal vertices are shown in Figure 6.5.

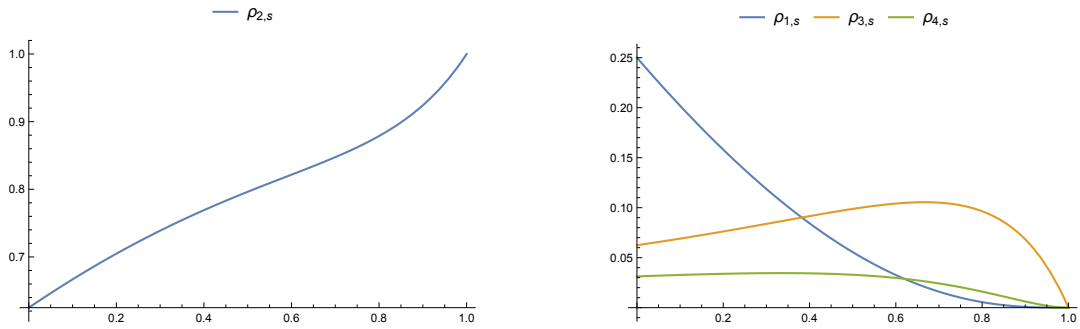


FIGURE 6.5: Let $t = 1$. The probability $\rho_{a,s}$ with $a = 2$ (left) and $a \in \{1, 3, 4\}$ (right).

6.3.2 Metric properties

Similar to the section before, metric properties of (typical) line segments have been studied by Cowan in [8]. Here, we specialize to (covering) I-segments of a given birth time. For this, we use the conditional density function for the length distribution of I-segments given its number of internal vertices and birth time. This function was given in Corollary 6.2.1 as

$$h_{\ell(\mathcal{I})|\beta(\mathcal{I})=s, \xi(\mathcal{I})=m}(x) = \frac{x^m (2(2t-s))^{m+1}}{\pi^{m+1} m!} \cdot e^{-\frac{2}{\pi} x(2t-s)}.$$

The length distribution of a segment within a STIT tessellation does not only depend on its type but also on the way sampling these segments. To clarify and distinguish between two ways of sampling, in what follows we write ℓ_Y^X for the length distribution of line segments of type Y when sampling according to segments of type X .

Length of a random edge on a typical I-segment sampled according its birth time s

In this first setting, we pick a typical I-segment with a given birth time s and ask about the length distribution of a randomly chosen edge on this I-segment. For this, we use [8, Corollary 3] which states that the probability density function of the length x of a random

edge lying on a typical I-segment with length y and m internal vertices. This is

$$h_{\ell(K)|\ell(\mathcal{I})=y, \xi(\mathcal{I})=m}(x) = \frac{m}{y} \left(1 - \frac{x}{y}\right)^{m-1}.$$

The proof of this identity uses the spacing properties of m internal vertices which are independent and uniformly distributed along the I-segment. This density does not depend on the birth time of the I-segment and can thus be used in our setup unchanged.

We can now conclude the density function for the conditional length distribution of an randomly chosen edge to be

$$\begin{aligned} \ell_K^{\mathcal{I}}(x|\beta(\mathcal{I}) = s) &= p_{0|s} \cdot h_{\ell(\mathcal{I})|\beta(\mathcal{I})=s, \xi(\mathcal{I})=0}(x) \\ &+ \sum_{m=1}^{\infty} p_{m|s} \int_x^{\infty} h_{\ell(\mathcal{I})|\beta(\mathcal{I})=s, \xi(\mathcal{I})=m}(y) \times \frac{m}{y} \left(1 - \frac{x}{y}\right)^{m-1} dy \\ &= \frac{2(2t-s)}{\pi} e^{-\frac{2}{\pi}x(2t-s)}. \end{aligned}$$

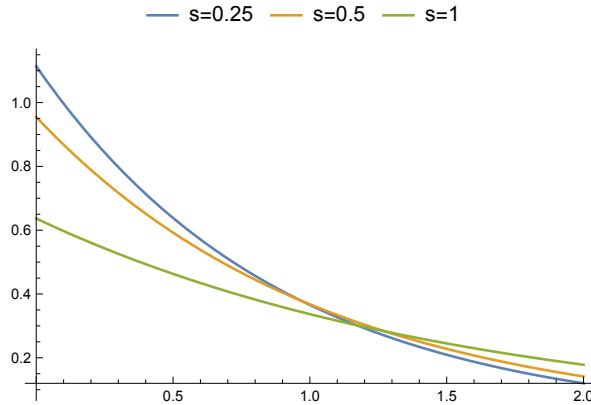


FIGURE 6.6: Let $t = 1$. Length of a random edge covered by a typical I-segment dependent on its birth time $s \in \{0.25, 0.5, 1\}$.

The mean length is $\frac{\pi}{2(2t-s)}$. The densities are visualized for some choices of s in Figure 6.6.

Length of an I-segment with birth time s covering a typical edge

In this setting, a typical edge \mathcal{K} , which is covered by an I-segment with birth time s , is picked out of the STIT tessellation. We are now interested in the length distribution of this covering I-segment. This way of sampling promotes picking I-segments with a higher number of edges and therefore segments with a higher number of internal vertices. Hence, the chosen I-segments with birth time s will contain m internal vertices with the probability

$$q_{\xi(\mathcal{I})|\beta(\mathcal{I})=s}^{\mathcal{K}}(m) = \frac{m+1}{\mathbb{E}[\xi(\mathcal{I})|\beta(\mathcal{I})=s] + 1} p_{m|s} = \frac{(m+1)s}{2t-s} p_{m|s}.$$

This leads to the following length distribution for I-segments covering a typical edge and with birth time s :

$$\begin{aligned} \ell_I^{\mathcal{K}}(x|\beta(I) = s) &= \sum_{m=0}^{\infty} h_{\ell(I)|\beta(I)=m, \xi(I)=s}(x) \cdot q_{\xi(I)|\beta(I)=s}^{\mathcal{K}}(m) \\ &= \frac{2s^2}{\pi(2t-s)} \left(1 + \frac{4}{\pi}x(t-s)\right) e^{-\frac{2}{\pi}sx}. \end{aligned}$$

The mean length in this setting is $\pi \left(\frac{1}{s} - \frac{1}{2(2t-s)}\right)$. The densities for some values of s are given in Figure 6.7.

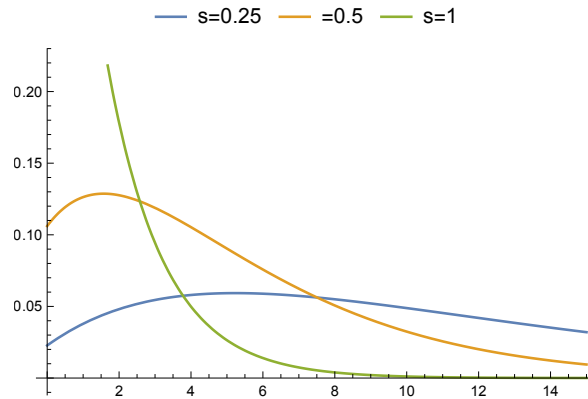


FIGURE 6.7: Let $t = 1$. Length of an I-segments with birth time $s \in \{0.25, 0.5, 1\}$ covering a typical edge.

Length of a random edge of an I-segment with birth time s covering a typical edge

For this way of sampling, we use the probability $q_{\xi(\mathcal{I})|\beta(\mathcal{I})=s}^{\mathcal{K}}(m)$ as before and write $I | \mathcal{K}$ for I-segments covering a typical \mathcal{K} -segment. Thus, the density function is

$$\begin{aligned} \ell_K^{I|\mathcal{K}}(x|\beta(\mathcal{I}) = s) &= q_{\xi(\mathcal{I})|\beta(\mathcal{I})=s}^{\mathcal{K}}(0) \cdot h_{\ell(I)|\beta(I)=s, \xi(I)=0}(x) \\ &\quad + \sum_{m=1}^{\infty} q_{\xi(\mathcal{I})|\beta(\mathcal{I})=s}^{\mathcal{K}}(m) \int_x^{\infty} h_{\ell(I)|\beta(I)=s, \xi(I)=m}(y) \cdot \frac{m}{y} \left(1 - \frac{x}{y}\right)^{m-1} dy \\ &= \frac{2(2t-s)}{\pi} e^{-\frac{2}{\pi}x(2t-s)}. \end{aligned}$$

The mean length in this setting is $\frac{\pi}{2(2t-s)}$.

Remark 6.3.2 This density equals the one for picking a typical I-segments and choosing a random \mathcal{K} -segment, *i.e.*, $\ell_K^{\mathcal{I}}(x | \beta(\mathcal{I}) = s)$. Nevertheless, the densities deduced by Cowan [8] for the respective processes without birth time dependency differ. They can be recovered by

either multiplying with $h_{\beta(\mathcal{I})}(s)$ or $h_{\beta(\mathcal{I}^{\xi+1})}(s)$. More precisely, this is

$$\begin{aligned}\ell_K^{\mathcal{I}}(x) &= \int_0^t \frac{2(2t-s)}{\pi} e^{-\frac{2}{\pi}x(2t-s)} \cdot \frac{2s}{t^2} ds, \\ \ell_K^{I\mathcal{K}}(x) &= \int_0^t \frac{2(2t-s)}{\pi} e^{-\frac{2}{\pi}x(2t-s)} \cdot \frac{2}{3t} \left(2 - \frac{s}{t}\right) ds.\end{aligned}$$

As for the length distribution of an I-segment, one can alter the question from above a little by picking those segments covering a typical side instead of a typical edge. Hence, I-segments with a higher number of internal sides are chosen preferably. Again, one may use the number of internal vertices to conclude that an I-segment with birth time s is picked with probability

$$q_{\xi(I)|\beta(I)=s}^{\mathcal{J}}(m) = \frac{m+2}{\mathbb{E}[\xi(I)|\beta(I)=s] + 2} p_{m|s} = \frac{(m+2)s}{2t} p_{m|s}.$$

Length of an I-segment with birth time s covering a typical side

The calculation strongly follows the one before. We only change the additional factor to be $q_{\xi(I)|\beta(I)=s}^{\mathcal{J}}(m)$. Thus, the length distribution is

$$\begin{aligned}\ell_I^{\mathcal{J}}(x|\beta(I)=s) &= \sum_{m=0}^{\infty} h_{\ell(I)|\beta(I)=s, \xi(I)=m}(x) \cdot q_{\xi(I)|\beta(I)=s}^{\mathcal{J}}(m) \\ &= \frac{2s^2}{\pi t} \left(1 + \frac{2}{\pi}x(t-s)\right) e^{-\frac{2}{\pi}sx}.\end{aligned}$$

The mean length in this setting is $\pi \left(\frac{1}{s} - \frac{1}{2t}\right)$. The densities for some s are given in Figure 6.8.

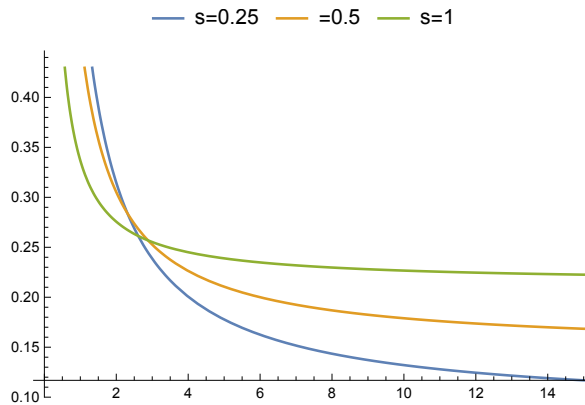


FIGURE 6.8: Let $t = 1$. Length of an I-segments with birth time $s \in \{0.25, 0.5, 1\}$ covering a typical side.

In Cowan's analysis [8], a more precise subdivision of edges was considered for detailed

examination. Thereby one takes into account, whether an edge is a side of zero, one or two cells. To further enhance the calculations incorporating birth time dependency, it would be worthwhile to extend the above considerations to these subdivisions. Another aspect worth investigating is exploring the birth times of edges and sides. However, it is important to note that these line segments not only have a birth time but also a time of death as edges and sides may be divided by the point process on their covering I-segment. Thus, conditioning on these particular parameters can be challenging.

Bibliography

- [1] BALOG, M., LAKSHMINARAYANAN, B., GHAHRAMANI, Z., ROY, D. M., AND TEH, Y. W. The Mondrian Kernel. *32nd Conference on Uncertainty in Artificial Intelligence* (2016), 32 – 41.
- [2] BENDER, E. A. Central and local limit theorems applied to asymptotic enumeration. *Journal of Combinatorial Theory, Series A* 15, 1 (1973), 91–111.
- [3] BETKEN, C., KAUFMANN, T., MEIER, K., AND THÄLE, C. Second-order properties for planar mondrian tessellations. *Methodology and Computing in Applied Probability* 25, 47 (2023).
- [4] BIEHLER, E. Consistency of constructions for cell division processes. *Advances in Applied Probability* 47, 3 (2015), 640 – 651.
- [5] BJÖRNER, A., AND BRENTI, F. *Combinatorics of Coxeter groups*, vol. 231 of *Graduate Texts in Mathematics*. Springer, New York, 2005.
- [6] BLEISTEIN, N., AND HANDELSMAN, R. A. *Asymptotic Expansions of Integrals*. Ardent Media, 1975.
- [7] BÓNA, M. Generalized descents and normality. *Electron. J. Combin.* 15, 1 (2008).
- [8] COWAN, R. Line segments in the isotropic planar stit tessellation. *Advances in Applied Probability* 45 (2013).
- [9] DALEY, D. J., AND VERE-JONES, D. *An Introduction to the Theory of Point Processes: Volume I: Elementary Theory and Methods*. Springer, 2003.
- [10] FÉRAY, V. Central limit theorems for patterns in multiset permutations and set partitions. *The Annals of Applied Probability* 30, 1 (2020).
- [11] FÉRAY, V., MÉLIOT, P.-L., AND NIKEGHBALI, A. *Mod- Φ convergence II: Estimates on the speed of convergence*. Springer International Publishing, Cham, 2019, pp. 405–477.
- [12] HUMPHREYS, J. *Reflection Groups and Coxeter Groups*. Cambridge Studies in Advanced Mathematics. Cambridge University Press, 1990.

-
- [13] JANSON, S. Normal convergence by higher semiinvariants with applications to sums of dependent random variables and random graphs. *The Annals of Probability* 16, 1 (1988), 305–312.
- [14] KAHLE, T., AND STUMP, C. Counting inversions and descents of random elements in finite Coxeter groups. *Math. Comp.* 89, 321 (2019), 437–464.
- [15] LAKSHMINARAYANAN, B., ROY, D. M., AND TEH, Y. W. Mondrian forests: Efficient online random forests. *Advances in Neural Information Processing Systems* 27 (2014), 3140–3148.
- [16] LAKSHMINARAYANAN, B., ROY, D. M., AND TEH, Y. W. Mondrian forests for large-scale regression when uncertainty matters. In *Artificial Intelligence and Statistics* (2016), PMLR, pp. 1478–1487.
- [17] MECKE, J., NAGEL, W., AND WEISS, V. Length distributions of edges in planar stationary and isotropic stit tessellations. *Journal of Contemporary Mathematical Analysis* 42 (2007), 28–43.
- [18] MECKE, J., NAGEL, W., AND WEISS, V. A global construction of homogeneous random planar tessellations that are stable under iteration. *Stochastics* 80, 1 (2008), 51–67.
- [19] MECKE, J., NAGEL, W., AND WEISS, V. The iteration of random tessellations and a construction of a homogeneous process of cell divisions. *Advances in Applied Probability* 40, 1 (2008), 49–59.
- [20] MECKE, J., NAGEL, W., AND WEISS, V. Some distributions for I-segments of planar random homogeneous STIT tessellations. *Mathematische Nachrichten* 284 (2011), 1483 – 1495.
- [21] MEIER, K., AND STUMP, C. Central limit theorems for generalized descents and generalized inversions in finite root systems, 2022.
- [22] NAGEL, W., JOSEPH, M., OHSER, J., AND WEISS, V. A tessellation model for crack patterns on surfaces. *Image Analysis and Stereology* 27 (2008).
- [23] NAGEL, W., AND WEISS, V. Limits of sequences of stationary planar tessellations. *Advances in Applied Probability* 35, 1 (2003), 123–138.
- [24] NAGEL, W., AND WEISS, V. Crack STIT tessellations: characterization of stationary random tessellations stable with respect to iteration. *Advances in Applied Probability* 37, 4 (2005), 859–883.
- [25] PETERSEN, T. *Eulerian numbers*. Birkhauser, New York, 2015.
- [26] PIKE, J. Convergence rates for generalized descents. *Electron. J. Combin.* 18, 1 (2011), Paper 236, 14.

- [27] SCHNEIDER, R., AND WEIL, W. *Stochastic and Integral Geometry*. Springer Science & Business Media, 2008.
- [28] SCHREIBER, T., AND THÄLE, C. Second-order properties and central limit theory for the vertex process of iteration infinitely divisible and iteration stable random tessellations in the plane. *Advances in Applied Probability* 42, 4 (2010), 913–935.
- [29] SCHREIBER, T., AND THÄLE, C. Second-order theory for iteration stable tessellations. *Probability and Mathematical Statistics* 32 (2012), 281 – 300.
- [30] SCHREIBER, T., AND THÄLE, C. Geometry of iteration stable tessellations: Connection with Poisson hyperplanes. *Bernoulli* 19, 5A (2013), 1637 – 1654.
- [31] SOMMERS, E. N. B -stable ideals in the nilradical of a Borel subalgebra. *Canad. Math. Bull.* 48, 3 (2005), 460–472.
- [32] STOYAN, D., KENDALL, W., CHIU, S., AND MECKE, J. *Stochastic Geometry and Its Applications*. Wiley Series in Probability and Statistics. Wiley, 2013.
- [33] STOYAN, D., KENDALL, W. S., AND MECKE, J. *Stochastic Geometry and its Applications*. Wiley, 1995.
- [34] THÄLE, C. Moments of the length of line segments in homogeneous planar stit tessellations. *Image Analysis and Stereology* 28 (2009).

Kathrin Meier

Lebenslauf

Persönliche Daten

Name Kathrin Meier
Geburtsdatum 20.06.1992
Geburtsort Dortmund
Mail Kathrin.Meier@ruhr-uni-bochum.de

Ausbildung

seit 2019 **Ruhr-Universität Bochum.**
Doktorandin
2017 – 2017 **Ruhr-Universität Bochum.**
Master of Education in Mathematik und Chemie
2014 – 2017 **Ruhr-Universität Bochum.**
Bachelor of Arts in Mathematik und Chemie
2011 – 2014 **Max-Planck Institut für Kohlenforschung**, Mülheim a.d. Ruhr.
Ausbildung zur Chemielaborantin
2002 – 2011 **Graf-Engelbert Schule**, Bochum.
Abitur

Dissertation

Titel *Probabilistic analysis of Coxeter statistics and STIT tessellations*
Betreuer & Gutachter Prof. Dr. Christian Stump (Bochum), Prof. Dr. Christoph Thäle (Bochum)

Masterarbeit

Titel *Was bleibt nach KEMIE?*
Betreuer Prof. Dr. Katrin Sommer (Bochum)
Gutachter Prof. Dr. Katrin Sommer (Bochum), Prof. Dr. Axel Rosenhahn (Bochum)

Bachelorarbeit

Titel *Zufällige Young Tableaus - Anzahl und Grenzform*
Betreuer Prof. Dr. Christoph Thäle (Bochum)
Gutachter Prof. Dr. Christoph Thäle (Bochum), Prof. Dr. Peter Heinzner (Bochum)

Preprints und Veröffentlichungen in Fachzeitschriften

- [1] Second-order properties for planar Mondrian tessellations
Betken, C., Kaufmann, T., Meier, K., and Thäle, C.
Methodology and Computing in Applied Probability 25 (2023), article 47
- [2] Central limit theorems for generalized descents and generalized inversions in finite root systems.
Meier, K., and Stump, C.
Preprint; arXiv:2202.05580

Vorträge

- 09/2021 86th Séminaire otharingien de Combinatoire, Bad Boll
Central limits for generalized descents and inversions in finite Weyl groups
- 08/2022 17. Doktorand:innentreffen der Stochastik, Klagenfurt
Central limit theorems for generalized descents and inversions in finite finite root systems

Bochum, April 2023

Eigenständigkeitserklärung

Ich versichere an Eides statt, dass ich die eingereichte Dissertation selbstständig und ohne unzulässige fremde Hilfe verfasst, andere als die in ihr angegebene Literatur nicht benutzt und alle ganz oder annähernd übernommenen Textstellen sowie verwendete Grafiken kenntlich gemacht habe.

Zudem versichere ich, dass die vorgelegte elektronische mit der schriftlichen Version der Dissertation übereinstimmt und die Abhandlung in dieser oder ähnlicher Form noch nicht anderweitig als Promotionsleistung vorgelegt und bewertet wurde.

Bochum, den

Kathrin Meier